People's Democratic Republic of Algeria

Ministry of Higher Education and Scientific Research

University of Oum El Bouaghi

Faculty of: Sciences and Applied Sciences

Thesis

Presented to obtain

3rd Cycle Doctorate

Branch: Electronics

Specialty: Instrumentation

Title:

Design of UWB Antennas for 5G Mobile Communications

Presented by:

SEYF EL ISLEM DAIRA

Publicly defended on 19/12/2024 in front of the following committee members:

N°	first and last name	Grade	University	Quality
01	Souheil Mouetsi	Prof.	University of Oum El Bouaghi	President
02	**Mohamed Lashab**	Prof.	University of Oum El Bouaghi	Supervisor
03	Mounir Belattar	Prof.	University of Skikda	Co-reporter
04	Djamel Khedrouche	Prof.	University of M'sila	Examiner
05	Abdesselam Hocini	Prof.	University of M'sila	Examiner
06	Abdelaziz Ait Kaki	MCA	University of Oum El Bouaghi	Examiner

Abstract

The advent of fifth-generation (5G) mobile communication systems has necessitated a paradigm shift in antenna design, compelling the development of antennas that can simultaneously offer ultra-wideband (UWB) capabilities, miniaturized dimensions, multi-band performance, and high gain. This PhD thesis addresses the complex challenges inherent in designing such advanced antennas for 5G and UWB applications. The research investigates the integration of innovative techniques, including fractal geometries, metamaterials, and advanced methods, to meet the stringent requirements imposed by modern communication networks.

The thesis begins with a thorough review of the literature on UWB and 5G antenna design, highlighting the evolution of antenna technologies and identifying key challenges and innovations within these domains. This comprehensive review sets the stage for the research, which focuses on developing novel antenna design that fulfill the demanding specifications of UWB and 5G communication systems.

The research first explores a metamaterial-based UWB patch antenna optimized for Sub-6 GHz 5G applications. By integrating Split Ring Resonator (SRR) unit cells and Defective Ground Structures (DGS), the antenna achieves significant improvements in bandwidth, gain, and overall electromagnetic performance, demonstrating the efficacy of metamaterials in enhancing antenna design. The study then presents an FSS unit cell design intended to filter electromagnetic signals across the entire UWB frequency range for filtering and shielding applications. Finally, the research presents a novel design of a UWB antenna using fractal techniques, achieving a broad impedance bandwidth and maintaining high gain across the UWB spectrum using Frequency Selective Surface technique. The fractal-based design effectively miniaturizes the antenna while preserving its performance, addressing a critical challenge in UWB antenna development.

ملخص

فرض ظهور أنظمة الاتصالات المتنقلة من الجيل الخامس تحولا جذريا في تصميم الهوائيات، مما استلزم تطوير هوائيات تتميز بقدرات النطاق العريض للغاية، أبعاد صغيرة، أداء متعدد النطاقات، وكسب عال. تتناول هذه الأطروحة للدكتوراه التحديات المعقدة المرتبطة بتصميم مثل هذه الهوائيات المنقدمة لتطبيقات الجيل الخامس و النطاق العريض للغاية. يستكشف البحث دمج تقنيات مبتكرة، بما في ذلك الهندسة الكسرية، والمواد الخارقة، وطرق متقدمة، لتلبية المتطلبات الصارمة التي تفرضها شبكات الاتصالات الحديثة.

تبدأ الأطروحة بمراجعة شاملة للأدبيات المتعلقة بتصميم هوائيات النطاق العريض للغاية و الجيل الخامس، مسلطة الضوء على تطور تقنيات الهوائيات وتحديد التحديات و الابتكارات الرئيسية في هذه المجالات. تمهد هذه المراجعة الطريق للبحث الذي يركز على تطوير تصاميم هوائيات جديدة تلبي المتطلبات الصعبة لأنظمة اتصالات الجيل الخامس.

يستكشف البحث أولا تصميم هوائي رقعة قائم على المواد الخارقة ومحسن لتطبيقات الجيل الخامس ضمن نطاق التردد الأقل من 6 جيغاهرتز. من خلال دمج خلايا رنانة حلقية منقسمة وهياكل أرضية معيبة، يحقق الهوائي تحسينات كبيرة في النطاق الترددي والكسب والأداء الكهرومغناطيسي العام، مما يظهر فعالية المواد الخارقة في تحسين تصميم الهوائيات. ثم يقدم البحث تصميم خلية وحدة سطح انتقائية التردد تهدف إلى ترشيح الإشارات الكهرومغناطيسية عبر النطاق الترددي الكامل لتطبيقات التصفية و التضليل. وأخيرا، يستعرض البحث تصميما جديدا لهوائي النطاق العريض للغاية باستخدام تقنيات الهندسه الكسرية، محققا نطاق مقاومة واسعا مع الحفاظ على كسب عال عبر طيف النطاق باستخدام تقنية السطح الانتقائي للتردد. يعمل التصميم القائم على الهندسة الكسرية على تصغير الهوائي بشكل فعال مع الحفاظ على أدائه، مما يعالج تحديا أساسيا في تطوير هوائيات النطاق العريض للغاية.

Dedications

In the Name of Allah, the Most Beneficent, the Most Merciful

All praise and thanks be to Almighty Allah. Choicest blessings and peace upon our Master, Allah's Noble Messenger Muhammad, His family, His companions, and all those who follow His guidance until the Last Day.

To my beloved parents, who planted the seed of knowledge in my mind and nurtured it with love, reminding me always that words have the power to change the world. Your unwavering support and encouragement have been my guiding light throughout this journey.

To my dear brother, sisters, grandparents, family, and friends, who have stood by my side, believed in me, and supported me with their love and prayers.

To the dear, sweet people of Gaza, I am deeply sorry that we have failed you, but know that you are never forgotten.

O Allah, help and protect the people of Gaza and Palestine. O Allah, ease their pain and suffering. O Allah, Bestower of Mercy, bestow Your mercy upon them. O Allah, grant them victory.

"From the river to the sea, Palestine, tomorrow will be free."

Acknowledgments

Alhamdulillah, all praise be to Allah, the Almighty, the Most Gracious, and the Most Merciful. I begin by thanking Allah for His countless blessings, guidance, and grace that have enabled me to complete this thesis and for everything He has bestowed upon me throughout my life. I also extend my praises to our beloved Prophet Muhammad (Peace Be Upon Him), who wisely stated, "Whoever takes a path upon which to obtain knowledge, Allah makes the path to Paradise easy for him."

I owe my deepest gratitude and heartfelt appreciation to my beloved parents, whose love, prayers, motivation, and endless support have been the cornerstone of my journey. Their unwavering belief in me has been a source of strength and encouragement, and I pray that Allah blesses them with health and happiness in this life and the hereafter.

I would like to express my profound thanks to my esteemed supervisor, Prof. Mohamed Lashab, for his invaluable supervision, support, and tutelage. His guidance has been instrumental in the completion of this work, and I am deeply grateful for his mentorship.

My gratitude also extends to the Doctoral Committee, colleagues, and staff of the Laboratory of Electronics and New Technologies (LENT), and the Department of Electrical Engineering, Faculty of Science and Applied Sciences at the University of Larbi Ben M'hidi. I am thankful for the opportunity to pursue my research, and complete this thesis.

I am particularly grateful to Prof. Ahmed Kishk for his invaluable supervision and support during my research internship at Concordia University. I would also like to extend my special thanks to the Laboratory of Advanced Technology on Antenna and Microwave Systems (LATAMS) and the Department of Electrical & Computer Engineering at Concordia University, Montreal, Canada, for their exceptional resources, support and inspiring academic environment.

Furthermore, I express my sincere thanks to Prof. Raed Abd-Alhameed from the University of Bradford for his collaboration and valuable insights during my research.

I am also deeply thankful to my dear friend Ramzi Farhi for his hospitality during my stay in Montreal, where he made me feel at home, providing not just a place to stay but also a sense of belonging.

Lastly, I wish to express my love and gratitude to my brother, sisters, grandparents, extended family, and friends for their constant encouragement and support. I am also grateful to everyone who has contributed to this endeavor in one way or another; your help and kindness have not gone unnoticed.

May Allah reward all of you abundantly.

Table of Contents

List of Tables

List of Figures

.

List of Acronyms

1G: First Generation of Mobile Telecommunications

2G: Second Generation of Mobile Telecommunications

3G: Third Generation of Wireless Mobile Telecommunications Technology

3GPP: Third Generation Partnership Project

4G: Fourth Generation of Broadband Cellular Network Technology

5G: Fifth Generation of Mobile Networks New Radio

5GPPP: 5G public private partnership

AI: Artificial Intelligence

AMPS: Advanced Mobile Phone System

AiP: Antenna-in-Package

ANN: Artificial Neural Networks

AoC: Antenna-on-Chip

BDMA: Beam-Division Multiple-Access

BS: Base Station

BSCs: Base Station Controllers

BSS: Base Station Subsystems

BW: Bandwidth

CDMA: Code-Division Multiple Access

CPW: Coplanar Waveguide

CSRR: Complementary Split Ring Resonator

CST: Computer Simulation Technology

DC: Direct Current

DGS: Defected Ground Structure

DR: Dielectric Resonator

EBG: Electromagnetic Band Gap

EDGE: Enhanced Data Rates for GSM Evolution

EM: Electro Magnetic

EMC: Electromagnetic Compatibility

EMI: Electromagnetic Interference

FBW: Fractional Bandwidth

FCC: The Federal Communications Commission

FHD: Full High Definition

FM: Frequency Modulation

FSK: Frequency Shift Keying

FR: Frequency Ratio

FR1: Frequency Range 1

FR2: Frequency Range 2

FSS Frequency Selective Structures

GA: Genetic Algorithms

Gbps: Giga bits per second

GHz: Giga Hertz

GPR: Ground-Penetrating Radar

GPRS: General Packet Radio Service

GPS: Global Positioning System

GSM: Global System for Mobile Communications

HFSS: High Frequency Structure Simulator

HSPA: High Speed Packet Access

IEEE: Institute of Electrical and Electronics Engineers

IoT: Internet of Things

IP: Internet Protocol

ISM: Industrial, Scientific, and Medical

IMT: Intelligent Manual Transmission

ITU: International Telecommunication Union

LTE: Long Term Evolution

MAC: Medium Access Control

MIMO: Multiple Input Multiple Output

MMW: Millimeter-Wave

MSC: Mobile Switching Center

MTM: Metamaterial

NR: New Radio

NTT: Nippon Telegraph and Telephone

PCB: Printed Circuit Board

PSD: Power Density Spectral

PSO: Particle Swarm Optimization

RCS: Radar Cross Section

RF: Radio Frequency

SAR: Specific Absorption Rates

SIW: Substrate Integrated Waveguide

SNR: Signal to Noise Ratio

SRR: Split Ring Resonator

TDMA: Time Division Multiple Access

UC: Unit Cell

UMTS: Universal Mobile Telecommunication Systems

UWB: Ultra-Wideband

VNA: Vector Network Analyzer

V2X: Vehicle to Everything

WiMAX: Worldwide Interoperability for Microwave Access

WLAN: Wireless Local Area Network

WPAN: Wireless Personal Area Network

WUSB: Wireless Universal Serial Bus

CHAPTER I
Introduction

1.1 Background and Context

The dawn of fifth-generation (5G) wireless communication networks has led to a thorough rethinking of antenna design, forcing a departure from traditional systems to meet modern communication network requirements for antennas, including ultra-wideband features, miniaturization properties, multi-band performance capability, and increased gain. This underscores the exigent demand posed by the 5G environment. Driven by the need for increased data rates, reduced latency, and enhanced connectivity, the previous age, characterized by the restrictions of prior generations, is replaced by 5G technology.

In this context, the research problem becomes the creation of antennas that can work with ultra-wideband transmission, small sizes (less than 3 centimeters), and high gain coefficients all at the same time. This calls for a creative mix of various design methods.

The main focus of this academic inquiry resides in identifying and addressing the multifaceted challenges that are inherent to the development of antennas for UWB and 5G applications. Combining fractal antennas, metamaterials, and different polarization methods seems like a smart way to deal with this problem, but it needs to be carefully studied to see how they can work together and what uses they can serve separately. As a result, this academic project uses a mix of theoretical knowledge, experimental interventions, and technological integration to give a thorough explanation of how the complex requirements for UWB antenna design interact with the transformative needs made clear by the 5G era.

1.2 Research Problem Statement

The pivotal research problem addressed in this scholarly study lies at the intersection of advanced antenna design requirements and the strict demands of the growing field of UWB applications and fifth-generation (5G) mobile communications. The emergence of UWB and 5G technologies requires antennas with certain properties such as wide frequency range, miniaturization, multi-band, and high gain. These features are crucial for the antennas that form the linchpin of modern wireless networks.

The crux of the research problem arises from the complex challenges in achieving all requirements of these specifications simultaneously within a single antenna framework. The research investigation is rooted in the need for antennas to function within the UWB spectrum (3 GHz to 10.6 GHz), thus requiring a detailed examination of design approaches that accommodate such wide frequency ranges. Furthermore, the prescribed antenna dimensions of less than 3 centimeters and the need for substantial gain impose challenging limitations that

necessitate creative solutions. The challenge goes beyond just combining these different characteristics; it involves a careful synthesis, creating a new paradigm in antenna design to effectively address the intricate demands of UWB applications and 5G mobile communication.

The identification of this research problem emphasizes the need for a thorough investigation into the integration of fractal antennas, metamaterials, and diverse polarization schemes. This will advance the academic discourse towards a practical understanding of the challenges involved in developing advanced antenna designs necessary for the effectiveness of UWB applications and 5G communication networks.

1.3 Thesis Description

This thesis's structure revolves around the development and analysis of innovative antenna designs specifically tailored for UWB and 5G mobile communication systems. This thesis presents research that combines multiple advanced design techniques to create antennas that meet the stringent requirements of UWB and 5G technology.

The primary focus is on designing UWB antennas that operate within the 3.1 GHz to 10.6 GHz frequency range, with an emphasis on achieving a miniaturized form factor of approximately less than 3 centimeters while maintaining a gain greater than a few decibels. To achieve these objectives, the thesis explores the use of fractal geometries, metamaterials, and various techniques.

Fractal antennas, known for their space-filling properties and self-similar patterns, are investigated for their potential to provide wideband performance and miniaturization. Metamaterials, which are artificial materials engineered to exhibit electromagnetic properties not found in nature, are explored for their ability to promote miniaturization and enhance antenna performance. The thesis also explores the design of multi-band antennas, specifically optimized for 5G sub-6 GHz mobile communications, to ensure their high efficiency across various frequency ranges.

Commercial simulation software, including CST Microwave Studio, is employed to model and simulate the suggested antenna designs. The final stage involves fabricating and testing the designed antennas to validate their performance and ensure their practical applicability for 5G mobile communication.

1.4 Objectives of the Thesis

The objectives of this thesis are as follows:

- Design of a UWB antenna based on the Fractal Technique: To develop a UWB antenna that employs fractal geometries, emphasizing the attainment of a broad impedance bandwidth, superior gain, and compact size.
- Design of an Antenna Using Metamaterials: To explore the use of metamaterials in antenna design with the aim of promoting miniaturization and improving overall performance.
- Design of a Multi-Band Antenna Suitable for 5G Mobile Communications: The aim is to develop a multi-band antenna that satisfies the unique frequency needs of 5G sub-6 GHz mobile communication, guaranteeing effective functioning in various bands.
- Utilization of Commercial Simulation Software: To employ commercial simulation tools, such as CST Microwave Studio, and HFSS for the modeling, simulation, and optimization of the proposed antenna designs.
- Fabrication and Testing of Designed Antenna: To manufacture and conduct experimental tests to validate their performance against theoretical and simulated results.

1.5Organization of the Thesis

The six comprehensive chapters that meticulously structure this thesis build upon each other, culminating in a detailed exploration and novel contributions to the field of UWB antenna design for 5G mobile communication.

The first chapter serves as the foundational cornerstone of the thesis and provides a comprehensive overview of the conducted research. This chapter begins by setting the stage with a background and context that delineate the evolution of antenna design within the framework of fifth-generation (5G) mobile communication systems. The research problem statement is then clearly stated, along with the major difficulties in creating UWB antennas that meet the strict requirements of 5G technology, including their high gain, wide frequency range, and small size. Following this, the thesis description offers a succinct summary of the research objectives, methodologies, and anticipated contributions. The thesis outlines the specific goals the research aims to achieve, including the design of UWB antennas using fractal techniques and metamaterials. Finally, the thesis organization provides readers with a roadmap of the following chapters, guiding them through the structured progression of the research work.

The second chapter presents a thorough review of the existing literature on UWB antenna design, offering a concise history of UWB technology to contextualize the subsequent discussions. We explore the basic concept of ultra-wideband technology in detail, highlighting its unique characteristics and how these have shaped antenna design principles. The chapter also examines the applications of UWB technology, highlighting its diverse uses across various domains and discussing its advantages over other communication technologies. We provide a comparison with narrowband and broadband systems to highlight the uniqueness of UWB technology, and then delve into the key features that are crucial for antenna design. The chapter then delves into antenna specifications for UWB technology, identifying the technical requirements that antennas must meet to be effective within UWB systems. Finally, an evaluation of UWB antennas in the time-domain is conducted, analyzing their performance metrics and identifying gaps in the current state of the art.

The third chapter shifts focus to the domain of 5G antenna design, providing a review of existing research and development in this rapidly evolving field. The chapter begins with an overview of the evolution of mobile networking technology, tracing the technological advancements that have culminated in the development of 5G. The chapter presents a detailed explanation of the fifth-generation wireless communications network (5G), highlighting its key features and highlighting its differences from previous generations. The chapter also covers 5G standardization and spectrum allocation, explaining the regulatory frameworks and frequency bands allocated for 5G communication. The chapter discusses the diverse applications of 5G and highlights its superior capabilities by comparing it with previous generations. The chapter then delves into 5G antennas and propagation, elaborating on the unique challenges and requirements for 5G antenna design. The chapter identifies key characteristics of 5G antennas, laying the groundwork for a detailed analysis of 5G antenna design considerations. This analysis provides insight into the critical factors that influence the design of effective 5G antennas.

In the fourth chapter, the thesis presents an innovative study on the integration of Split Ring Resonator (SRR) unit cells and Defective Ground Structure (DGS) techniques in a UWB patch antenna, specifically aimed at enhancing performance for Sub-6 GHz 5G applications. The chapter details the antenna design, which incorporates SRRs near the feed line to maximize electromagnetic field intensity and employs DGS on the ground plane to create a strong resonance effect, leading to enhanced coupling between electric and magnetic fields. The

design's Miniaturization is noteworthy, achieving dimensions of 20×28×16 mm^3, while still maintaining desirable operational characteristics. The bandwidth is expanded from 2.26 GHz to 5.4 GHz, with a markedly enhanced S-11 parameter of -33 dB at 3.5 GHz. The Gain Improvement is also significant, with a peak of 4.15 dB at 5.2 GHz. The chapter explores the Electromagnetic Properties of the SRR unit cells, confirming their role as a metamaterial with near-zero values of permeability, permittivity, and refractive index, which contribute to the antenna's superior performance. This chapter underscores the potential of SRR and DGS integration in advancing antenna design for 5G communication systems, offering a promising pathway for future research and development in this field.

The fifth chapter presents the conception and study of a single-layered Ultra-Wideband Frequency Selective Surface (UWB-FSS) intended for band-stop spatial filtering and electromagnetic shielding applications. The proposed FSS structure is implemented on a low-cost FR4 substrate and features a novel unit cell design comprising a square patch with reverse hexagonal slots. The unit cell demonstrates an ultra-wide stop-band performance, with a significant stop-band attenuation of -10 dB. The shielding effectiveness (SE) remains consistently above 10 dB within the obtained frequency band. The performance of different array configurations was also investigated. Larger arrays demonstrated enhanced electromagnetic characteristics, including improved stop-band performance and higher shielding effectiveness. The compact size and high shielding effectiveness of the proposed FSS design make it well-suited for UWB applications requiring efficient spatial filtering and EMI suppression. The study concludes that the proposed structure provides an effective solution for UWB filtering and shielding, with promising results for practical implementation.

The sixth chapter introduces a novel design approach that integrates a curved single-layer FSS with a compact coplanar waveguide (CPW) UWB antenna to enhance gain. The chapter provides a comprehensive description of the design, which involves a CPW-fed UWB monopole antenna developed on an FR-4 substrate. The antenna is strategically placed atop an 11 × 11 bended FSS reflector, also manufactured from FR-4 material, with each UC measuring 13 × 13 mm. The chapter meticulously details the design's Impedance Bandwidth, which spans 2.66 GHz to 17.98 GHz, covering the whole UWB spectrum, and emphasizes the substantial Gain Enhancement achieved by the curved reflector, with values fluctuating between 0.2 and 14.9 dB. The Radiation Patterns are directed efficiently, with a peak gain boost of 10 dB at 10.6 GHz. A comparative analysis is conducted, juxtaposing the conventional FSS approach with the proposed design through both simulations and experimental tests, demonstrating the

superior performance of the new design. The findings highlight the applicability of the proposed structure in UWB and ground-penetrating radar systems, setting a benchmark for future antenna designs in these fields.

The final chapter synthesizes the key contributions of the research, providing a comprehensive summary of the findings across the various chapters. The chapter emphasizes the novel insights gained from the study, particularly in the design and development of UWB antennas for 5G mobile communication systems. The practical implications of the research are discussed. The chapter ends with a discussion of future work, including possible areas for further investigation. For example, the authors suggest looking into more metamaterial structures, using the proposed designs in different frequency bands, and creating more advanced fabrication techniques to improve the performance of antennas. The chapter serves as a closing reflection on the research journey, positioning the work within the broader context of ongoing developments in the field of antenna design.

This organization ensures a logical progression of ideas, leading the reader from foundational concepts through to advanced research findings and ultimately culminating in a set of well-defined conclusions and recommendations for future research.

CHAPTER II

Literature Review and State of the Art

Part One:

UWB Antennas

2.1 Ultra-Wideband Antennas

2.1.1 Concise History of UWB Technology

The origins of UWB tech go back more than one hundred years. The examination of electromagnetic wave propagation brought UWB technology to the public's attention in the early 1960s [1]. In the past, UWB devices employed impulse radio, which sends data at very high speeds by sending pulses with an interval of just a few nanoseconds [2]. Guglielmo Marconi applied his spark gap radio transmitter to send Morse code over the Atlantic Ocean on December 12, 1901, which he originally developed in the late 1890s [3]. This radio transmitter generated pulses with an extremely broad bandwidth [4]. At that time, it wasn't possible to effectively restore wideband energy or tell one wideband signal from many others. In the end, wideband transmission stopped being used. The world of information switched to narrowband radio transmitters, which were easy to control and coordinate. From 1942 to 1945, work was done to cut down on disturbance and make the system more reliable. Multiple patents were filed on this subject, and because of this, most patents were put on hold because the U.S. government thought they could be used in the military [5].

In the 1960s, there were two very important advances in UWB technology. Gerald F. Ross invented a way to measure impulses that can be used to figure out how radio networks behave during transient events. Hewlett-Packard made the sampling oscilloscope in 1962. This tool was employed for the aim of observing, studying, and measuring the impulse reaction of microwave networks, and also for allowing the synthesis of sub-nanosecond pulses by catalyzed methods. During the 1960s, antenna manufacturers designed antennas that demonstrated a nearly constant pattern and impedance despite the specific frequency. Rumsey and Dyson were the creators of logarithmic spiral antennas [6, 7]. Ross used techniques for measuring impulses to build the wideband radiating antenna [8], which made short-pulse radar interactions better. In April 1973, Ross filed the first approved UWB patent, which was for a short-pulse detector [9].

In the middle of the 1980s, unlicensed wideband communication was authorized for Industrial, Scientific, and Medical (ISM) uses. WLAN and Wi-Fi have grown a lot since then. After that, people in the communication business started to look into the advantages and consequences of communications with a broader bandwidth.

The DARPA's radar study from 1990 was the first time the word "UWB" appeared [10]. In the beginning, UWB signals were thought to be "carrier-free" or "baseband," with a very short rising time. Pulses have been employed as broadband signals to get a wide-band receiver excited. Improvements in semiconductor technology have made UWB more useful for commercial purposes.

The FCC updated its regulations on February 14, 2002, so people could use the 7.5 GHz bandwidth from 3.1 to 10.6 GHz without a license [11]. Because of this grant, the study and advancement of RF circuits and antennas for UWB communications grew a lot. Additional funding has been invested in this new technology so that businesses can offer a greater variety of services to clients. UWB technology is an invention that is seen as a possible way to communicate at a high data rate.

In 2007, the IEEE Institute standardized UWB under IEEE 802.15.4a [12]. UWB PHY then evolved into an IR-UWB technology that focuses on low-data-rate wireless transmission and precision ranging. IEEE 802.15.6 [13] became the standard for Wireless Body Area Networks (WBAN) in 2012. It describes short-range wireless communications that can happen near or inside a human body.

In 2020, the UWB PHY improvement to the IEEE 802.15.4 standard, named IEEE 802.15.4z [14], came out. The two main goals of the improvement were to make the measurements more accurate and to improve their integrity, which made it possible to use them for a variety of applications, such as 5G. Some of the improvements are more coding and preamble choices with proportionally smaller sets of zero-valued elements that make detection work better.

2.1.2 Basic Concept of Ultra-Wideband technology

UWB is an approach for a wireless network to send data that has an extremely large bandwidth, as the name implies. A UWB system is defined as a signal that has a fractional bandwidth (bandwidth divided by the center frequency) larger than 20% or a bandwidth of −10 dB that is either equal to or greater than 500 MHz of the spectrum [11]. The bandwidth is determined by measuring the signal level in areas where the emission is 10 decibels lower than the peak. The fractional bandwidth and center frequency are both determined by calculating the upper and lower points, denoted as f_H and f_L, respectively, as shown in equations (1) and (2) [15].

$$BW = \frac{2(f_H - f_L)}{(f_H + f_L)} \quad (1)$$

$$f_C = \frac{(f_H + f_L)}{2} \quad (2)$$

The majority of narrowband systems use less than 10% of the bandwidth centered around the frequency and are transmitted at significantly higher power levels. For instance, if a system were to utilize the complete UWB band ranging from 3.1 to 10.6 GHz and position itself around any frequency within that range, the required bandwidth would need to exceed 100% of the center frequency in order to cover the whole UWB frequency spectrum. In comparison, a wireless system that operates at a frequency of 2.4 GHz and has a bandwidth of 80 MHz utilizes a bandwidth that is equivalent to only 1% of the central frequency.

Currently, there is a strong focus on employing these signals for efficient, low-power, close-range communication at high data rates. Using signals with a very large frequency spectrum may be the best way to deal with the problem of interference that comes up in narrowband communications. Worldwide regulatory bodies have reached an agreement that the transmission of UWB signals without a license can be permitted under specific conditions. The primary constraint is that the Power Spectral Density (PSD) must not go greater than the predefined limitations established by a PSD mask. The requirements of the mask vary based on its particular application and geographical location as well, but one constant characteristic is that the PSD is always limited to −41.3 dBm/MHz or lower.

The FCC in the United States grants authorization for UWB communications across the frequency range of 3.1 to 10.6 GHz. Regulatory organizations in other countries engage in active research to make decisions concerning UWB regulations. While they are undoubtedly affected by the FCC's decisions, it doesn't mean that they will completely follow its rules. The Electronic Communications Committee (ECC) in Europe completed the preliminary paper regarding security standards for wireless data networks against UWB-related [16]. Unlike the FCC's approach, which uses a single emission mask level for the whole UWB range, this paper suggests dividing the UWB band into two sub-bands: a low band from 3.1 GHz to 4.8 GHz and a high band from 6 GHz to 8.5 GHz. The UWB PSD mask for both FCC and ECC is shown in Figure 2.1.

Figure 2.1 shows the FCC and ECC Power Spectral Density mask for indoor applications in the United States and Europe, respectively.

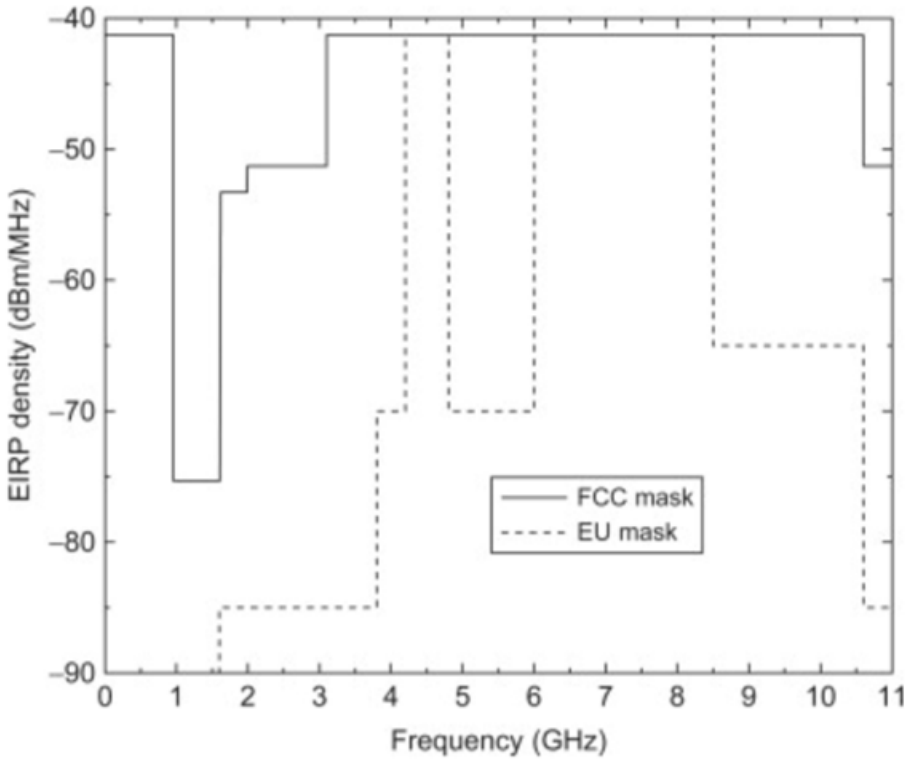

Figure 2.1. FCC and ECC Power Spectral Density mask for indoor applications [11][16].

The PSD mask guarantees that the power emitted by a UWB system within the range of a typical communication system remains at a relatively low level to prevent any substantial interference. The PSD limit in certain bands is set below -41.3 dBm/MHz to provide more safety for specific existing services, such as GPS. The restricted PSD of ultra-wideband systems usually limits their effective range to approximately 10 m. The extensive bandwidth leads to potentially enormous data transfer rates. The Shannon-Hartley rule is used to figure out the theoretical channel capacity, which is shown in Figure 2.2 as a variable that depends on both the bandwidth and the signal-to-noise ratio (SNR).

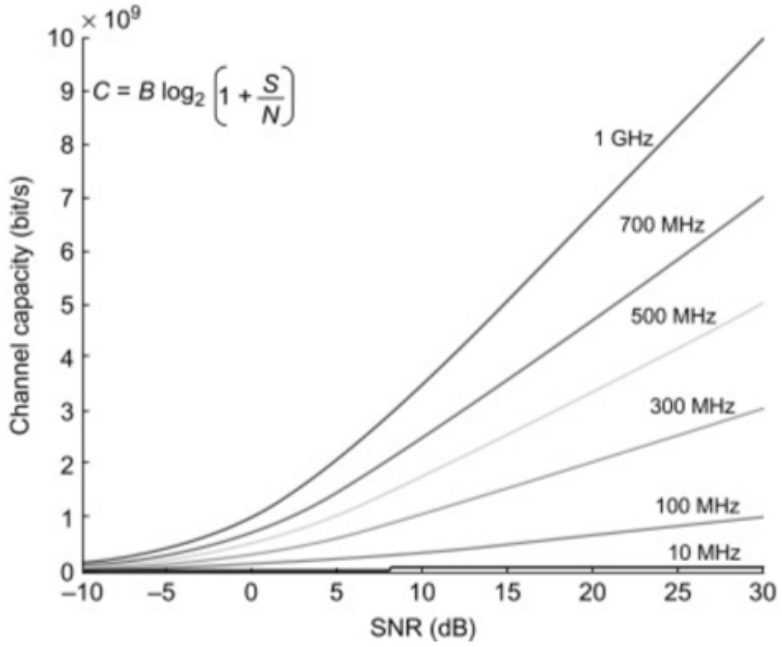

Figure 2.2. Comparison of channel capacity in relation to signal-to-noise ratio (SNR) and bandwidth.

Figure 2.3 shows the UWB PSD mask limited to –41.3 dBm by FCC for indoor and outdoor UWB communications.

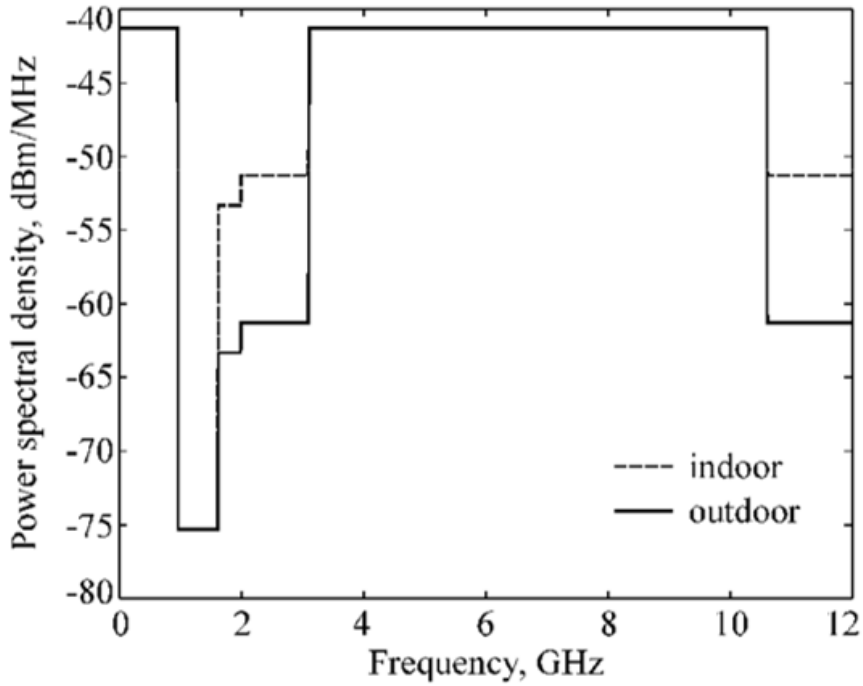

Figure 2.3 UWB PSD mask limitation to –41.3 dBm by FCC for indoor and outdoor UWB communications [11].

Table 2.1 provides a concise overview of the emission values for indoor and handheld UWB devices as defined by the FCC. The emissions must remain below the average limits when monitored with a resolution bandwidth of 1 MHz.

Table 2.1. FCC restrictions for Indoor and handheld systems.

Frequency (MHz)	Indoor PSD (dBm)	Handheld PSD (dBm)
960-1.610	-75.3	-75.3
1.610-1.990	-53.3	-63.3
990-3.100	-51.3	-61.3
3.100-10.600	-41.3	-41.3
Above 10.600	-51.3	-61.3

2.1.3 Applications of UWB Technology

UWB short-range technology stands ahead of traditional carrier wave systems due to its low transmit power consumption, ultra-wide signal bandwidth, and enormous data rate which makes it one of the most attractive radio technologies. These characteristics facilitate the concurrent running of several different user signals and programs within a particular bandwidth. UWB is commonly used in multiple systems to improve performance in applications including accurate distance measurement, location, and data transmission. Key applications encompass:

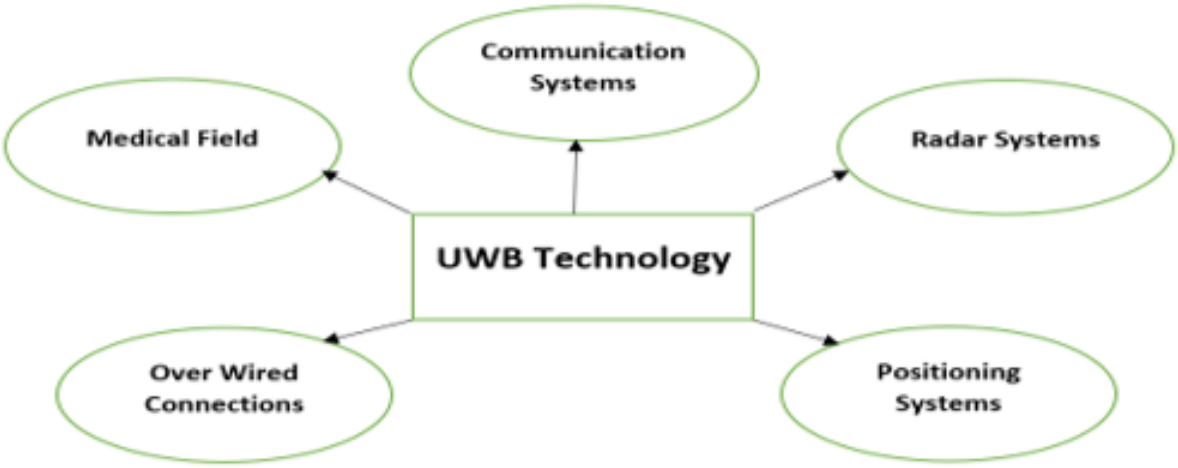

Figure 2.4 UWB Major Application Areas

2.1.3.1 Communication Systems

UWB networks have become practical by employing this technology and the wide RF bandwidths that are currently available. The vast bandwidth helps to establish a high-speed wireless local area network (WLAN) with data rates close to gigabits per second. UWB transmissions have the advantage of being available at low frequencies, which results in substantially less attenuation due to building materials than high-bandwidth systems using mm Waves. Functioning at lower frequencies reduces route losses and decreases the necessary radiated power, resulting in enhanced performance [17].

The enormous data rate capability of UWB leads it to be particularly suited for use in Wireless Personal Area Networks (WPAN) applications. The data is transmitted across a maximum distance of 10 meters, with speeds ranging from 100 to 500 megabits per second. It is possible to link personal computers to scanners, keyboard, joystick, printers, monitors, cameras, and storage devices via the high-speed wireless universal serial bus (WUSB). UWB in WPANs enables the download and upload of high-quality videos from smartphones and tablets, listening on music players, wireless high-definition multimedia, and wireless connection of speakers [18]. The requirement for cables to link the aforementioned items is eliminated.

UWB is utilized as a transmission bridge in a sensor network. Sensor networks are comprised of a number of sensors that are strategically placed throughout a certain area to carry out surveillance functions. The sensor nodes can be classified as either fixed or portable. The sensor nodes possess mobility when attached to vehicles, firefighters, robots, troops, and emergency response scenarios [19]. The desired qualities of sensor networks, such as low power, robustness, cheap cost, and multi-functionality, can be achieved by applying UWB technology. UWB communication systems provide the efficient collection and distribution of an immense amount of sensory information in a short period of time. A significant reduction in installation and maintenance expenses can be achieved without the need for wired connections [20].

Ultrawideband pulses are utilized to deliver exceptionally high data transmission rates in multi-user networked services. These brief waveforms are fairly resistant to the interference caused by multipath cancellation, which is commonly found in outdoor and indoor settings. Furthermore, the implementation of package bursting and Time Division Multiple Access (TDMA) techniques for multiple user connections is easily achieved due to the very brief waveforms [21].

2.1.3.2 Medical field

Ultra-wideband technology is a very attractive option to facilitate communication in the healthcare sector because of its low signal strength. The weak signal remains unaltered by surrounding interference and jamming equipment, and it also has a small effect on the human body. In order to track patient data, sensors are inserted both on the body and inside the body, which then transmit data to a control center located nearby. An ultra-wideband sensor network eliminates the need for wired sensors, providing the patient with freedom from entangled wires. Sensors are employed in medical scenarios to measure pulse rate, temperature, and other vital life indicators [17]. UWB is utilized for wireless transmission of sensor data and can also serve as a sensor for monitoring breathing, heart rate, and even for medical imaging purposes. This enables it to possibly replace X-ray systems in healthcare diagnosis and perform tasks such as through-wall imaging and ground-penetrating radar for rescue operations [20].

2.1.3.3 Radar Systems

In radar apps, the aforementioned brief pulses offer exceptional range accuracy and precise abilities for determining distance and location. The extensive bandwidth results in outstanding radar resolution, enabling the differentiation of tightly positioned targets. Even when traversing lossy materials like plants, earth, and even walls and floors, this great resolution is still achieved. UWB short pulses have additional benefits, such as being resistant to passive interference from fog, rainfall, congestion, aerosols, and other factors. They also have the capability to detect targets that are moving really slowly or are immobile [3].

Ultrawideband antenna arrays play a crucial role in radars by providing precise and accurate measurements of both distance and angle. Within the domain of the radar cross-section (RCS) range, a solitary UWB antenna serves as a substitute for a substantial array of narrowband antennas typically employed to encompass the entire frequency range of significance. UWB signals provide cost-effective, high-quality radar. Radar will be employed in unconventional domains such as vehicle sensors, programmable air bags, smarter highway projects, accuracy mapping, and even in a variety of homeland security applications [4].

The UWB regulations allow for the use of directional antennas on cars to operate vehicular radar in the frequency range of 22 to 29 GHz. These devices can figure out where things are and how they're moving that are close to a vehicle. This makes it easier for functions like avoiding close collisions, improving air bag deployment, and making suspension systems better able to adapt to traffic conditions [4].

2.1.3.4 Positioning Systems

The Global Positioning Satellite System (GPS) relies on time to precisely identify position and location, enabling precision within a range of 10 m. Particular procedures are employed to improve precision. Boosting the bandwidth has an immediate impact on precision. Therefore, by raising the bandwidth, the accuracy of positional measurements increases as well. With the use of UWB approaches, it becomes possible to achieve highly accurate positioning, such as sub-centimeter and even sub-millimeter accuracy [21]. This makes UWB technology an excellent choice for indoor positioning and tracking apps, as it offers higher data rates at shorter ranges. The improved tracking system enables precise tracking of things moving within an indoor space with a precision of millimeters [4]. They can be utilized to ascertain the location of objects or individuals who are lost or missing in scenarios such as a blazing structure, casualties in an isolated region, and similar circumstances [2].

In the field of satellite communications, wideband feeds are utilized to conserve space and reduce weight by enabling multiple lines of communication to be supported by a single antenna. Hence, the deployment of UWB will significantly enhance the accuracy of intrusion detection radar, accuracy, positioning systems, and protected ground connectivity for military personnel, surpassing any potential negative effects it could have on various other systems.

2.1.3.5 Ultra-Wideband over Wired Connections

UWB technology can be sent over wired connections and cables, which gives it the potential to efficiently increase the bandwidth accessible by cable television (CATV) networks by two times without requiring any changes to the current infrastructure. Coaxial cable-based wired networking offers a maximum downstream speed of 1.2 Gbps and a maximum upstream speed of 480 Mbps, providing more bandwidth on various CATV systems at cheap prices. The wire-line Ultra-Wideband technology doesn't cause any disruption or deterioration to television, web browsing, or other services that are currently served by the Cable Television infrastructure [4].

2.1.4 Advantages of UWB Technology

UWB is frequently seen as a superior option for radar and communications tasks due to its distinct advantages over alternative technologies. The following are some of the primary benefits of UWB technology [3].

- The transceiver architecture is uncomplicated and cost-effective.
- Minimal disruption to existing systems.

- Large channel capacity.
- Low Power Spectral Density.
- Exhibits a high level of resistance to multipath interference.
- Improved precision in measuring distance and distinguishing between different distances.
- Reduced probability of detection and interception.

As per Hartley-Shannon's capacity formula, the channel capacity experiences a linear rise in relation to the bandwidth [22]. If there is sufficient bandwidth available for Ultra-Wideband transmissions, typically operating in the gigahertz range, it indicates that data speeds of Gbps could be attained. UWB technology utilizes brief pulses transmitted across a wide frequency range spanning from 3.1 to 10.6 GHz, resulting in a substantial bandwidth benefit. Nevertheless, the speed of UWB transmission is constrained by the power constraint, which allows only short ranges of up to 10 m [23]. Consequently, UWB provides a greater capacity and faster data rates, making it an exceptional option for these applications.

UWB employs waveforms without a carrier frequency to transfer data. Consequently, the need for carrier oscillations to move the carrier frequency for the transfer of signals is eliminated. This means that the receiving end doesn't need to do a carrier restoration step, and the UWB transceiver doesn't need any intermediate frequency components, modulators, or demodulators [24, 25]. The UWB transceiver's simplicity in design renders it lighter and more advantageous in comparison to narrowband transmissions. Moreover, these qualities lead to a substantial decrease in the system's power usage. Furthermore, the UWB system's simplicity and the lower dimensions of its chips contribute to a decrease in the overall cost of the system.

Multipath is the occurrence when an electromagnetic signal takes many routes during transmission because of elements like signal refraction, absorption, dispersion, and scattering caused by items in the surroundings [22,26]. UWB systems have a wide bandwidth, enabling them to function at high data rates, therefore rendering them highly resilient. In addition, they exhibit high performance in low-SNR channels of communication, offering resistance to multipath circumstances. UWB communication is highly suitable for indoor location applications because of this particular aspect. Moreover, UWB systems exhibit excellent resistance to multipath interference and are unaffected by channel degradation. UWB signals have a low average PSD due to their short-pulse nature. This puts them on the noise floor, typically at -40 dBm/MHz. As a result, UWB signals require less transmission power, leading to improved power efficiency and resistance toward jamming and interceptions.

2.1.5 UWB Comparison with Narrowband and Broadband

UWB signals exhibit distinct characteristics in the frequency range compared to conventional narrowband and broadband signals, mostly due to their broader bandwidth. If we consider the concept of relative bandwidth, a signal is considered narrowband if its proportional bandwidth is less than 1%. The relative bandwidth of wideband signals ranges from 1% to 20%. UWB signals possess a relative bandwidth exceeding 20% or a total bandwidth above 500 MHz [27].

In addition, UWB signals possess the notable attribute of having a broad frequency spectrum and energy evenly distributed throughout the whole range of frequencies, leading to a flat spectral profile. On the other hand, narrowband signals have a smaller range of frequencies and usually show strong power peaks focused on their central frequency, which indicates distinct spectral peaks. Although broadband signals often possess a broader frequency bandwidth, they are unable to reach the same level of spectral spread as UWB broadcasts. The reason for this is that UWB signals have the ability to cover a frequency range wider than 500 MHz, spanning multiple gigahertz. UWB signals exceed the traditional concept of broadband transmissions with regard to spectral width, thereby resulting in superior performance.

Simply put, narrowband signals use a smaller frequency range and need less power to transmit compared to broadband signals. On the other hand, UWB signals are short pulses that convey information by momentarily occupying a significant section of the conventional communications frequency range.

Figure 2.5 presents a schematic representation of the comparative bandwidth and PSD for the three aforementioned communication types, and Table 2.2 shows their relative bandwidth.

Table 2.2. Relative bandwidth for the three communication types.

Communication Band	**Relative Bandwidth**
Narrow-band	$(f_H - f_L) < 0.01 f_C$
Broadband	$0.01 f_C < (f_H - f_L) < 0.2 f_C$
UWB	$0.2 f_C < (f_H - f_L)$

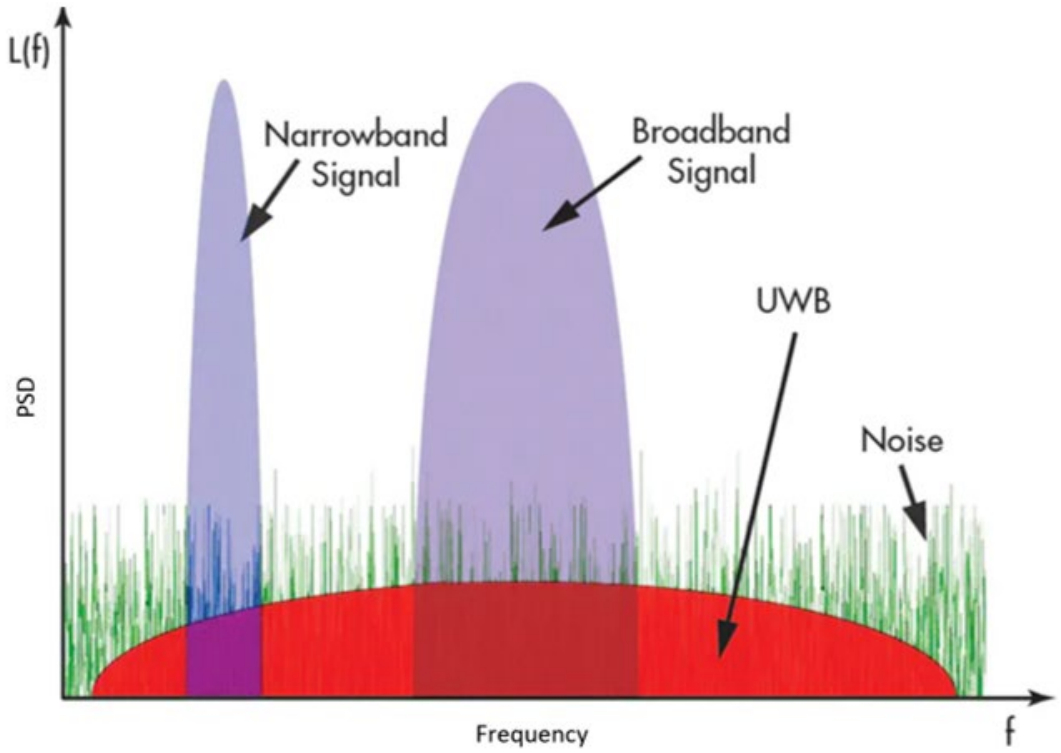

Figure 2.5. Schematic representation of the comparative bandwidth and PSD for the three communication forms.

2.1.6 Key features of UWB technology

UWB technology possesses distinct attributes that render it highly promising for utilization in particular domains.

2.1.6.1 Low power consumption:

Pulse-based ultra-wideband technology commonly employs irregular pulse transmission for the purpose of data exchange. UWB positioning systems usually have operational cycles ranging from 0.2 ns to 1.5 ns, which leads to minimal power usage. UWB systems in ultra-fast communication have power consumption ranging from tens to hundreds of watts [28], [29]. Thus, in comparison to traditional wireless technology, UWB positioning tools provide superior battery life and reduce electromagnetic radiation.

2.1.6.2 High immunity to interference from other devices:

UWB signals have extensive coverage over the frequency range, occupying an enormous spectrum of frequencies. This distinctive feature in the frequency domain allows UWB transmissions to effectively avoid narrow-band interference signals. The transmitted

power is distributed throughout the frequency range, enhancing its resistance to interference [28].

2.1.6.3 Higher security:

UWB transmissions offer a higher level of confidentiality and are more challenging to detect in comparison to non-UWB wireless transmissions [27]. The reason for this is that UWB signals cover a broad frequency range and may bear resemblance to signals that mimic noise. Simply put, background noise across a wide range of frequencies obscures UWB signals, making their detection difficult. Every bit is commonly encoded as a multitude of extremely weak pulses, frequently with amplitudes that fall below the threshold of detectable noise. These attributes facilitate the secure transfer of data with a minimal chance of being detected (LPD) or intercepted (LPI).

2.1.6.4 Limited interference with other devices:

The use of spectrum resources by UWB in conjunction with various wireless communication technologies. The system employs a frequency range of 3.1 GHz to 10.6 GHz, without the need for specific or exclusive frequency bands. UWB prevents interference with other electronic devices by restricting transmitting power. The ability to utilize the spectrum in an adaptable way is a key factor in the notable advancement of this technology, particularly in scenarios where there is a limited availability of spectrum resources [27], [30].

2.1.6.5 Low signal attenuation and strong penetration:

IR-UWB transmissions have minimal signal attenuation and high penetration due to their large band coverage. This indicates that IR-UWB signals employ a wide spectrum of frequency resources concurrently when transmitting. IR-UWB signals have a greater dispersion of energy over the spectrum as compared to standard narrowband signals. This leads to less signal power at certain frequencies and mitigates the effects of frequency-selective fading [31].

2.1.6.6 Time resolution and robustness against multipath interference:

In conventional wireless networks, the majority of radio frequency (RF) transmissions are characterized by continuous waveforms. Consequently, these electromagnetic waves are susceptible to the impact of multipath propagation, which can adversely affect both signal strength and transmission speed. UWB communication employs short-duration periodical

pulses, often with pulse widths ranging from a few nanoseconds up to dozens of picoseconds. Such pulses possess diminutive cycle times and short operation intervals, hence preventing temporal overlapping multipath signals in the time domain. Nevertheless, as a result of the exceptionally brief duration of the pulse, ultra-wideband signals manifest as remarkably sharp pulses within the temporal domain. The signals that bounce off the surfaces separating the transmitter and receiver are unlikely to coincide in time [32]. By using time-domain processing, ultra-wideband receivers can tell the difference between direct and reflected signals, which effectively lowers the negative effects of multipath interference [28].

2.1.6.7 High data rates:

$$C = Blog_2\left(1 + \frac{S}{N}\right) \quad (3)$$

The Shannon Formula, displayed above, allows for the calculation of the ultimate attainable data rate or channel capacity (C) of a channel used for communication [22]. This is done by utilizing Shannon's channel capacity formula, in which B stands for the channel bandwidth, N indicates the Gaussian white noise PSD, and S stands for the typical signal strength. UWB technology offers exceptionally high data rates by augmenting the process of transmitting bandwidth. Usually, the maximum data transfer speed varies between dozens and hundreds of Mbits/s.

2.1.7 Comparison between various short-range wireless technologies

The benefits of UWB can be determined through a comparison with frequently employed short-range wireless technologies. The detailed comparisons are displayed in Table 3. The benefits of UWB when it comes to precision are apparent. The UWB technology demonstrates an exceptional capacity to accurately calculate distance and position within a range of 5 to 10 cm. Conversely, wireless technologies such as Wi-Fi and Bluetooth, among others, are limited to precision within a range of a few meters. In addition, UWB distinguishes itself by exhibiting considerably reduced power usage in comparison to Wi-Fi. Nevertheless, it is important to acknowledge that UWB has a drawback in terms of its restricted interoperability and interaction capabilities with modern tablets and smartphones, where gadgets equipped with Wi-Fi and Bluetooth outperform it. However, some firms are aggressively embracing UWB by creating hybrid products that use a combination of UWB and either Wi-Fi or Bluetooth technologies. The goal is to merge the superior characteristics and benefits of each technology.

Table 2.3. Comparison of several short-range wireless technologies [33].

Wireless Technology	Data Rate	Accuracy	Complexity	Frequency band	Channel Bandwidth	Range	Power Consumption	Topology	Areas of focus
ZigBee	20,40, 250 Kbits/s	0.5 m	Low	868/915 MHz; 2.4 GHz	0.3/0.6 MHz; 2MHZ	10-100 m	Medium	Ad-hoc, peer to peer star, mesh	manufacturing control and surveillance, systems for sensors, architectural automation, residential control, and robotics in games and toys.
Bluetooth	1 Mbits/s	Few meters	High	2.4 GHz	1 MHz	10 m	High	Ad-hoc, very small networks	Wireless communication enables the interconnection of devices, such as cellphones, PDA, computers, and headsets.
Wi-Fi	11, 54 Mbits/s	Few Meters	High	2.4 GHz; 5 GHz	22 MHz	50-100 m	Very Low	Point to hub	The ability to connect to a local area network without the need for physical cables. Wideband Internet access.
UWB	110 Mbits/s , over 500 Mbits/s in future	5-10 cm	Medium	3.1-10.6 GHz	500 MHz-7.5 GHz	170 m	Low	Point to point	Manufacturing control and surveillance, systems for sensors, architectural automated processes, house controlling video streaming, and household entertainment apps.

2.1.8 Antenna Specifications for UWB Technology

The approach to designing ultra-wideband antennas is more complicated compared to narrowband antennas due to the need to incorporate a greater number of performance characteristics during the design stage. The substantial bandwidth demand of UWB antennas distinguishes them from other types of antennas. According to FCC standards, an appropriate UWB antenna must have a minimum absolute bandwidth of 500 MHz or a minimum fractional bandwidth of 20%. Typically, the UWB antenna must be operational across the whole frequency spectrum of 3.1–10.6 GHz.

It is necessary for the UWB antenna to maintain stable performance across the entire frequency range. Optimally, effective impedance matching, high gain, and a consistent radiation pattern across the whole frequency range are sought after. In certain applications, it is necessary to incorporate a band-rejection characteristic in UWB antennas to ensure compatibility with other conventional systems [34–35]. An omni-directional or directional antenna can be utilized based on the specific application requirements. The necessary radiation characteristics of the antenna vary from one application to another. In the context of mobile and hand-held communication devices, an omnidirectional antenna is the preferable choice as it allows for signal reception from all directions. The UWB antenna exhibits a gain of around 5 dBi throughout the whole frequency band. Directional antennas are employed in applications that necessitate high gain, such as radar surveillance systems.

The PSD of transmitted pulses in UWB systems is subject to a fairly severe constraint. If losses mount, the system's performance might decrease. In order to maximize radiation efficiency, it is imperative to minimize losses to the greatest extent possible. Utilizing lower-loss dielectric materials results in increased radiation efficiency, provided adequate impedance matching is preserved at the input port. Implementation should prioritize the execution of minimized-size approaches. To ensure compatibility with modern mobile and handheld systems, the UWB antenna must be both compact and planar, possess the characteristics of being modest in dimensions, and be able to work effectively with printed-circuit-board (PCB) technology [20].

In addition to the frequency domain performance requirements mentioned above, UWB antennas are also required to have favorable time-domain properties. The NB antenna maintains consistent effectiveness across its entire bandwidth, but similar results cannot be expected for a UWB antenna due to its extensive operational spectrum. The UWB antenna has a substantial effect on the signal that is being broadcast. The group delay should exhibit

minimal variation across the entire bandwidth, indicating that the phase response must show linearity. This reduces the deformation of the pulse shape. The period of the ringing must be minimized to avoid inter-symbol interference (ISI) [20]. The specific criteria for a UWB antenna designed for extremely fast communication are outlined in Table 2.4.

Table 2.4. UWB Antenna parameter specification.

Parameter	Specification
Bandwidth	3.1 – 10.6 GHz
Gain	Few decibels
Radiation Pattern	Omni directional
Size	Compact and Planar
Phase	Nearly Linear

2.1.9 Evaluation of UWB Antennas in the Time-Domain

UWB systems utilize the transmission and reception of ultra-short electromagnetic pulses with restricted practical radiated power. The characteristics of the radiators, which must adhere to strict time and frequency domain criteria across the entire working spectrum [36], are the main determinants of the system's efficiency. To do this, you need a phase center that doesn't move around, radiation and impedance that stay the same across the frequency range, and no higher-order modes being stimulated [37]. Planar antennas that have large functioning bands frequently have multi-resonant designs that exhibit good impedance matching. Ultrawideband antennas are utilized for the transmission and reception of brief pulses, typically on the scale of picoseconds, inside the temporal domain. In order to successfully integrate impulse-radio systems, it is imperative to examine the impulse response of antennas that emit signals across a broad range of frequencies. The efficiency of UWB antennas in the time domain is assessed using a range of criteria. Additional parameters are established and exploited to describe wideband antennas. The parameters consist of group delay, system fidelity factor (SFF), and impulse response. A UWB antenna could be represented as a two-port network, as illustrated in Figure 2.6 [38].

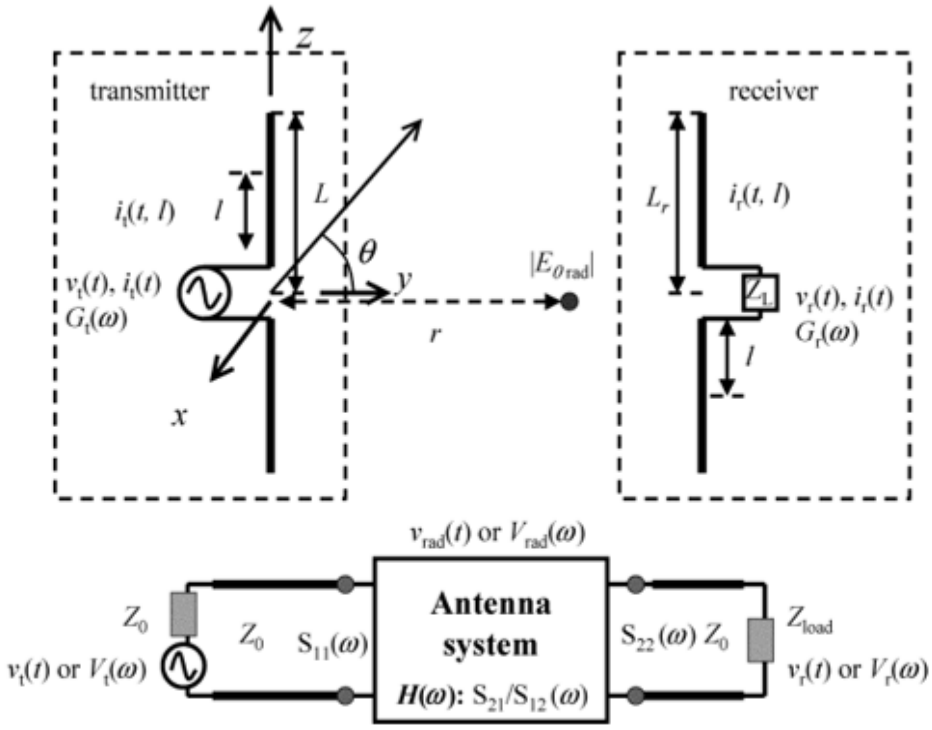

Figure 2.6. Schematic representation of a 2 ports network UWB antenna system [38].

The analysis of the system is typically conducted in an outdoor environment, taking into account real-world conditions, rather than in an anechoic chamber, as shown in Figure 2.7. Each antenna setup has two identical ultra-wideband transmitters that are linked to a pair of vector network analyzer (VNA) ports. Considering the highest possible power output of the VNA, the antennas are typically positioned at a short distance from each other. Two distinct spatial orientations between the receiver and the transmitter are being explored for the assessment of system efficiency. In one scenario, the antennas maintain an opposing orientation, but in the second scenario, they are oriented next to one another. In a face-to-face configuration, the two front sides of the antennas are positioned towards one another, while in a side-by-side perspective, the front sides of the antennas are aligned in an identical way [20].

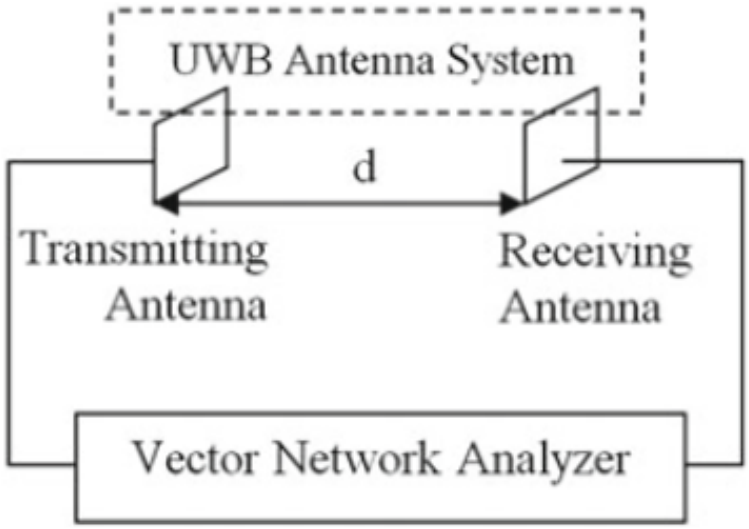

Figure 2.7. Measuring a UWB antenna system with a VNA.

The analysis of antenna dispersion features can be performed using the transfer function's (TF) magnitude of the system (S21) and group delay. If the phase of S21 shows nonlinear behavior at the magnitude fall region in the S21 plot, the transmitted pulses will show distortion. However, the TF cannot reliably determine the magnitude of pulse distortions.

The GD parameter is sometimes seen when defining devices with two ports. GD quantifies the cumulative phase distortion that occurs between the input and output signals. Equation (4) represents the TF of the device, whereas equation (5) describes the GD as the derivative of the phase response with respect to frequency.

$$H(\omega) = |H(\omega)|e^{j\angle \mathrm{H}(\omega)} \tag{4}$$

$$\tau = -\frac{\partial}{\partial \omega}\angle \mathrm{H}(\omega) = -\frac{1}{360^\circ}\frac{\partial}{\partial f}\angle \mathrm{H}(\mathrm{f}) \tag{5}$$

The antenna's dispersion is reduced as the size of the TF changes minimally and the GD remains relatively constant across the required frequency range. The S21 phase exhibits a relatively straight direction, and there is a slight change in the GD (<1 ns) across the whole ultra-wideband spectrum. This guarantees that pulse transmission occurs with low distortion. The technique of Hermitian processing, as described in [39], could be used to derive the impulse response of the antenna system. To produce the pass-band signal, no padding can be applied from the very lowest frequency recorded in the Vector Network Analyzer to the DC. The complex conjugate of the signal can be derived, and when mirrored across the negative

frequencies, it produces a symmetrical spectral response. The reason for doing this is to adhere to the characteristic of genuine TD signals, which states that the Fast Fourier Transform (FFT) of actual signals exhibits a conjugate symmetric character. Therefore, the inverse IFFT of the complex conjugate produces a signal with true values. The resulting spectrum obtained after reflection is a true signal spectrum. Next, the inverse fast Fourier transform is applied to the dual-sided spectrum in order to derive the IR in the TD. The procedure for acquiring the impulse response is illustrated in Figure 8. The received signal can be acquired through the process of converging the IR with the signal that was sent.

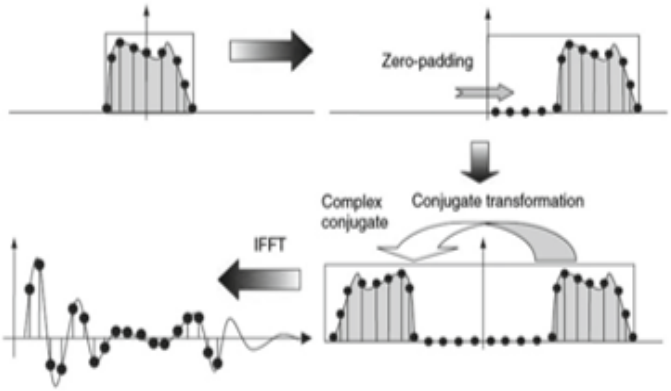

Figure 2.8. Zero padding, reflecting the conjugate, and obtaining the consequent IR[39].

The transmitted signal experiences dispersion due to both the antenna and the channel. The fidelity factor measures the degree of similarity between the input radiated waveform and the driving voltage of an antenna that transmits [40]. The fidelity factor [41] is defined by the correlation between the standardized input signal and the standardized radiated field. Measuring the radiated field is challenging in real-world situations. Alternatively, SFF can be characterized as the correlation between the signal that is transmitted and the signal that is received. The S21 factor of the antenna, which includes the transmitting antenna, channel, and receiving antenna, quantifies the degree of similarity among the broadcast signal and the signal that was received, known as SFF. The fidelity factor considers the distortion brought about by the transmitted antenna alone as opposed to the fidelity factor, which considers the distortion brought about by both the send and receive antennas [42]. The relationship between the standardized sent pulse and the standardized received pulse yields the Signal Fidelity Factor (SFF).

$$SFF = max_{\tau} \frac{\int_{-\infty}^{\infty} T_s(t).R_s(t+\tau)dt}{\left[\int_{-\infty}^{\infty} |T_s(t)|^2\, dt\right]^{1/2} \left[\int_{-\infty}^{\infty} |R_s(t)|^2\, dt\right]^{1/2}} \qquad (6)$$

Normalization is done to look at the shape of the signals without measuring their strength, since the strength of what was obtained was always weaker than the signal that was sent [43]. The SFF value ranges from 0 to 1. When the SFF number is 0, the received signal differs completely from the transmitted one. However, when the SFF number is 1, the received signal is exactly the same as the transmitted one. The signal becomes unidentifiable when the level of distortion exceeds 50% or when the Signal Fidelity Factor is less than 0.5. Ringing is the term used to describe the occurrence of unwanted oscillations in a signal. The ringing effect in antennas occurs as a result of energy that is retained or numerous reflections among the input port and the antenna [44]. The period for the waveform of a signal h(t) to decrease from its maximum value to a specific lesser number (5% of the maximum) is referred to as the ringing duration.

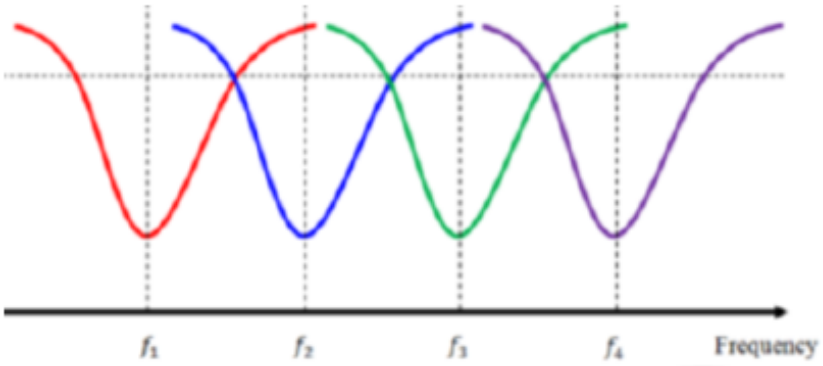

Figure 2.9. The principle of overlapping multiple resonance modes.

2.1.10 Recent research trends in UWB antennas

Recent advancements in ultra-wideband (UWB) antenna research have explored a variety of innovative solutions to meet the demands of modern communication systems. Notably, several key areas of focus have emerged. One significant trend is the integration of artificial intelligence (AI) into UWB antenna systems. AI-enhanced UWB antennas have been developed to optimize system performance dynamically, adapting to environmental and application-specific conditions. For instance, [46] demonstrated an AI-driven UWB antenna array capable of adaptive beamforming to mitigate interference. Computational intelligence techniques, such as particle swarm optimization (PSO), genetic algorithms (GA), and artificial neural networks (ANN), have become increasingly important in the design and optimization of UWB antennas. These techniques facilitate enhanced antenna performance, compact design, and optimized parameters for modern communication devices. PSO, for example, has been

employed to increase the efficiency of UWB patch antennas, addressing complex electromagnetic optimization challenges [47].

Another prominent area of exploration is the integration of UWB antennas with other electronic components. This includes Antenna-in-Package (AiP) designs, where UWB antennas are embedded within package substrates to minimize size and cost while preserving performance. A notable study in [48] proposed a multilayer substrate AiP design that achieved wide bandwidth and a low profile. Additionally, research has focused on Antenna-on-Chip (AoC) solutions, where UWB antennas are integrated directly onto integrated circuits, enabling fully integrated wireless systems. An example of this is a silicon-based AoC design that achieved both high gain and low radiation efficiency [49].

Wearable technology has also driven significant research into flexible and wearable UWB antennas. These designs frequently incorporate electromagnetic bandgap (EBG) structures or metasurfaces to enhance performance while maintaining flexibility and a low profile, making them ideal for body-centric communications and biomedical applications. Efforts have also been directed at reducing the specific absorption rate (SAR) of wearable devices to ensure compliance with safety standards [50]. Reconfigurable UWB antennas are another area of interest, offering dynamic adjustments in response to varying operating conditions. For instance, [51] proposed a reconfigurable UWB antenna with tunable bandwidth and impedance matching using PIN diodes.

Additionally, the utilization of metamaterials and frequency-selective surfaces (FSS) has gained attention for improving UWB antenna performance. These materials contribute to the development of compact, high-gain antennas with improved directional characteristics and electromagnetic interference (EMI) shielding. FSS has been utilized in the creation of broadband absorbers that protect against EMI without compromising antenna performance [50].

Finally, efforts to miniaturize UWB antennas have led to the development of compact designs that maintain wide frequency range capabilities. Band-notching techniques have been employed to filter out specific frequency bands, such as those used by WiMAX or WLAN, ensuring that UWB antennas can coexist with other communication systems in a crowded RF spectrum [47,50].

REFERENCES

[1] C.L. Bennett, G.F. Ross, Time-domain electromagnetics and its applications. Proc. IEEE 66(3), 299–318 (1978)
[2] J. Liang, Antenna study and design for ultra-wideband communication, Ph.D. thesis, Queen Mary, University of London, United Kingdom (2006)
[3] R.J. Fontana, Recent system applications of short-pulse ultra-wideband (UWB) technology. IEEE Trans. Microwave. Theory Tech. 52(9), 2087–2104 (2004)
[4] K. Siwiak, D. McKeown, Ultra-wideband radio technology (Wiley, New Jersey, 2004)
[5] G.R. Aiello, G.D. Rogerson, Ultra-wideband wireless systems. IEEE Microw. Mag. 4(2), 36–47 (2003)
[6] V. Rumsey, Frequency independent antennas. IRE Natl. Conv. 5, 114–118 (1957)
[7] J. Dyson, The unidirectional equiangular spiral antenna. IRE Trans. Antennas Propag. 7, 329–334 (1959)
[8] G. Ross, A time domain criterion for the design of wideband radiating. IEEE Trans. Antennas Propag. 16, 355–356 (1968)
[9] G. Ross, Transmission and reception system for generating and receiving base-band duration pulse signals for short base-band pulse communication system, U.S. Patent 3728632 (1973)
[10] C. Fowler, J. Entzminger, J. Corum, Assessment of ultra-wideband (UWB) technology. IEEE Aerosp. Electron. Syst. Mag. 5(11), 45–49 (1990)
[11] Federal Communication Commission, First report and order, revision of part 15 of the commission's rules regarding ultra-wideband transmission (2002)
[12] "IEEE Standard for Information technology-- Local and metropolitan area networks-- Specific requirements-- Part 15.4: Wireless Medium Access Control (MAC) and Physical Layer (PHY) Specifications for Low-Rate Wireless Personal Area Networks (WPANs): Amendment 1: Add Alternate PHYs," in IEEE Std 802.15.4a-2007 (Amendment to IEEE Std 802.15.4-2006) , vol., no., pp.1-210, 31 Aug. 2007, doi: 10.1109/IEEESTD.2007.4299496.
[13] IEEE, 802.15.6-2012, "IEEE Standard for Local and Metropolitan Area Networks—Part 15.6: Wireless Body Area Networks", pp. 1-271, 2012.
[14] IEEE, 802.15.4z-2020, "IEEE Standard for Low-Rate Wireless Networks—Amendment 1: Enhanced Ultra Wideband (UWB) Physical Layers (PHYs) and Associated Ranging Techniques", pp. 1-174, 2020.
[15] Kazimierz Siwiak, Debra Mc. Keown, "Ultra-Wideband Radio Technology," John Wiley & Sons, Ltd, 2004. Chapter 2, pp. 30-31.
[16] Electronic Communications Committee (ECC) Report 64, "The Protection Requirements of Radio Communications Systems below 10.6 GHz from Generic UWB applications," February 2005.
[17] Rahayu, Yusnita, et al. "Ultra wideband technology and its applications." 2008 5th IFIP International Conference on Wireless and Optical Communications Networks (WOCN'08). IEEE, 2008.
[18] Ultra-wideband (UWB) technology enabling high-speed wireless personal area networks, Intel White Paper (2004)
[19] L. Yang, G. Giannakis, Ultra-wideband communications: an idea whose time has come. IEEE Signal Process. Mag. 21(6), 26–54 (2004)
[20] Jagannath, M., P. Amalendu, and M. V. Kartikeyan, Compact Antennas for High Data Rate Communication, 1st Edition, Springer Topics in Signal Processing, Vol. 14, 1–90, Springer, Berlin/Heidelberg, Germany, 2018.
[21] Robert J. Fontana, "A Brief History of UWB Communications," Multispectral Solutions, Inc., Kluwer Academic/Plenum Publishers, 2000. http://www.multispectral.com/history.html.
[22] Lecointre, A.; Dragomirescu, D.; Plana, R. IR-UWB channel capacity for analog and mostly digital implementation. In Proceedings of the International Semiconductor Conference, Sinaia, Romania, 13–15 October 2008; pp. 403–406.
[23] R.C. Qiu, H. Liu, X. Shen, Ultra-wideband for multiple access communications. IEEE Commun. Mag. 43(2), 80–87 (2005)
[24] Shams, N.; Kakhki, A.P.; Nabavi, M.; Nabki, F. An OOK and Binary FSK Reconfigurable Dual-Band Noncoherent IR-UWB Receiver Supporting Ternary Signaling. IEEE Trans. Very Large Scale Integr (VLSI) Syst. 2023, 31, 644–657.
[25] Wang, S.-F.; Xie, Y.-Z.; Qiu, Y.-X. A Kind of Tightly Coupled Array with Nonuniform Short-Circuited Branches for the Radiation of UWB Pulses. IEEE Trans. Antennas Propag. 2023, 71, 2259–2267.
[26] Niemelä, V.; Haapola, J.; Hämäläinen, M.; Iinatti, J. An Ultra Wideband Survey: Global Regulations and Impulse Radio Research Based on Standards. IEEE Commun. Surv. Tutor. 2017, 19, 874-890.
[27] Z. Zaichen and B. Guangguo, "On the analysis of UWB key technologies and development strategy," Journal of EEE, vol. 6, pp. 6–10, 2004.
[28] X. Chen, M. Fu, Z. Liu, C. Jia, and Y. Liu, "Harris hawks optimization algorithm and bp neural network for ultra-wideband indoor positioning," Mathematical Biosciences and Engineering, vol. 19, no. 9, pp. 9098–9124, 2022.
[29] Z. Zhao, Z. Lou, R. Wang, Q. Li, and X. Xu, "I-WKNN: Fast-speed and high-accuracy WIFI positioning for intelligent sports stadiums," Computers & Electrical Engineering, vol. 98, p. 107619, 2022.
[30] R. Wang, M. A. Kishk, and M.-S. Alouini, "Evaluating the accuracy of stochastic geometry based models for LEO satellite networks analysis," IEEE Communications Letters, vol. 26, no. 10, pp. 2440–2444, 2022.
[31] A. Subbarao and S. Raghavan, "A novel ultra-wideband planar antenna with rejection of WLAN and ITU bands," The Applied Computational Electromagnetics Society Journal (ACES), pp. 821–828, 2013.
[32] A. Alarifi, A. Al-Salman, M. Alsaleh, A. Alnafessah, S. Al-Hadhrami, M. A. Al-Ammar, and H. S. Al-Khalifa, "Ultra wideband indoor positioning technologies: Analysis and recent advances," Sensors, vol. 16, no. 5, p. 707, 2016.
[33] M. V. N. Katare, "Comparative analysis and interpretation of various short-range wireless technologies," International Journal of Scientific & Engineering Research, vol. 3, no. 8, pp. 775–779, 2012.
[34] M. Nabil Srifi, O. El Mrabet, F. Falcone, M. Sorolla, M. Essaaidi, A novel compact printed circular antenna for very ultra-wideband applications. Microw. Opt. Technol. Lett. 51(4), 1130–1133 (2009)

[35] K.H. Kim, Y.J. Cho, S.H. Hwang, S.O. Park, Band-notched UWB planar monopole antenna with two parasitic patches. Electron. Lett. 41(14), 786–788 (2005)
[36] Ghosh D, De A, Taylor MC, Sarkar TK, Wicks MC, Mokole EL. Transmission and reception by ultra-wideband (UWB) antennas. IEEE Antennas and Propagation Magazine. 2006;48(5):67–99.
[37] Galvan-Tejada GM, Peyrot-Solis MA, Aguilar HJ. Ultra-wideband antennas: design, methodologies, and performance. CRC Press; 2017.
[38] Z.N. Chen, X.H. Wu, H.F. Li, N. Yang, M.Y. Chia, Considerations for source pulses and antennas in UWB radio systems. IEEE Trans. Antennas Propag. 52(7), 1739–1748 (2004)
[39] I. Oppermann, M. Hamalainen, J. Iinatti, UWB theory and applications (Wiley, New Jersey, 2004)
[40] D.H.Kwon, Effect of antenna gain and group delay variations on pulse-preserving capabilities of ultrawideband antennas. IEEE Trans. Antennas Propag. 54(8), 2208–2215 (2006)
[41] D. Lamensdorf, L. Susman, Baseband-pulse-antenna techniques. IEEE Antennas Propag. Mag. 36(1), 20–30 (1994)
[42] G. Quintero, J.-F. Zurcher, A.K. Skriverviky, System fidelity factor: a new method for comparing UWB antennas. IEEE Trans. Antennas Propag. 59(7), 2502–2512 (2011)
[43] E.A. Akbari, M.-N. Azarmanesh, S. Soltam, Design of miniaturized band-notch ultrawideband monopole-slot antenna by modified half-mode substrate-integratedwaveguide. IET Microw. Antennas Propag. 7, 26–34 (2013)
[44] W.Wiesbeck,G.Adamiuk, C. Sturm, Basic properties and design principles ofUWBantennas. Proc. IEEE 97(2), 372–385 (2009)
[45] J. Liang, Antenna study and design for ultra-wideband communication, Ph.D. thesis, Queen Mary, University of London, UK (2006)
[46] Chen, W., Liu, Y., & Wang, J. (2021). An intelligent ultra-wideband antenna array using artificial intelligence. IEEE Transactions on Antennas and Propagation, 69(12), 6789-6797.
[47] Sarkar, D., Khan, T., Talukdar, F.A. et al. Computational intelligence paradigms for UWB antennas: a comprehensive review of analysis, synthesis and optimization. Artif Intell Rev 56, 655–684 (2023).
[48] Li, Y., Zhang, Y., & Yang, H. (2023). A compact and broadband antenna-in-package for ultra-wideband applications. IEEE Transactions on Antennas and Propagation, 71(1), 437-444.
[49] Kim, J., Lee, S., & Park, J. (2022). A fully integrated antenna-on-chip for ultra-wideband wireless communication. IEEE Transactions on Microwave Theory and Techniques, 70(12), 5678-5686.
[50] Thalakotuna, D.N., Esselle, K.P., Matekovits, L., Ranga, Y. (2024). Making UWB Antennas Unidirectional: Phase Coherence with an Ultra-Wide Band Frequency Selective Surface Reflector. In: Lakhtakia, A., Furse, C.M., Mackay, T.G. (eds) The Advancing World of Applied Electromagnetics. Springer, Cham.
[51] Kim, J., Lee, S., & Park, J. (2022). A reconfigurable ultra-wideband antenna using PIN diodes. IEEE Transactions on Antennas and Propagation, 70(6), 3210-3217.

CHAPTER III

Literature Review and State of the Art

Part Two:

5G Antennas

3.1 5G Antennas

3.1.1 Evolution of the G mobile networking technology

In 1819, Christian Oersted established the essential relationship between magnetism and electricity. This indicates that the search has officially commenced. Currently, the term "magnetic field" is familiar to the majority of individuals in our modern society. In 1832, Michael Faraday made a notable breakthrough in the generation of electricity by applying the principles of electromagnetic theory to his examination of this matter. Subsequently, in 1865 and 1873, James Clerk Maxwell delivered demonstrations to the scientific world. Maxwell's equations define the fundamental principles that will underpin the most significant technological advancements in many years. In 1895, Guglielmo Marconi became the first person to successfully transmit a radio telegraph signal over the English Channel. The incident sparked the initial development of radio communication. This work adds to the innovative research that other scientists conducted during the same period. AT&T Bell Labs advanced the voyage by conducting the first voice-over radio transmission in 1914 and the first long-distance TV broadcast in the US in 1927. Both of these accomplishments occurred in the US, and momentous events occurred. In 1935, Armstrong introduced the concept of frequency modulation (FM), which has since become a significant advancement in the field of communication. The mobile communications era commenced in 1980, and since then, wireless networking has gone through substantial transformations and witnessed tremendous expansion [1].

1G: The initial iteration of wireless telephone technology, took place in the 1980s, before the release of 2G digital telecommunications. NTT first introduced these systems in Japan in 1979 and subsequently extended them to Europe, enabling the provision of speech services through analog transmission. The main analog systems used were Nordic Mobile Telephones (NMT) and Total Access Communication Systems (TACS). Nevertheless, achieving interoperability across different countries was a significant issue. In 1982, the United States implemented the Advanced Mobile Phone System (AMPS) with 832 channels and a data rate of 10 kbps. AMPS employed directional antennas to enhance cell reuse, implementing a 7-cell reuse scheme. The device functioned within the frequency range of 800 to 900 MHz, with communications taking place over both forward and reverse channels. Both AMPS and TACS utilized frequency modulation (FM) and traffic multiplexing through FDMA (frequency division multiple access) [2].

2G: Second-generation mobile systems, which emerged in the late 1980s, provided digital multiple access technologies like TDMA and CDMA to offer low-bit-rate data and speech services. 2G systems offered greater spectrum efficiency, enhanced data services, and increased roaming capabilities in comparison to 1G. Europe adopted GSM as the standard, ensuring uninterrupted services across the continent. The Global System for Mobile Communications (GSM) underwent a gradual development process spanning twenty years, resulting in the emergence of 2.5G systems. In the United States, the IS-54, IS-136 (TDMA), and IS-95 (CDMA One) technologies were developed alongside the introduction of GSM-1900 into the market. Japan implemented the Personal Digital Cellular (PDC) system. GSM networks included Base Station Subsystems (BSS) and Network Switching Subsystems (NSS), which facilitated fundamental services and expansions to landline telephony networks. Second-generation systems incorporated base station controllers (BSCs) to reduce the workload on the mobile switching center (MSC), with a focus on promoting compatibility and standardization. Mobile-assisted handoff and services such as voice mail and Short Message Service (SMS) were included. GSM advanced with the introduction of GPRS, which allowed for packet-switching protocols and wireless internet access at speeds of up to 150 kbps. This development marked the transition to 2.5G. GPRS efficiently utilizes network resources by selectively allocating them for packet handling, enabling adaptable data transmission speeds, and maintaining uninterrupted network connectivity. This is a substantial advancement towards 3G. EDGE improves the data rates of GSM up to 384 kbps with only small modifications to the hardware and has the potential to reach 2 Mbps while operating alongside 3G WCDMA. While second-generation digital cellular networks remain the primary choice, a range of technoeconomic factors restrict the adoption of 3G systems [2].

3G: The implementation of EDGE technology facilitated the transfer of large amounts of data but maintained a circuit-switch-like operation, resulting in a decrease in efficiency. The emergence of 3G allowed for the creation of internationally standardized networks that are not dependent on specific technology platforms. UMTS in Europe and CDMA2000 in the US were implementations of the IMT-2000 standard set by the ITU [3]. 3G networks have extended their services to encompass wide-area wireless communication for voice, video calls, and high-speed internet access with HSPA capabilities that can achieve download speeds of up to 14.4 Mbps and upload speeds of up to 5.8 Mbps. Global commercial launches commenced in 2001 [4], first with NTT DoCoMo's FOMA in Japan and then expanding to South Korea, Europe,

the US, and Africa. The project's implementation was delayed due to the exorbitant fees associated with obtaining spectrum licenses and the need for equipment improvements. Certain nations, such as Indonesia, are still waiting to receive their licenses. In 2009, China introduced 3G technology, and key firms in the country picked different protocols. China Mobile chose TD-SCDMA, China Unicom chose WCDMA, and China Telecom chose CDMA2000. Despite facing obstacles, the implementation of 3G networks represented notable progress in the field of mobile telecommunications, allowing for improved services and faster data transmission rates on a global scale [2].

4G: The advent of fourth-generation mobile communication systems seeks to fulfill increasing user requirements by incorporating pre-existing technologies such as GSM, GPRS, IMT-2000, Wi-Fi, and Bluetooth [5]. Adopting an all-IP framework enables cost savings and facilitates faster data transport. 4G offers an improved user experience, increased capacity for multiple services, the ability to choose services freely, and cost-effective pricing. Commenced in 2010, 4G services are expected to become widely available to the general public by 2014–15. The ITU-R has established IMT-Advanced standards, which enable quicker data access, improved roaming capabilities, unified messaging, and broadband multimedia services. The United Nations' Millennium Development Goals align with the substantial socio-economic consequences of wireless broadband technology progress. The Third Generation Partnership Project (3GPP) and WiMAX Forum are now working on the development of LTE-Advanced and WiMAX-m, respectively, in order to fulfill the requirements of 4G technology. This progression signifies a transition towards more rapid and comprehensive mobile communication technologies [2].

5G: Fifth generation represents the next advancement in the progression of mobile communications. The purpose of its design was to enhance data transfer rates, reduce latency, and enhance dependability in comparison to prior iterations. This advancement facilitates new applications and revolutionizes several industries. 5G networks have the capability to accommodate a significantly higher number of devices compared to earlier generations. Additionally, they are capable of handling more data-intensive applications such as virtual and augmented reality, driverless vehicles, and the Internet of Things (IoT). The advent of 5G has brought out a plethora of novel advancements and prospects across diverse industry sectors like healthcare, manufacturing, transportation, and entertainment. 5G is a significant catalyst for technologies like edge computing and artificial intelligence. The expansion and

advancement of 5G technology is ongoing as Mobile Service Providers (MSPs) worldwide are implementing their 5G networks. It will be fascinating to witness the emergence of new applications and possibilities that 5G provides in the 2020s.

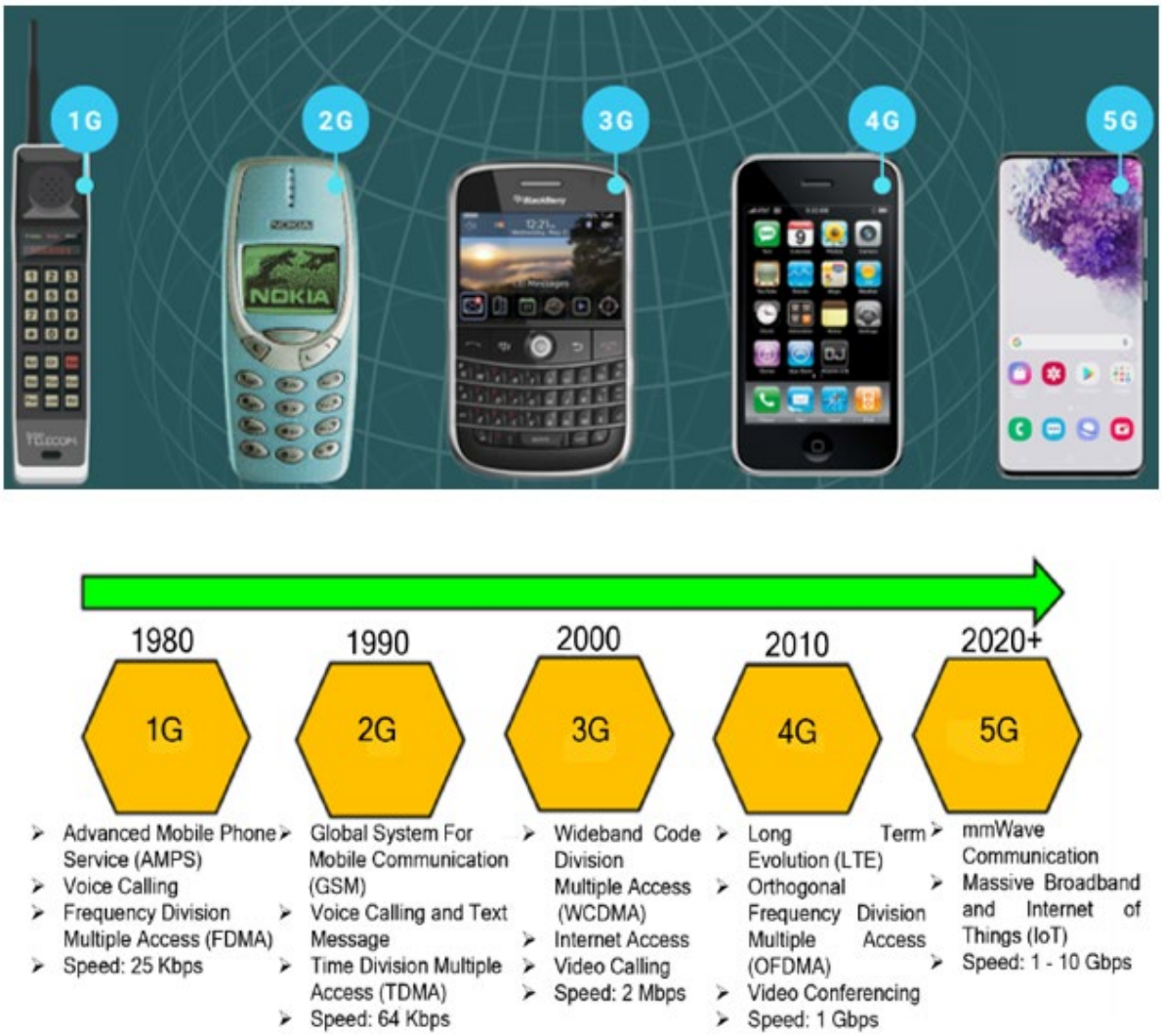

Figure 3.1. Evolution of Wireless Connectivity from 1G to 5G.

3.1.2 Fifth-generation wireless communications network (5G)

5G is expected to provide quicker and more reliable wireless connectivity, reduced latency, and increased network capacity compared to previous generations. Experts have confirmed the widely recognized potential of this technology to transform various industries, including medical care, entertainment, and public transportation [6].

Two significant bands, millimeter wave (MMW) and sub-6 GHz, serve as the foundation for 5G technology. The sub-6 GHz frequency spectrum offers an extended range,

wider coverage, and enhanced obstacle-piercing capabilities. Nevertheless, it provides reduced velocity and capacity. Conversely, the MMW frequency spectrum offers fast data transmission, large data capacity, and minimal delay, but it has a limited range and is vulnerable to obstructions [7]. 5G technology provides a multitude of benefits compared to previous wireless technologies. Increased download and upload speeds, expanded network capacity, and reduced latency facilitate the development of novel applications in areas such as improved wireless broadband, IoT, and vital communications.

Implementing 5G technology is complex. A major hindrance is the absence of adequate infrastructure. The utilization of the MMW frequency range requires a more concentrated network of tiny cells and antennas to ensure adequate coverage and capacity, which in turn requires substantial expenditures in infrastructure and technology. Moreover, the limited coverage of the MMW frequency band poses difficulties in implementing it in rural regions [8]. Another obstacle is the protection and confidentiality of data carried across 5G systems. 5G networks are more susceptible to cyberattacks due to their improved connections and higher data transfer rates. Hence, it is imperative to implement strong security and privacy measures in order to safeguard sensitive data [9].

5G offers substantial benefits compared to 4G in mobile connectivity [10]. Expected to be up to 100 times faster than 4G, 5G is a novel worldwide wireless standard. Unlike 4G, 5G technology extends beyond cellular phones and laptops. According to Ericsson's assertion, the implementation of 5G technology would revolutionize various industries and greatly enhance everyday tasks [11]. When compared to earlier generations, 5G offers greater advantages in terms of channel access methods for accommodating multiple users. It is capable of supporting both Code-Division Multiple Access (CDMA), which is used in 3G and 4G networks, and Beam-Division Multiple Access (BDMA), which allows for simultaneous data transfer to several users via distinct antenna beams from the base station. 5G has a superiority over 4G in terms of reduced latency, which refers to the duration it takes for data to move between two points. Applications such as video games, augmented and virtual realities, and remote surgery require low latency. 5G has the capability to significantly decrease latency to as little as one millisecond, whereas 4G generally exhibits a latency of over 50 milliseconds. The decreased latency facilitates instantaneous communication between gadgets, a crucial requirement for applications like driverless vehicles or industrial automation systems [12, 13]. Furthermore, 5G has the capacity to accommodate a substantially higher number of connected gadgets per

square kilometer in comparison to 4G. 5G has the capability to link up to one million devices, whereas 4G can only accommodate up to 100,000 devices. This enhanced capability is especially advantageous in wireless scenarios with a large number of devices, like at a mall or workplace [14].

Ultimately, 5G functions at elevated frequencies compared to 4G, which allows for the transmission of a greater volume of data within a reduced timeframe. Nevertheless, the increased frequency of 5G also leads to a reduced range compared to 4G, making it more susceptible to obstruction by structures such as trees and buildings. However, this feature can be beneficial in mobile connectivity since it enables more accurate and focused interaction among devices and enhances security in point-to-point connections [15, 16].

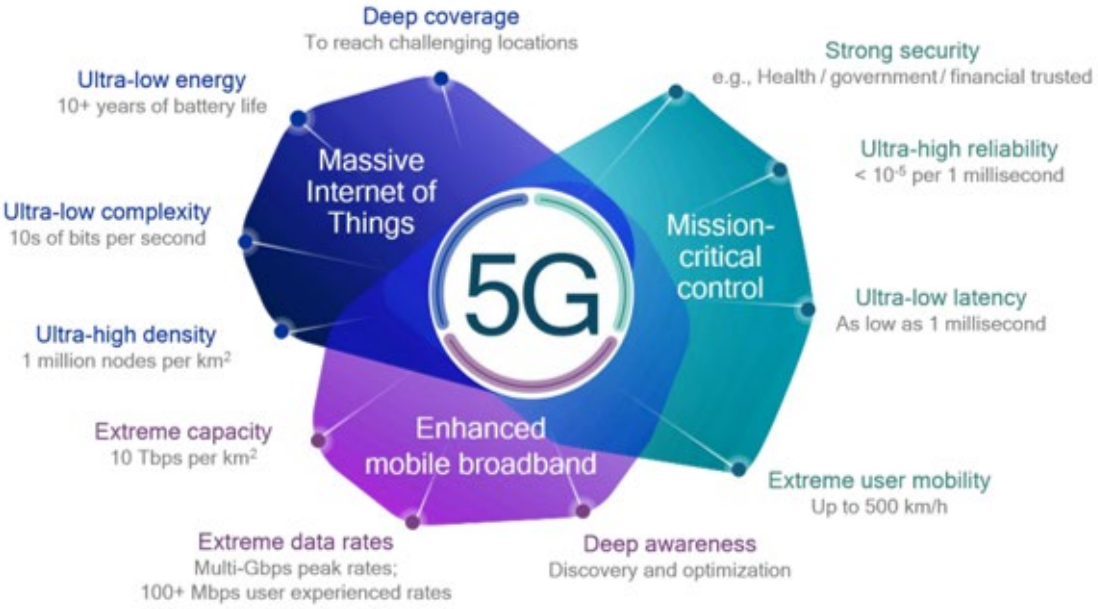

Figure 3.2. 5G capability to expand and adjust to a diverse set of requirements [17].

3.1.3 5G standardization and spectrum allocation

The shift to mm-waves in the electromagnetic spectrum offers several benefits, including shorter wavelengths that enable smaller antenna sizes, unoccupied bandwidth that can be utilized to improve channel width, broadband spread-spectrum capacity that reduces multipath, and accessibility to high-attenuation bands for safe point-to-point connectivity [18, 19]. The primary factors to take into account when designing the 5G standardization framework, the primary factors to consider include addressing capacity-related challenges,

ensuring compatibility with high-speed short-range interactions, handling path loss constraints, enhancing security, improving connection, and reducing latency. Global regulatory agencies are highly interested in a spectrum assignment that reduces transmission losses and attenuations. Multiple architectural concepts have been proposed, advocating for the use of millimeter waves as the future of 5G network connectivity [20]. The International Telecommunication Union's (ITU) primary mandate is to provide protocols for harmonized communications, facilitating the seamless integration of technological devices and networks worldwide and ensuring the unrestricted availability of communications services. In terms of IMT technologies, the ITU governs every component of the radio network. The ITU is responsible for ensuring consistency and standardization of frequency band specifications for mobile communication systems. This is done to facilitate compatibility and seamless operation between existing and upcoming technologies across different platforms. The International Telecommunication Union is responsible for supervising, evaluating, and formulating the specifications for the 5G standard [21]. The ITU Radio rules delineate the spectrum allocations that ITU-R has been diligently developing for many services and apps. IMT technologies now occupy multiple spectrums. While some preferences have yet to be defined, it is theoretically possible to operate 5G across all of the designated frequency bands. The United States is inclined to utilize the 3.5 GHz (3550–3700 MHz) common band as well as the 600 MHz authorized spectrum (617–652/663–698 MHz). For 5G, Europe has selected the 700 MHz band (694–790 MHz) as a radio band below 1 GHz. However, the primary and innovative spectrum for fifth-generation must fall in the range of 3.4–3.8 GHz. In order to increase the number of transmissions, there is a proposal to include the 1.5 GHz bandwidth (1427–1452/1492–1518 MHz) [22, 23]. Other countries are now exploring the most effective frequency range to implement their 5G networks. Japan is now assessing the suitability of the frequency ranges 3600–4200 MHz and 4400–4900 MHz for the purpose of evaluating and implementing 5G technology. Nigeria is currently evaluating the 3500 MHz and 26,000 MHz frequency ranges, and China is examining the 3300–3600 MHz and 4800–4990 MHz ranges [24,25,26]. Given the continuous growth in data usage, additional spectrum assets are necessary to sustain future wireless communication networks. Moreover, it is important to keep in mind that each country will have distinct requirements for its domestic frequency range. The 5G standard divides the radio band spectrum into two distinct regions called FR1 and FR2.

3.1.3.1 FR1

5G mobile communications use the lower frequency band known as FR1. This band covers the frequency range between 410 MHz and 7.125 GHz, sometimes referred to as the sub-6 GHz spectrum. Despite not significantly outperforming 4G's FR1 at 2.5 to 2.69 GHz, 5G offers significantly faster connectivity due to its wider bandwidth of approximately 6.5 GHz. As the number of wireless links increases, the signal's reach decreases and the connection rate rises. This frequency band offers an advantageous equilibrium of coverage and capacity, making it suitable across rural as well as urban locations [27].

Some of the main benefits of 5G FR1 include its ability to use sophisticated techniques such as beamforming and massive MIMO. It is particularly advantageous in highly populated metropolitan regions where structures and other barriers may block or bounce back radio frequencies.

3.1.3.2 FR2

The FR2 spectrum encompasses frequencies ranging from 24.25 GHz to 71.0 GHz. It functions at a higher frequency than the FR1, resulting in a greater bandwidth but a narrower range [28]. The initial sub-band, n257, functions within the band of 26.5 GHz to 29.5 GHz and is especially advantageous in highly populated regions, like metropolitan areas, since it enables high-capacity connectivity. Additionally, it is well-suited for facilitating high-rate wireless broadband offerings, such as broadcasting 4K content and utilizing virtual reality apps. The n258 sub-band operates within the 24.25 GHz to 27.5 GHz range. Interior applications specifically design it to provide high-bandwidth, low-latency communications. This specific frequency range is very beneficial in smart houses, as it enables the quick transmission of substantial amounts of data across equipment. The third sub-band, n260, works within the spectrum of 37 GHz to 40 GHz and possesses a broader band compared to the other sub-bands in FR2. This feature makes it highly suitable for apps that necessitate extremely fast data transfer, such as AR and 8K resolution video sharing. Nevertheless, because of its limited range and increased vulnerability to interference, it is better suited for outdoor applications. The fourth and last sub-band, n261, functions within the spectrum of 27.5 GHz to 28.35 GHz and exhibits notable efficacy in compact interior spaces, like workplaces or residences. It offers fast and reliable communications with minimal delay, making it ideal for apps that demand low latency, including gaming and VR [28].

Table 3.1. Allocation of 5G frequency bands [29].

Classification	General Classification	5G Frequency Band	Sample Application	Comments
Low-band	Below 1 GHz	600 MHz, 700 MHz	Broadcast TV	Spectrum at the lower band (below 1 GHz) is ultimate for deploying 5G coverage and enabling IoT services in urban, suburban, and rural areas.
Mid-band	Above 2 GHz	2300 MHz, 2600 MHz, 3300–3800 MHz, 3800–4200 MHz, 4400–4900 MHz	Fixed satellite, fixed service (point-to-point, point-to-multipoint)	The 3.5 GHz frequency of the mid-band spectrum provides an excellent balance of capacity and coverage.
High-band	Above 6 GHz	26 GHz (24.25–27.5 GHz), 28 GHz (27.5–29.5 GHz), 37–43.5 GHz, 45.5–47 GHz, 47.2–48.2 GHz, 66–71 GHz	Satellite service, space research, earth exploration	High-band spectrum is ideal for ultra-high-speed, short-range applications that require low latency (such as at 26 and 40 GHz).

Figure 3.3. 5G Spectrum.

3.1.4 5G Applications

Today, 5G technology facilitates a diverse array of applications that elevate the user experience to an unprecedented level in the realm of mobile communication. Some applications are mentioned here.

- Adoption of AI: Prominent corporations possessing extensive data will need to employ AI to efficiently analyze their voluminous information, and the implementation of 5G technology will undoubtedly expedite these operations. Moreover, in the context of smart cities, the transmission of data from newly installed sensors is essential to ensuring their timely deployment. There is a strong need for cellular sensors in many applications, such as metering, traffic and parking monitoring, city lighting, and other purposes.

- Applications in the Agriculture Sector: Although the most ancient industry in business, the agricultural industry of every nation will also see significant advantages from 5G services. Enhancing the industry's security would entail the installation of surveillance sensors and the provision of essential crop information, including water requirements, pest control, preventing illnesses, and other factors that contribute to the prompt and proper development of agricultural products. Furthermore, 5G Internet of Things (IoT) devices can conveniently and remotely track the well-being of livestock, including cows and sheep.

- Self-driving Vehicles: In the present era of 5G, individuals will have the chance to operate autonomous cars, which is a novel technological advancement. Only the implementation of 5G technology, which offers high speed and minimal latency services, can achieve these benefits. An important usage of self-driving cars is the Vehicle-to-Everything (V2X) system, which enables 5G customers to link their automobiles with a variety of equipment.

- In the realm of multimedia and entertainment, the act of streaming videos constitutes the major part of the total wireless web traffic. Undoubtedly, future advancements will increase this tendency, resulting in a more extensive dissemination of video streaming. 5G technology will enable high-speed 4K video downloading and unmistakable audio, allowing handheld devices to create a high-definition virtual world. 5G's low-latency and high-resolution broadcast will greatly simplify the deployment of VR and AR in the years to come.

- The provision of advanced medical services is crucial for the functioning of vital applications in the healthcare sector. Consequently, all classes are able to establish connections

using 5G networks. Participating in classes and conferences will be easier. Using 5G technology platforms, patients can now seek virtual consultations with doctors for counseling. Intelligent Medical serves as a scientific tool to support individuals grappling with chronic illnesses. 5G networks allow the medical field to use smart gadgets, medical internet, advanced sensors, high-definition imaging devices, and smart analytic tools. Utilizing 5G technology enables convenient global access to cloud storage and medical information.

- Smart Homes: The current demand for intelligent house devices and technology is significant. The 5G network enables rapid communication and facilitates smart appliance surveillance, advancing the realization of smart houses. The 5G network's highly efficient, low-latency connectivity allows for easy access and installation of smart home goods from remote areas.

- Utilizing drones for Internet of Things applications: Drones capture stunning aerial images from multiple perspectives. They are also crucial for conducting security inspections of the environment. By utilizing drone services enabled by 5G technology, individuals can obtain high-quality images and videos that are suitable for security, monitoring, and various filmmaking needs.

- Satellite services: The lack of ground-based stations (BS) significantly restricts connectivity in remote areas. The implementation of 5G technology will involve the deployment of satellite systems, which will offer network services and guarantee uninterrupted access in remote areas through a constellation of multiple small satellites.

- The introduction of 5G will bring about a significant revolution in the realm of augmented and virtual reality (AR and VR), particularly in this area. This is due to the specific development of 5G, which boasts exceptional characteristics designed to enhance high-definition gaming experiences. Moreover, virtual reality has surfaced as the most recent advancement in the technology industry. As 5G connectivity technology advances, VR and its variations will inevitably become more prominent. In addition to gaming, the implementation of 5G technology will enable individuals to partake in virtual reality experiences and attend sporting events remotely.

- The upcoming 5G wireless network technology, provides extremely rapid download speeds ranging from 10 to 20 Gbps. The 5G system operates in a manner very similar to that of a broadband fiber-optic link. Unlike previous mobile communication devices, 5G efficiently

provides both high-speed data transfer and voice communication. 5G's connectivity latency of less than one millisecond is highly advantageous for essential and autonomous vehicular applications. 5G technology utilizes millimeter waves to transmit data, offering significantly greater capacity and data speed compared to lower-frequency LTE bands.

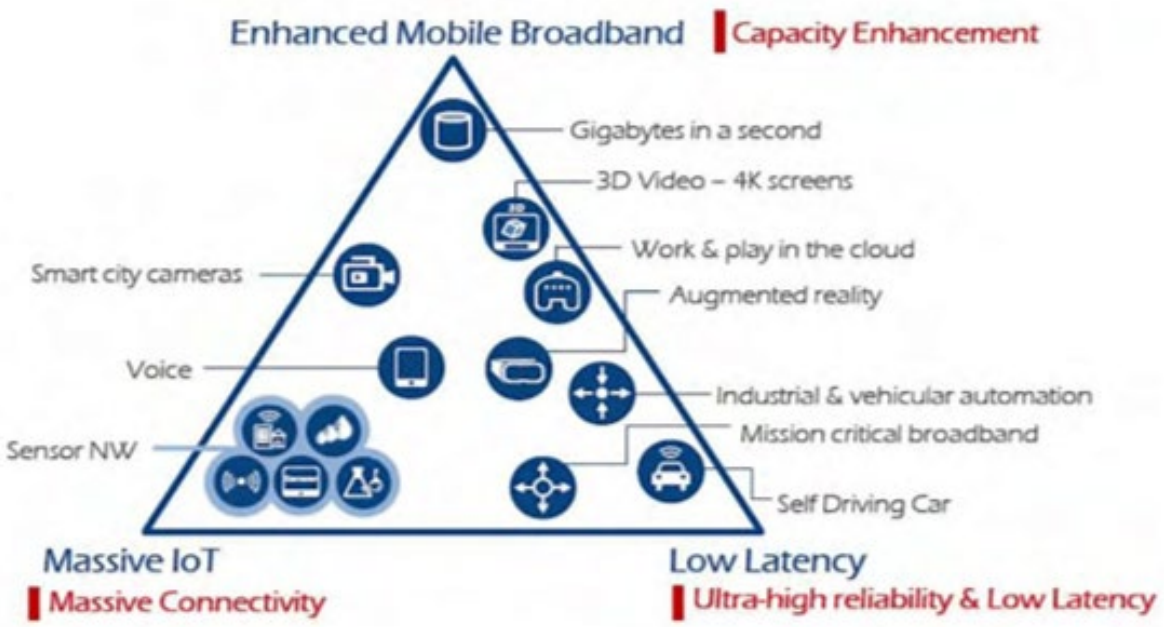

Figure 3.4. Some 5G applications [30].

3.1.5 Comparison with previous generations

The development of mobile communications has made significant progress since the inception of the initial generation (1G) in the 1980s. It has facilitated continuous connectivity regardless of our location, be it at home, at work, or while traveling. Each successive generation of mobile phone technology, from 1G to 5G, has exhibited advancements that have enabled us to achieve higher levels of productivity, speed, and efficiency. While evaluating cell networks, there are numerous aspects to consider. Table 2 presents a comparison between 5G and preceding generations.

The advent of 1G introduced the initial cellular networks, which offered fundamental analog voice services. Shortly after, the implementation of 2G introduced text messages, digital voice services, and data services, including image messaging. 3G and 4G networks have significantly enhanced data rates and services, enabling customers to effortlessly connect to the internet, effortlessly stream videos and audio files, and effortlessly utilize complex

applications. 5G is the latest generation that offers quicker speeds and enhanced stability. The comparison clearly highlights the disparities in the technologies and definitely demonstrates that their potential is seemingly boundless.

Table 3.2. A comparison of mobile technology from the first to the fifth generation. [29].

Generation	1G	2G	2.5G	3G	3.5G	4G	5G
Access Technology	FDMA, AMPS	GSM, TDMA, CDMA	GPRS, EDGE, CDMA 2000	WCDMA, UMTS, CDMA 2000, HSUPA/HSDPA	HSPA, EVDO	LTEA, OFDMA, SCFDMA, WiMAX	BDMA, NOMA FBMC
Switching Techniques	Circuit Switching	Circuit Switching	Circuit Switching	Circuit and Packet Switching	Packet Switching	Packet Switching	Packet Switching
Error-Correction Mechanism	-	-	-	Turbo Codes	Concatenated Codes	Turbo Codes	LDPC
Data Rate	2.4 kbps	10 kbps	144 kbps	384 kbps to 5 Mbps	5 Mbps to 30 Mbps	100 Mbps to 200 Mbps	10 Gbps to 50 Gbps
Frequency Band	800 MHz	800 MHz, 900 MHz, 1800 MHz, 1900 MHz	850 MHz, 900 MHz, 1800 MHz, 1900 MHz	800 MHz, 900 MHz, 1800 MHz, 1900 MHz 2100 MHz	800 MHz, 850 MHz, 900 MHz, 1800 MHz 1900 MHz, 2100 MHz	2.3 GHz, 2.5 GHz, and 3.5 GHz initially	1.8 GHz, 2.6 GHz, and 30–300 GHz
Bandwidth	30 kHz	200 kHz	200 kHz		5 MHz	3.5 MHz, 5 MHz, 7 MHz, 8.75 MHz, and 10 MHz	FR1 (100 MHz) FR2 (400 MHz)
Application	Voice	Voice and Data		5 MHz		Voice, Data, Video calling, HD Television, etc.	Voice, Data, Video calling, Ultra HD video, VR application
Description	Voice conversation	Messaging and Improved data services	-	Voice, Data, and Video calling	-	Voice and Data over fast broadband Internet	Improvement of broadband services to allow IoT and V2X.
Deployment	1980	1990	2000	Surfing the Internet and Introduction of mobile applications	2006	2010	2020
Core Network	PSTN	PSTN and Packet	Packet Network	2001	Internet	Internet	Internet
Security	Poor	Good		Internet			
Handoff	Horizontal	Horizontal	Horizontal/ Vertical		Horizontal/ Vertical	Horizontal/ Vertical	Horizontal/ Vertical
Advantages	Mobility	Security, Mass adoption, Longer battery life	Security, Mass adoption, Longer battery life	Horizontal/Vertical	Better Internet experience	High data rate and Wearable devices	Wider coverage, Improved speed, Fast handover, and Very low latency.
Disadvantages	Poor spectral efficiency and Poor handoff	Low data rate and Low capacity	Slight increase in the data rate	Better Internet experience		Expensive	
				Failure of performance for Internet			

3.1.6 5G in Antenna and Propagation

The 5G studies have placed significant emphasis on antennas, which are the central component of wireless networks. Innovative methods have been devised to elevate the performance of 5G antennas to an advanced degree. For example, a metamaterial is expected to have significant promise, particularly in antenna design, because of its ability to manipulate electromagnetic waves and provide control over them. Metamaterial-based antennas have several advantageous characteristics, including size reduction, increased bandwidth, and improved signal amplification, which can greatly benefit modern 5G connections [31]. UWB antennas are necessary in these connections in order to increase the channel width, resulting in greater efficiency and higher data transmission speeds. Furthermore, the use of UWB antennas in a MIMO arrangement can greatly enhance spatial variety at the antenna front ends, allowing for concurrent multiple-channel connection [32].

The development of wireless transceivers has seen significant interest in the use of an entirely integrated system-on-chip (SoC) method, which offers numerous significant benefits. Some of those benefits encompass reduced complexity, affordability, miniaturization/compactness, and reduced power consumption for the embedded wireless components. The SoC-based wireless system proposes a close-knit combination of the antenna, radio frequency, analog, and digital components on a single substrate, consequently eliminating lossy linkages. The shorter wavelength at millimeter waves enables the antenna to decrease in size, making it possible to integrate it onto a chip. The antenna used in this technology is called an antenna-on-chip, and it provides numerous benefits compared to traditional off-chip antennas [32]. For example, (1) improving the impedance matching control across the antenna and the radio frequency front-end parts enables the use of conjugate matching methods to achieve improved system optimization, (2) reducing the power needs of the system, (3) creating smaller integrated circuits with simpler packaging, and (4) providing design flexibility, particularly in regarding antenna layout [33].

A major obstacle in utilizing mm-wave technology is the substantial freespace route loss, which greatly diminishes the signal power when encountering obstacles or over lengthy transmitting distances. Compact massive MIMO antennas are considered an intelligent solution since they achieve higher gain by incorporating more radiating parts to offset the loss of mm-wave signals. Moreover, it is possible to create specialized high-gain antenna arrays that have been fitted with a phasing network, allowing for the adjustment of the signal phase for every

single antenna using phase shifters. Those phased arrays consist of a highly focused radiation pattern and are equipped with an automated phase shifting device for obtaining beamforming. The beamforming gain is directly related to the overall dimensions and size of the antenna arrangement which is advantageous because of the compact nature of the mm-wave massive MIMO [34]. From the standpoint of 5G system viewpoints, the implementation of MIMO techniques, such as beamforming, can significantly enhance the dependability of transmission and offer increased data speeds. It is anticipated that the use of mm-waves at the transceiver would result in an increased amount of antenna elements in a small space. This boost in antenna elements is predicted to provide stronger variety and multiplexing gains, and the channel matrix is likely to have favorable characteristics. Depending on the system specifications, beamformers can be built using analog methods, digital, or hybrid techniques [35]. Furthermore, a reflect array consists of a collection of antennas that are lit by a feed and have the capability to generate a concentrated beam by adjusting the phasing. The reflect array functions similarly to a phased array antenna, however it lacks the need for a power divider or extra phase shifters. It incorporates the benefits of both reflector antennas and phased arrays, such as an easier layout and lower power consumption. This makes it a cost-effective option for 5G systems [36,37].

3.1.7 Key characteristics of 5G antennas

5G antennas are required to have the capability to adjust their beam coverage based on the specific application situations and distribution of user device. In order to achieve beam control and accurate coverage in the desired area while effectively suppressing interference in undesired areas, it is essential for 5G antennas to operate in conjunction with the Radio Access Network (RAN). Hence, it is imperative that 5G antennas provide flexibility to accommodate various band arrangements and adaptable beam control [4,5]. Furthermore, in order to achieve high data rates and effectively handle the capacity and movement of 5G traffic, the 5G antenna must fulfill the following requirements:

- It should be able to operate in both the sub-6 GHz frequency band and the mm-wave 5G allocated frequencies, like 28 and 39 GHz.

- Adaptive beamforming techniques should be employed to put the antenna's focus in the wanted area, thereby minimizing interference and maximizing data rates.

In order to meet the demands of high spectrum and power efficiency, and connecting density, 5G antennas must be capable of supporting the following:

- Multiuser beamforming is a technique that involves the simultaneous transmission of multiple signals to many users using a single antenna array. This will enable the adaptive beam to utilize frequency and time assets, resulting in an enhanced system performance in general. Nevertheless, the negative impact of resource sharing can be reduced by implementing null directional control in advanced antenna system (AAS).

- Adaptive beamforming facilitates accurate pattern manipulation in AAS, allowing for the concentration of radiated energy in a specific location to enhance power efficiency.

The user did not provide any text. In order to maximize the density of connections, it is crucial to reduce losses in antenna elements and RF links, ensuring the identical amount of radiation energy can provide extensive and comprehensive coverage.

In order to optimize the strength of the transmitted signal and improve the signal quality by minimizing interference and noise, it is crucial to employ beamforming methods in 5G antennas. This technology allows for the creation of narrow beams with the proper width and directionality. Figure 3.5 illustrates the beamforming method used in 5G antennas, which involves the precise movement of a narrow beam throughout a specific region. This movement ensures that there are no gaps in coverage and minimizes any unnecessary overlap. In addition, in order to generate a focused beam that covers a wide range of angles and allows for beam steering, massive antenna arrays are split into smaller sub arrays, with two separate chains used for each sub array.

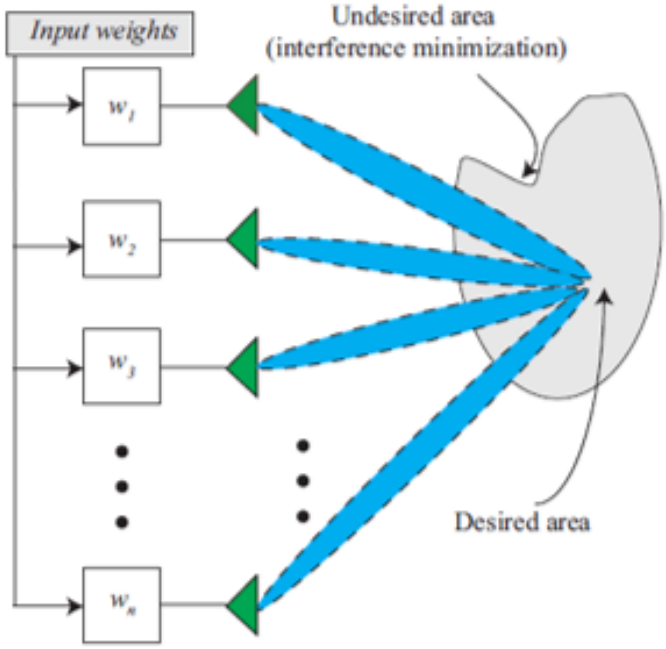

Figure 3.5. A depiction of the beamforming concept used in 5G antennas [32]

Figure 3.6 illustrates the situation where antennas are arranged in a rectangular form and a sub-array consists of two antennas. Increasing the amount of antenna subarrays would lead to a more focused and concentrated beam [32].

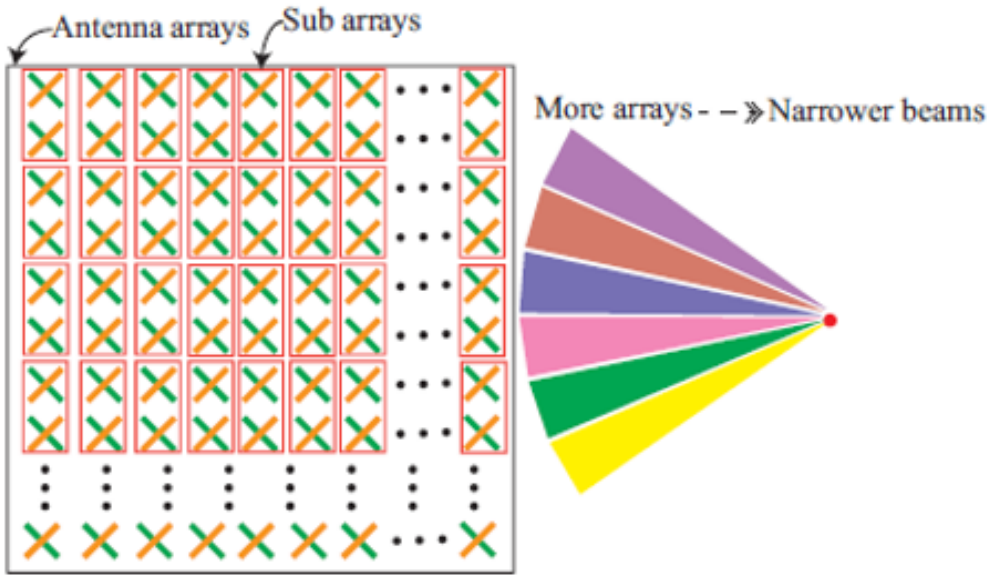

Figure 3.6. The use of a narrower directional beamforming of an antenna array and its sub arrays in the context of 5G technology [32].

The fifth-generation antenna system must be capable of supporting MU beamforming towards multiple User Equipment (UE) while accurately null steering towards other UEs. Figure 3.7 illustrates a potential situation of MU beamforming, where 4 aimed beams are precisely catering to four customers inside the coverage region of their corresponding base stations, and the null-steering effect, which is a necessary characteristic of 5G antenna design. MU beamforming is crucial for achieving precise coverage of 5G broadcasting and traffic beams. High-precision beamforming, alongside adaptive null steering, is seen as an essential requirement for 5G antenna arrays. In addition to MU beamforming and adaptive null steering, 5G antennas shall also enable beam visibility and network connectivity center control as achievable characteristics. The network should autonomously detect situations and beam arrangement using AI algorithms combined with 5G antennas.

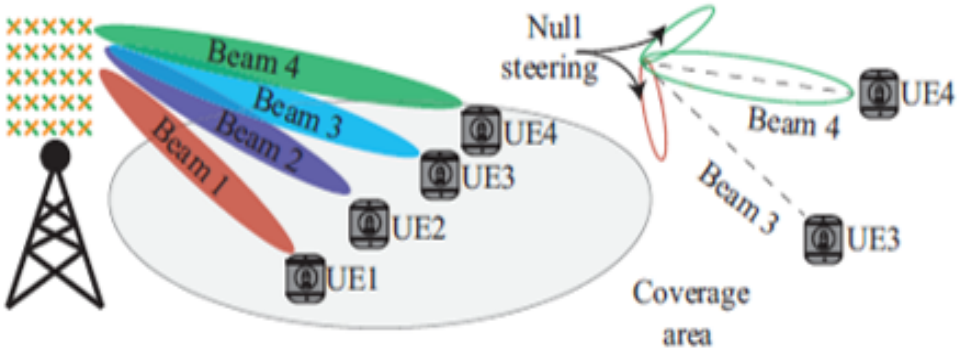

Figure 3.7. Multi-user beamforming and null steering techniques are employed in 5G networks to achieve precise coverage [32].

Figure 3.8 depicts an example showcasing the visibility of a beam in several circumstances, including dwellings, high-rise buildings, and roadways. Where the roadways necessitate directed beams, while tall buildings demand wide vertical beams. The antenna array topologies for 5G must possess the capability to modify the azimuth and elevation beamwidth, which can be managed by the network management center. This would contribute to enhancing the efficiency of the 5G network.

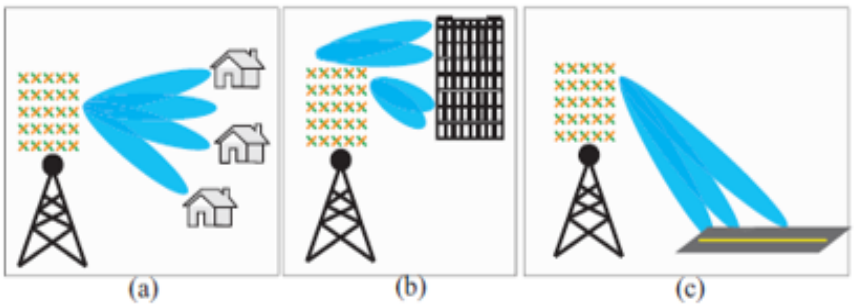

Figure 3.8. The three coverage situations of beam visibility: (a) dwellings or low-rise coverage, (b) vertical beam for high-rise coverage, and (c) narrow and aimed beam for roadways and walkways [32].

Figure 3.9 depicts a visual representation of beam adjustment. In order to prevent disruptions in the 5G network, it is necessary for 5G antennas to possess the capability to intelligently deactivate specific channels by adjusting the activation levels of the individual antenna components. This would additionally contribute to enhancing network coverage by considering the density of User Equipment (UE).

Figure 3.9. Beam alignment in a 5G antenna array [32].

3.1.8 5G Antenna Design Considerations

The 5G mobile communication significantly differs from previous networking standards. In the past, antennas were mostly constructed for frequencies below 3 GHz. However, for 5G networks, the bands that are most useful are those above 3 GHz, specifically the mm-Wave bands. Antennas utilized in 5G transceivers are required to provide a secure wireless connection that ensures dependable transmission, capable of handling speeds of gigabits per second (Gbps) [38]. The primary design considerations for a 5G antenna are as follows.

3.1.8.1 Frequency Range:

The antenna must be capable of covering a wide range of frequencies in order to support existing and upcoming cellular communication protocols. This requires having multiband features to span various microwave and mm-Wave frequency bands [39]. The microwave and mm-Wave band are both applicable in 5G for indoor micro cellular connectivity and MIMO applications. This can be achieved by utilizing a common aperture multi band microstrip antenna array [40]. A broad frequency range is necessary, with a reflection coefficient below -10 dB, and minimal variation in both gain and side lobe magnitude across the full operational spectrum.

3.1.8.2 Antenna Size:

In order to achieve optimal radiation efficiency and reduce the amount of energy stored in the nearby areas, it is recommended that the dimensions of every antenna should be no larger than a quarter of the wavelength that is steered. The thickness of a cell phone PCB is frequently less than 1 mm [38]. Increasing the thickness of the printed circuit board (PCB) in electronic products results in higher manufacturing costs. The free space wavelength at a frequency of 28 GHz measures about 10.71 mm. It limits the ability to adjust the direction of the beam in the vertical plane. Utilizing fan beams effectively resolves this issue.

3.1.8.3 Radiation Pattern:

The antenna of a cell phone faces challenges in accurately determining the angle from which signals arrive, due to the phone's mobility. As a result, an omnidirectional radiation pattern was selected for 3G/4G mobile phones, with a gain ranging from -8dB to 0 dBi [41, 42]. In scenarios where users are evenly distributed across extensive spaces, like auditoriums and shopping malls, it is necessary to have radiation patterns that cover all directions

horizontally and have focused radiation patterns vertically in order to conserve power [43]. However, due to the significant signal deterioration at mm-Wave frequencies, it is preferable to have antennas with exceptionally high gain and narrow primary lobe radiation at every angle within the hemisphere. Therefore, for 5G cellular phone antennas and base stations, a steerable narrow beam pattern is wanted [38, 44, 45, 46]. Covering the entire region employing a steerable narrow beam directional phased array antenna is far more difficult than employing an omnidirectional antenna [42]. At millimeter-wave frequencies, the wavelength is tiny, resulting in difficulties with diffraction around barriers [38, 45, 47]. Obstacles cause absorption, which leads to a decrease in the propagation of signals in a direct line-of-sight. Additionally, non-line-of-sight propagation is affected by high attenuation and minimal multipath connectivity. mm-Wave technology has challenges in its ability to penetrate solid objects [3]. The multipath delay spread is greater in densely populated urban areas due to the presence of highly reflecting surfaces. To mitigate the effects of small-scale fading and shadowing at millimeter-wave frequencies, a highly directional and high-gain steerable antenna is necessary [44, 48, 49]. A symmetrical radiation pattern is desired for space scanning in both planes [45]. The endfire fan beam is favored over the broadside array for 5G mobile phones [50].

3.1.8.4 Beamwidth:

When employing 1D beam steering, a greater beamwidth is necessary in the elevation plane, while a narrower beamwidth is required in the azimuth plane. This form of beam is sometimes referred to as a fan beam [51, 52]. The fan beam is predominantly favored in cellular phones. In order to achieve 2D beam steering, it is necessary to have a low beamwidth in both planes. This specific type of beam, known as a pencil beam, is favored at base stations [38, 53].

3.1.8.5 Placement of the antenna in a mobile device:

is important for its performance. While cellular antennas are often developed and tested in free space, it is crucial to take into account the physical conditions while analyzing their performance in a mobile phone. The presence of a highly conductive metallic surface in the body of a mobile phone affects the radiation properties of the antenna. The cell phone contains an LCD, batteries, cameras, microphone, and other sensors [38]. The upper and lower portions of the cellphone are designated for 4G LTE antennas, GPS, Wi-Fi, and antennas for various apps. Therefore, the left and right edges are the appropriate locations for the 5G antenna [54]. In modern times, the majority of cellphones are equipped with a completely metallic housing. Therefore, the antenna design must be able to function well under these circumstances. The

optimal position must be selected to minimize the impact on the radiation characteristics of the antenna. The antenna should be positioned on the PCB beside the radio-frequency integrated circuit (RFIC) in a certain manner to minimize the insertion loss among them, as indicated by previous research [45,50,52,55]. The scanning area of the array is constrained by the diffraction and refraction effects generated by the cell device frame, LCD panel, and other components. Research presented in articles [52,56] indicates that the human body absorbs near 95% of the radiation that enters at mm-Wave frequencies. Users experience a reduction in gain of 9.5 dB when they totally cover the antenna array area with their hands. For optimal performance, it is recommended to deploy MIMO antennas both at the highest and lowest points of the structure.

3.1.8.6 Side Lobe Levels:

To achieve optimal scanning, the side lobe levels in the radiation pattern must be below -10 dB for all beam scan angles. Additionally, when the primary beam is scanned at various angles, the loss in scanning must be minimal. Controlling the direction of a high gain antenna across a large range of angles in two dimensions without affecting its directivity, beamwidth, and lowest side lobe levels is a highly difficult task [57].

3.1.8.7 Specific Absorption Rate (SAR):

is a crucial metric for 5G mobile antennas as it quantifies the amount of electromagnetic energy absorbed by the human body in terms of mass. It is imperative to adhere to the regulations set forth by the Federal Communications Commission. The maximum allowable value for specific absorption rate (SAR) in the human body, as stated by IEEE/ANSI/FCC [58], is 1.6 W/kg for a mass of 1g.

3.1.9 5G Antenna Design Challenges

5G deployment is imminent, utilizing systems that operate at mm-Wave frequencies to provide faster speeds, more dependable and secure connections, lower latency, and increased capacity. No reports of ideal antennas have been published in the literature to yet. Several unresolved problems exist in the design of 5G antennas. Researchers have made many endeavors to create a low-cost, small-sized, and high-performing planner antenna for 5G usage [59].

- The antenna's efficiency and its ability to direct radiation in a specific direction primarily determine the efficiency of radio frequency energy. Antenna efficiency refers to the ratio of the power transmitted by the antenna to the amount of power delivered to the antenna's

feeds. Reducing the size of an antenna results in a decrease in both bandwidth and efficiency. For instance, in the case of a massive multiband antenna, maximizing the efficient use of the entire antenna volume can enhance its effectiveness. However, it is common for only a portion of the antenna to be actively radiating at a certain frequency, while the remaining parts remain inactive. This inactive portion affects the overall efficiency of the antenna. Another factor contributing to low efficiency is the antenna's fixed nature, which prevents it from adapting its performance to different scenarios. The mobile antenna is highly effective at emitting radiation in open space. However, its functioning is not adaptable to the user's specific needs and proximity, resulting in reduced radiation efficiency [59].

- Beam scanning over a broader angular range is a significant challenge due to the degradation of the radiation pattern at greater scanning angles. This results in decreased gain, larger beamwidth, and deeper side lobes. Attaining consistent radiation properties at all scanning angles is a challenging task. PCB antennas can experience impedance mismatching at specific beam scanning angles [60]. It is quite difficult to achieve lower side lobe levels while expanding the array size.

- The gain and beamwidth of massive MIMO systems need to be consistent across all operational frequencies in order to provide effective coverage for every megabase station. Stationary element spacing causes beamwidth fluctuation, which significantly challenges the achievement of seamless control comparable to gain. To minimize beamwidth oscillations, it is important to carefully select the boundary [61].

- The coexistence of millimeter-wave and microwave antennas in the same space is a significant development. 5G mobile networks will utilize millimeter-wave antennas in addition to LTE or sub-6 GHz antennas. Co-locating several antennas in a common space is a significant problem. Proximity between antennas can alter their individual performance. The high screen-to-body ratio poses a significant difficulty in the design of mobile devices [59].

- In order to decrease the dimensions of an antenna array, or MIMO antenna, the distance between the individual elements needs to be lowered. However, this leads to a rise in mutual coupling as well as a decrease in gain, bandwidth, and efficiency.

- Massive MIMO antennas pose a multidisciplinary challenge that aims to improve coverage, efficiency, and service quality. At base stations, the implementation of a MIMO

antenna system presents several obstacles, including cooling, passive interference, high power consumption, reliability, mutual coupling, and phase stability [60].

- It's hard to make a wideband high-gain circularly polarized antenna that works over a wider frequency range because it's hard to keep the phase shift between the two elements oriented along the x- and y-axes stable over a wider frequency range. Across the entire range of frequencies used, the axial ratio ought to be under 3 dB, and the return loss must be less than 10 dB [62].

- It is quite a difficult task to achieve both significant gain and broad bandwidth in a small space simultaneously. An antenna needs to be capable of operating across a wide range of frequencies to effectively handle high data rates. In order to overcome the effects of environmental diminution along with major link loss, achieving notable gain is crucial at mm-Wave. Compact-size antennas for cellular devices can help save on manufacturing costs. Increasing the bandwidth of an antenna often results in a decrease in gain. Reducing the antenna's dimension leads to an increase in mutual coupling and losses, ultimately leading to a reduction in gain.

- Phase shifting across a wide variety of frequencies with few losses while keeping costs low is a significant challenge. 5G apps will employ phased array technology. Beamforming necessitates the use of multiple phase shifters within a phased array antenna. Scientists are devising phase shifting systems for microwave bands, but at mm-Wave frequency ranges, the main challenges for practical use are the significant reduction in signal strength and the substantial expense. SIW approaches are utilized to tackle this problem [62].

- Achieving reconfigurability with regard to frequency, polarization, and radiation pattern at the same time poses a significant challenge. A multiband reconfigurable antenna is the ideal choice for 5G applications, as it can accommodate various bands of operation while maintaining a compact antenna shape. The purpose of a pattern reconfigurable antenna is to dynamically alter its pattern to meet specific requirements and achieve optimal signal sending and receiving. Polarization reconfigurable antennas have the capability to alter their polarization state, transitioning between linear and circular polarization (both right and left-handed circular polarization, as well as elliptical polarization) [59].

- The choice of patch width typically impacts the resonance frequency and radiation pattern, while the patch length normally influences both parameters as well. The patch's width

has a negligible impact on these factors. Decreasing the patch width results in a reduction in both size and radiation efficiency. The formula provides a precise minimum width for a patch antenna that decreases its dimension to a specified limit without affecting the radiation efficiency [63]. Equation (7) provides the formula.

$$W\min(in\,mm) = (72/f\min) - (L/6.28) \quad (7)$$

Where Wmin represents the minimum width in millimeters, fmin represents the minimum operational frequency, and L represents the length of the patch.

- The excitation technique of phased arrays involves using phased array technology to generate a narrow and controllable beam of radiation with elevated gain. This technique is considered to be highly effective and efficient [64]. There are actually two methods to stimulate a phased array. The first method is parallel feeding, which uses several power dividers. Power dividers enlarge the device's size, while false radiation and dielectric loss constrain performance. The direction of a parallel feed array's beam is determined by the frequency. Another option is a series-feeding structure. The utilization of short microstrip lines in symmetrical series-fed phased arrays leads to a reduction in size and a boost in efficiency. However, a challenge arises when beam squints occur. Larger series-fed arrays have a narrow bandwidth, significant losses, and low efficiency. Changes in frequencies do not affect the beam steering of a series-fed array. Metallic waveguides can enhance efficiency [67].

- Choosing the appropriate substrate material for higher frequency ranges poses significant challenges. One must analyze the characteristics of the material, including its relative permittivity, loss tangent, and ease of production. A cell device integrates the RFIC and antenna into a single system package. The substrate loss tangent is a critical factor to consider for high-frequency systems. We should carefully select the substrate's permittivity. If the permittivity is high, the size of the antenna decreases. The antenna's bandwidth and efficiency significantly decrease when the thickness of substrates exhibiting greater permittivity equals that of substrates with less permittivity [68].

- When it comes to choosing how to feed an antenna, the coaxial feeding approach has the drawbacks of low mechanical strength and limited bandwidth. However, proximity coupling can overcome these limitations by enhancing both the gain and frequency range within the same aperture, albeit at the expense of increasing the antenna's thickness. Additional

methods include microstrip line feed and aperture-linked feeding. The selection of feeding mechanisms relies on the effective transmission of power via the feeding and radiating components [63].

- To achieve optimal bandwidth and gain when utilizing stacking at mm-Wave frequencies, it is necessary to ensure that the gap between two substrates is smaller than 0.1 times the wavelength. At mm-Wave frequencies, maintaining an air gap of 0.1 times the wavelength between two substrates is extremely difficult. We can utilize an acrylic polymer spacer in the form of a three-dimensional manufactured window. Furthermore, its low permittivity diminishes the surface wave and enhances the surrounding field and radiation power [63].

- Stacked patches are the recommended method for increasing bandwidth inside a single aperture while maintaining a steady gain. However, at mm-Wave frequencies, the use of a multilayer structure might lead to misalignment issues in antenna fabrication [69]. The combination of decreased substrate layers, an easy compact structure, simplicity in manufacture, and broadband capabilities makes antennas highly appealing for prospective 5G apps [70].

REFERENCES

[1] S. R. Jena, A. Deka, J. P. Kalita, H. Byeon, "5G TECHNOLOGY AND IT'S APPLICATION", Dabra, Xoffencer International Publication, 2023.
[2] P. Gupta, "Evolvement of mobile generations: 1G To 5G", Int. J. Technol. Res. Eng.1 (3) (Nov. 2013)
[3] Transition to 4G: 3GPP Broadband Evolution to IMT Advanced. Rysavy Research/3G America's, 2010.
[4] UMTS World (2009), UMTS/3G History and Future Milestones. [Online] Available at: www.umtsworld.com/umts/history.html.
[5] Ajay K. Mishra. Fundamentals of Cellular Network Planning and Optimization, 2G/2.5G/3G..Evolution Of 4G. John Wiley and Sons, 2004.
[6] S. Hossain, "5G wireless communication systems," Am. J. Eng. Res., vol. 2, no. 10, pp. 344–353, 2013.
[7] J. Rodriguez, Fundamentals of 5G Mobile Networks. John Wiley & Sons, 2015.
[8] Y. Corre, T. Tenoux, J. Stéphan, F. Letourneux, and Y. Lostanlen, "Analysis of outdoor propagation and multi-cell coverage from ray-based simulations in sub-6GHz and mmwave bands," in 2016 10th European Conference on Antennas and Propagation (EuCAP), 2016, pp. 1–5.
[9] S. Sicari, A. Rizzardi, and A. Coen-Porisini, "5G In the internet of things era: An overview on security and privacy challenges," Comput. Networks, vol. 179, p. 107345, 2020, doi: 10.1016/j.comnet.2020.107345.
[10] S. Čaušević and A. Medić, "4G to 5G network evolution: Advantages and differences," SAR J., vol. 4, no. 4, pp. 153–159, 2021, doi: 10.18421/SAR44-01.
[11] "What is 5G? how will it Transform our world?" Ericsson, 30-Mar-2023. [Online]. Available: https://www.ericsson.com/en/5g. [Accessed: 05-Apr-2023].
[12] T. Zemen, "Wireless 5G ultra reliable low latency communications: European and Austrian research initiatives," Elektrotechnik und Informationstechnik, vol. 135, no. 7, pp. 445–448, 2018, doi: 10.1007/s00502-018-0645-0.
[13] X. Ge, "Ultra-reliable low-latency communications in autonomous vehicular networks," IEEE Trans. Veh. Technol., vol. 68, no. 5, pp. 5005–5016, 2019, doi: 10.1109/TVT.2019.2903793.
[14] D. Jiang and G. Liu, "An Overview of 5G Requirements," 5G Mobile. Commun., pp. 3–26, 2016.
[15] J. L. Carcel, B. Mouhouche, M. Fuentes, E. Garro, and D. Gomez-Barquero, "IMT-2020 key performance indicators: Evaluation and extension towards 5G new radio point-to-multipoint," in BMSB, 2019, pp. 1–5, doi: 10.1109/BMSB47279.2019.8971948.
[16] A. Tamayo-Dominguez, J.-M. Fernandez-Gonzalez, and M. S. Castaner, "Low-cost millimeter-wave antenna with simultaneous sum and difference patterns for 5G point-to-point communications," IEEE Commun. Mag., vol. 56, no. 7, pp. 28–34, 2018.
[17] Qualcomm white paper: Making 5G NR a reality. https://www.qualcomm.com/media/documents/files/whitepaper-making-5g-nr-a-reality.pdf
[18] R. N. Gurzhi and S. M. Shevchenko, "Thermal conductivity theory of thin dielectric models", Soviet Physics - Journal of Experimental and Theoretical Physics, vol. 25, no. 3, pp. 534–536, 1967.
[19] G. T. Ruck, "Radar Cross Section Handbook", Plenum Press, New York, 1970.
[20] R. Vaughan and J. Andersen, "Channels, Propagation and Antennas for Mobile Communications", IET, London, 2003.
[21] ITU. Provisional Final Acts. In Proceedings of the World Radiocommunication Conference 2019, Sharm El-Sheikh, Egypt, 28 October–22 November 2019; 2019.
[22] Lee, J.; Tejedor, E.; Ranta-aho, K.; Wang, H.; Lee, K.-T.; Semaan, E.; Mohyeldin, E.; Song, J.; Bergljung, C.; Jung, S. Spectrum for 5G: Global Status, Challenges, and Enabling Technologies. IEEE Commun. Mag. 2018, 56, 12–18.
[23] Sowande, O.A.; Idachaba, F.E.; Ekpo, S.; Faruk, N.; Uko, M.; Ogunmodimu, O. Sub- 6 GHz 5G Spectrum for Satellite-Cellular Convergence Broadband Internet Access in Nigeria. Int. Rev. Aerosp. Eng. (IREASE) 2022, 15, 85.
[24] Morgado, A.; Huq, K.M.S.; Mumtaz, S.; Rodriguez, J. A Survey of 5G Technologies: Regulatory, Standardization and Industrial Perspectives. Digit. Commun. Netw. 2018, 4, 87–97.
[25] Shafi, M.; Molisch, A.F.; Smith, P.J.; Haustein, T.; Zhu, P.; De Silva, P.; Tufvesson, F.; Benjebbour, A.;Wunder, G. 5G: A Tutorial Overview of Standards, Trials, Challenges, Deployment, and Practice. IEEE J. Sel. Areas Commun. 2017, 35, 1201–1221.
[26] Union, A. Report of the 3rd Ordinary Session of the Specialized Technical Committee on Communication and ICT, Sharm El Sheikh, Egypt, 25–26 October 2019. 2020.
[27] Y. Wang, J. Li, L. Huang, Y. Jing, A. Georgakopoulos, and P. Demestichas, "5G mobile: Spectrum broadening to higher-frequency bands to support high data rates," IEEE Veh. Technol. Mag., vol. 9, no. 3, pp. 39–46, 2014.
[28] R. Dilli, "Analysis of 5G wireless systems in FR1 and FR2 frequency bands," in 2020 2nd International Conference on Innovative Mechanisms for Industry Applications (ICIMIA), 2020, pp. 767–772.
[29] Imam-Fulani, Y.O.; Faruk, N.; Sowande, O.A.; Abdulkarim, A.; Alozie, E.; Usman, A.D.; Adewole, K.S.; Oloyede, A.A.; Chiroma, H.; Garba, S.; et al. 5G Frequency Standardization, Technologies, Channel Models, and Network Deployment: Advances, Challenges, and Future Directions. Sustainability 2023, 15, 5173.
[30] A. Baratè, G. Haus, L. A. Ludovico, E. Pagani, and N. Scarabottolo, ''5G technology and its applications to music education,'' in Proc. MCCSIS,2019, pp. 65–72.
[31] Zhu S, Liu H, and Wen P. A new method for achieving miniaturization and gain enhancement of Vivaldi antenna array based on anisotropic metasurface. IEEE Trans. Antennas Propag. 2019;67(3):1952–6.
[32] Abbasi, Q.H.; Jilani, S.F.; Alomainy, A.; Imran, M.A. Antennas and Propagation for 5G and Beyond; Institution of Engineering and Technology: Stevenage, UK, 2020.

[33] Karim R, Iftikhar A, Ijaz B, and Mabrouk IB. The potentials, challenges, and future directions of on-chip-antennas for emerging wireless applications—A comprehensive survey. IEEE Access. 2019;7:173897 934.
[34] Cho YJ, Suk G, Kim B, Kim DK, and Chae C. RF lens-embedded antenna array for mmwave MIMO: Design and performance. IEEE Commun. Mag. 2018;56(7):42–8.
[35] Payami S, Ghoraishi M, and Dianati M. Hybrid beamforming for large antenna arrays with phase shifter selection. IEEE Trans. Wireless Commun. 2016;15(11):7258–71.
[36] Dahri MH, Jamaluddin MH, Abbasi MI, and Kamarudin MR. A review of wideband reflectarray antennas for 5G communication systems. IEEE Access. 2017;5:17803–15.
[37] Huang J, and Encinar JA. Reflectarray antennas. Piscataway, NJ/New York: IEEE Press/Wiley, 2008.
[38] Hong, W., Baek, K. H., Lee, Y., Kim, Y., & Ko, S. T. (2014). Study and prototyping of practically large-scale mmWave antenna systems for 5G cellular devices. IEEE Communications Magazine, 52(9), 63–69.
[39] Yassin, M. E., Mohamed, H. A., Abdallah, E. A. F., & El-Hennawy, H. S.(2019). Single-fed 4G/5G multiband 2.4/5.5/28 GHz antenna. IET Microwaves, Antennas and Propagation, 13(3), 286–290.
[40] Diawuo, H. A., & Jung, Y.-B. (2018). Broadband proximity-coupled microstrip planar antenna array for 5G cellular applications. IEEE Antennas and Wireless Propagation Letters, 17(7), 1286–1290.
[41] A White Paper on Enabling 5 G in India. (2019). TRAI.
[42] Ojaroudiparchin, N., Shen, M., Zhang, S., & Pedersen, G. F. (2016). A switchable 3-D-coveragephased array antenna package for 5G mobile terminals. IEEE Antennas and Wireless Propagation Letters, 15, 1747–1750.
[43] Mao, C. X., Khalily, M., Xiao, P., Brown, T. W. C., & Gao, S. (2019). Planar sub-millimeter-wave array antenna with enhanced gain and reduced sidelobes for 5G broadcast applications. IEEE Transactions on Antennas and Propagation, 67(1), 160–168.
[44] Rappaport, T. S., Sun, S., Mayzus, R., Zhao, H., Azar, Y., Wang, K., & Gutierrez, F. (2013). Millimeter wave mobile communications for 5G cellular: It will work! IEEE Access, 1, 335–349.
[45] Sazegar, M., Zheng, Y., Kohler, C., Maune, H., Nikfalazar, M., Binder, J. R., & Jakoby, R. (2012). Beam steering transmitarray using tunable frequency selective surface with integrated ferroelectric varactors. IEEE Transactions on Antennas and Propagation, 60(12), 5690–5699.
[46] Asma, K., Wakrim, L., Saida, I., & Hassani, M. (2022). Beam-steerable ultra-wide-band miniaturized elliptical phased array antenna using inverted-L-shaped modified inset feed and defected ground structure for 5G smartphones millimeter-wave applications. Wireless Personal Communications.
[47] Mohajer, M., Faraji-Dana, M., & Safavi-Naeini, S. (2014). Effects of resonance-based phase shifters on Ka-band phased array antenna performance for satellite communications. Progress In Electromagnetics Research B, 60, 259–274.
[48] Habaebi, M. H., Janat, M., & Rafiqul, I. M. (2018). Beam steering antenna array for 5G telecommunication systems applications. Progress In Electromagnetics Research M, 67, 197–207.
[49] Andrews, J. G., Buzzi, S., Choi, W., Hanly, S. V., Lozano, A., Soong, A. C. K., & Zhang, J. C. (2014). What will 5G be? IEEE Journal on Selected Areas in Communications, 32(6), 1065–1082.
[50] Askari, G., & Kamarei, M. (2017). Frequency and time domain design, analysis and implementation of a multi-gbps uwb wilkinson power divider for 5g new spectrum and CAR applications. Progress In Electromagnetics Research B, 77, 103–116.
[51] Roh, W., Seol, J.-Y., Park, J., Lee, B., Lee, J., Kim, Y., & Aryanfar, F. (2014). Millimeter-wave beamforming as an enabling technology for 5G cellular communications: theoretical feasibility and prototype results. IEEE Communications Magazine, 52(2), 106–113.
[52] Gandhi, O. P., & Riazi, A. (1986). Absorption of millimeter waves by human beings and its biological implications. IEEE Transactions on Microwave Theory and Techniques, 34(2), 228–235.
[53] Verma, A., Arya, R. K., & Nallanthighal, R. (2022). Wireless personal communications metasurface superstrate beam steering antenna with AMC for 5G/WiMAX/WLAN applications. Wireless Personal Communications.
[54] Yu, B., Yang, K., Sim, C.-Y.-D., & Yang, G. (2018). A novel 28 GHz beam steering array for 5G mobile device with metallic casing application. IEEE Transactions on Antennas and Propagation, 66(1), 462–466.
[55] Zhou, H., & Aryanfar, F. (2013). Millimeter-wave open ended SIW antenna with wide beam coverage. In 2013 IEEE Antennas and Propagation Society International Symposium (APSURSI) (pp.658–659).
[56] Zhadobov, M., Chahat, N., Sauleau, R., Le Quement, C., & Le Drean, Y. (2011). Millimeter-wave interactions with the human body: State of knowledge and recent advances. International Journal of Microwave and Wireless Technologies, 3(2), 237–247.
[57] Khalily, M., Tafazolli, R., Xiao, P., & Kishk, A. A. (2018). Broadband mm-wave microstrip array antenna with improved radiation characteristics for different 5G applications. IEEE Transactions on Antennas and Propagation, 66(9), 4641–4647.
[58] Li, G., Zhai, H., Ma, Z., Liang, C., Yu, R., & Liu, S. (2014). Isolation-improved dual-band MIMO antenna array for LTE/WiMAX mobile terminals. IEEE Antennas and Wireless Propagation Letters, 13, 1128–1131.
[59] Nahar, T.; Rawat, S.A. A Review of Design Consideration, Challenges and Technologies Used in 5G Antennas. Wirel. Pers.Commun. 2023,129, 1585–1621.
[60] Viikari, V., Luomaniemi, R., Ala-Laurinaho, J., Kurvinen, J., Kähkönen, H., Lehtovuori, A., & Leino, M. (2019). 5G Antenna Challenges and Opportunities. In 2019 16th International Symposium on Wireless Communication Systems (ISWCS) (pp. 330–334).
[61] Wu, Z., Wu, B., Su, Z., & Zhang, X. (2018). Development challenges for 5G base station antennas. In 2018 International Workshop on Antenna Technology (iWAT) (pp. 1–3).

[62] Mittra, R. (2018). Some Challenges in Millimeter Wave Antenna Designs for 5G. In 2018 International Symposium on Antennas and Propagation (ISAP) (pp. 1–2).
[63] Ershadi, E., Keshtkar, A., Abdelrahman, A., Xin, H., & Ershadi, E. (2017). Wideband high gain antenna subarray for 5G application. Progress In Electromagnetics Research C.
[64] Khalily, M., Tafazolli, R., Rahman, T. A., & Kamarudin, M. R. (2016). Design of phased arrays of series-fed patch antennas with reduced number of the controllers for 28-GHz mm-wave applications. IEEE Antennas and Wireless Propagation Letters, 15, 1305–1308.
[65] Kuo, F.-Y., & Hwang, R.-B. (2014). High-isolation X-band marine radar antenna design. IEEE Transactions on Antennas and Propagation, 62(5), 2331–2337.
[66] Ehyaie, D., & Mortazawi, A. (2011). A 24-GHz modular transmit phased array. IEEE Transactions on Microwave Theory and Techniques, 59(6), 1665–1672.
[67] Garcia-Marin, E., Masa-Campos, J. L., & Sanchez-Olivares, P. (2019). Planar array topologies for 5G communications in ku band [Wireless Corner]. IEEE Antennas and Propagation Magazine, 61(2), 112–133.
[68] Huang, H.-C. (2018). Overview of antenna designs and considerations in 5G cellular phones. In 2018 International Workshop on Antenna Technology (iWAT) (pp. 1–4).
[69] Stanley, M., Huang, Y., Wang, H., Zhou, H., Alieldin, A., & Joseph, S. (2018). A Capacitive coupled patch antenna array with high gain and wide coverage for 5G smartphone applications. IEEE Access, 6, 41942–41954.
[70] Yin, J., Wu, Q., Yu, C., Wang, H., & Hong, W. (2019). Broadband symmetrical E-shaped patch antenna with multimode resonance for 5G millimeter-wave applications. IEEE Transactions on Antennas and Propagation, 67(7), 4474–4483.

CHAPTER IV

A Metamaterial-Based UWB Patch Antenna for Sub-6 GHz 5G Mobile Communications

4.1 Introduction

Every year, mobile wireless networking witnesses a surge in information exchange, primarily due to the steadily growing demand for data-intensive electronic gadgets and smartphone apps. Many places worldwide have already deployed 5G wireless networks to meet the growing demand. 5G technologies differ from previous generations in several key aspects. These include an information transfer rate of gigabits per second, a latency duration of milliseconds, a significant traffic density, a large number of interactions, improved spectrum energy, as well as cost effectiveness [1]. Typically, in mmWave bands, electromagnetic waves encounter challenges such as signal fading, significant route loss, and atmospheric absorptions. Network operators are utilizing current base station sites originally designed for frequencies below 6 GHz to facilitate the seamless and efficient deployment of 5G technology. The frequency spectrum beneath 6 GHz, commonly referred to as the sub-6 GHz, is considered to be the main frequency range used for the implementation of 5G technology, particularly for the (3.3-4.2, 3.3-3.8, 4.4-5.0 GHz) bands [2].

Antennas play a crucial role in wireless communications by establishing the connection between both transmitter and receiver. With the implementation of 5G networks in several nations, there is a high demand for antenna design for 5G transmission towers and smartphones. In order to achieve optimal performance for 5G applications, the antenna must possess several resonance modes that can effectively span the entire sub-6 GHz band of the 5G spectrum. Hence, it is crucial to develop an antenna that has broad frequency range capabilities in order to effectively encompass all the sub-6 GHz ranges, in addition to the pre-existing 4G (LTE) spectrum. An appropriate 5G antenna should include dimensions that allow for compatibility with handheld wireless technologies. For seamless integration into mobile devices, we particularly want an antenna with a low-profile design and easy integration with a PCB. Planar antennas have specific properties that make them the most commonly chosen option for small antennas [3]. However, the limitations of these antennas require additional methods to achieve a wider bandwidth [4].

Multiple publications have stated that Split Ring Resonator (SRR) can boost antenna performance by altering its electromagnetic characteristics [5, 6]. The dual electromagnetic characteristics of SRR, which can function as either a single negative or double negative material, facilitate the modification of antenna qualities. Materials like SRR are typically categorized as metamaterials, meaning that they are artificial materials designed to possess

electromagnetic properties that are not commonly seen in natural materials, including negative refractive index (NRI) and artificial magnetism [7]. Metamaterial antennas achieve a NRI through the use of SRRs and complementary SRRs (CSRRs) configurations. Current demands for simple integration, smaller dimensions, and light weight of the antenna drive the design of these components. The direction and positioning of the SRR's gap relative to the transmission line significantly affect the overall performance of the antenna.

In this chapter, a study about the effectiveness of integrating Split Ring Resonator (SRR) unit cells and a Defective Ground Structure (DGS) technique in enhancing the performance of a UWB rectangular patch antenna for 5G Sub-6 GHz applications. The modified antenna design achieved significant improvements in bandwidth, gain, and overall electromagnetic behavior. The integration of SRRs near the feed line, where the electromagnetic field intensity is highest, and the strategic application of DGS on the ground plane, facilitated a strong resonance effect, effectively coupling the electric and magnetic fields. This configuration not only miniaturized the antenna ($20\times28\times16mm^3$) while maintaining desirable operational characteristics but also expanded the bandwidth from 2.26 GHz to 5.4 GHz, with a markedly enhanced S-11 parameter of -33 dB at 3.5 GHz. The improved gain, with a peak of 4.15 dB at 5.2 GHz, further demonstrates the efficacy of the proposed design. The negative or near-zero values of permittivity, permeability, and refractive index confirm the SRR unit cell's role as a metamaterial, enabling unique electromagnetic properties that contribute to the antenna's superior performance. These findings highlight the potential of SRR and DGS integration in advancing antenna design for modern communication systems, offering a promising pathway for further research and development in this field.

4.2 Methodology

This section outlines the design procedures for a rectangular microstrip patch antenna, followed by the design of an SRR unit cell metamaterial, and finally the patch's integration with the SRR metamaterial.

4.2.1 Antenna Design

The antenna is specifically engineered to have resonance at a specific frequency of 3.5 GHz. To maintain consistency and minimize changes to the original structure of the feed, a proper substrate and modeling software are used to achieve uniformity. The substrate used is only one layer of 1.6 mm thickness (h) of FR-4 material, which has a dielectric constant (ε_r)

of 4.4, a dielectric loss tangent (tan δ) of 0.025. The mathematical equations utilized for the rectangular microstrip structure [8, 9, 10] are listed as follows:

The width of the microstrip patch is calculated using Eq. 8.

$$W_p = \frac{c}{2f_r\sqrt{\frac{\varepsilon_r+1}{2}}} \tag{8}$$

The effective dielectric constant is derived from Eq. 9.

$$\varepsilon_{reff} = \frac{\varepsilon_r+1}{2} + \frac{\varepsilon_r-1}{2}\left[1 + 12\left(\frac{h}{W_p}\right)\right]^{-1/2} \tag{9}$$

The patch's effective length is determined using Eq. 10.

$$L_{eff} = \frac{c}{2f_r\sqrt{\varepsilon_{reff}}} \tag{10}$$

The length extension is subtracted from the original length of the patch while keeping the actual length of the patch untouched. Eq. 11 demonstrates that consideration of the surrounding field leads to length extension.

$$\Delta L = 0.412h\frac{\left[\varepsilon_{reff}+3\right]\left[\frac{w}{h}+0.264\right]}{\left[\varepsilon_{reff}-0.258\right]\left[\frac{w}{h}+0.813\right]} \tag{11}$$

The actual length of the patch is determined by utilizing Eqs. 12 and 13.

$$L_{eff} = L_p + 2\Delta \tag{12}$$

$$L_p = L_{eff} - 2\Delta \tag{13}$$

The dimensions of the ground plane are determined. When dealing with both finite and infinite planes, it is necessary for the ground plane to have a size that is six times larger than the dimensions of the patch, taking into account the substrate thickness (h), across the whole perimeter of the patch [10]. Therefore, the dimensions of the ground plane for this design are determined as follows:

$$L_g = L_p + 6h \tag{14}$$

$$W_g = W_p + 6h \quad (15)$$

Table 4.1 provides the parameters of the rectangular patch antenna operating at a frequency of 3.5 GHz, while Figure 4.1 illustrates the design of the monopole.

Table 4.1 Values of the basic design parameters.

Parameter	**Value (mm)**
W_{sub}	35
L_{sub}	30
W_p	25
L_p	20
W_f	3
L_f	5
W_g	35
L_g	30
S_1	1
S_2	4.5

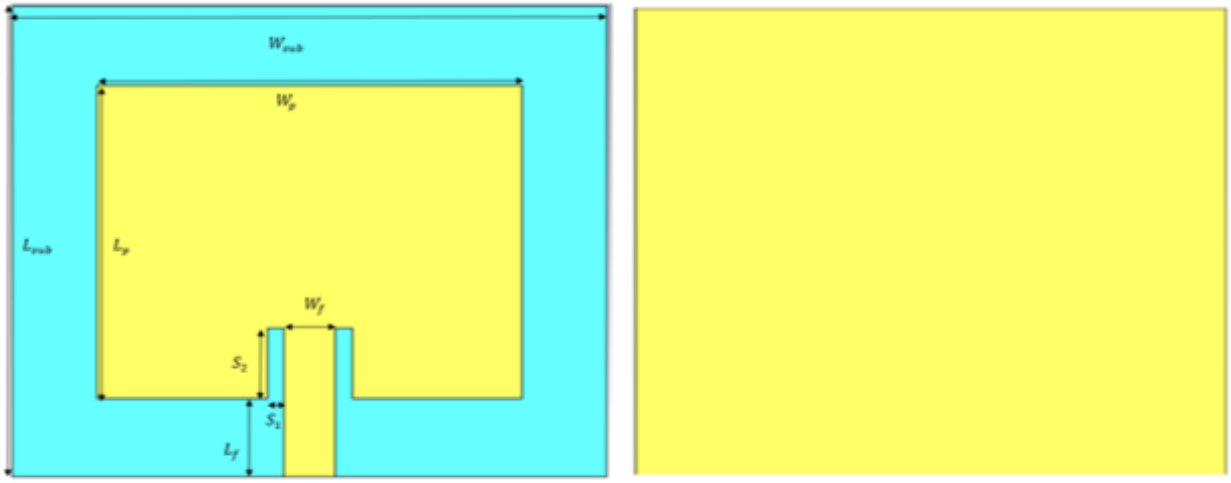

(a) (b)

Figure 4.1 Basic design of the rectangular patch antenna. (a) Top view. (b) Back view.

4.2.2 SRR Design

To meet specific resonance frequency requirements, the dimensions of a unit cell are adjusted based on its form and size. Generally, the unit cell size is somewhere between one-tenth and one-twentieth of the functioning wavelength, as indicated in equation 16:

$$\frac{\lambda_0}{10} \leq R \leq \frac{\lambda_0}{20} \tag{16}$$

To retrieve effective settings from reflection and transmission data, the overall unit-cell measure must be smaller than the working wavelength. Therefore, by taking one-fifteenth of the guided wavelength of the reference monopole (3.5 GHz) as the outside length of the metamaterial (MTM), the outer ring length of the MTM can be obtained from the wavelength and the guided wavelength which are calculated using the following equations:

$$\lambda_0 = \frac{c}{f_r} \tag{17}$$

$$\lambda_g = \frac{\lambda_g}{\sqrt{\varepsilon_{eff}}} \tag{18}$$

Where:

λ_0: is the operating wavelength

λ_g: is the guided wavelength

For this study, the selected shape of the MTM is the split ring resonator (SRR), primarily chosen for its simplicity of design and evaluation. The parameters of the SRR, such as the outer radius (R), the ring width (w) and the gap (g), can be adjusted to tune the resonant frequency within the desired range. Generally, we determine these dimensions in the following manner:

$$R \approx \frac{\lambda_g}{15} \approx 0.15\lambda_g \tag{19}$$

$$g \approx 0.1R \tag{20}$$

$$w \approx g - 0.1 \tag{21}$$

The final dimensions of the unit cell are obtained using a simulation software optimization tool. The parameters of the SRR metamaterial unit cell are given in Table 4. 2, and the design arrangement is depicted in Figure 4.2.

Table 4.2 Parameters of the SRR metamaterial unit cell.

Parameter	Value (mm)
R	2.9
g	0.29
w	0.2

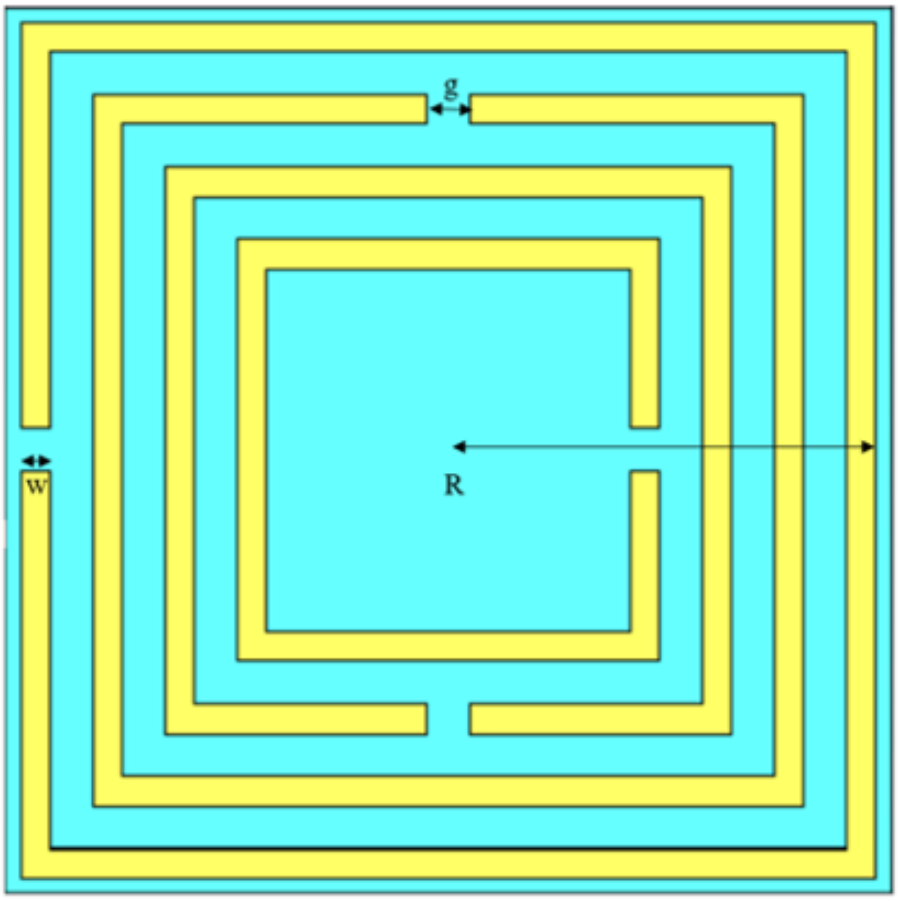

Figure 4.2 Design configuration of the SRR unit cell.

4.2.3 Antenna with SRR Unit Cell

To achieve the miniaturization of the antenna while maintaining coverage of the target frequency band, specifically the mid-band of the Sub-6 GHz spectrum, two pre-designed SRR unit cells were integrated with the patch antenna. Additionally, a defective ground structure (DGS) technique was employed on the ground plane. This combination effectively reduced the overall antenna dimensions and enhanced performance. The optimized parameters of the antenna are presented in Table 4.3, and the proposed design configuration is illustrated in Figure 4.3.

Table 4.3 Parameters of the proposed design.

Parameter	Value (mm)
W_{sub}	20
L_{sub}	28
W_p	14
W_f	2
L_f	13
S_3	3
S_4	18

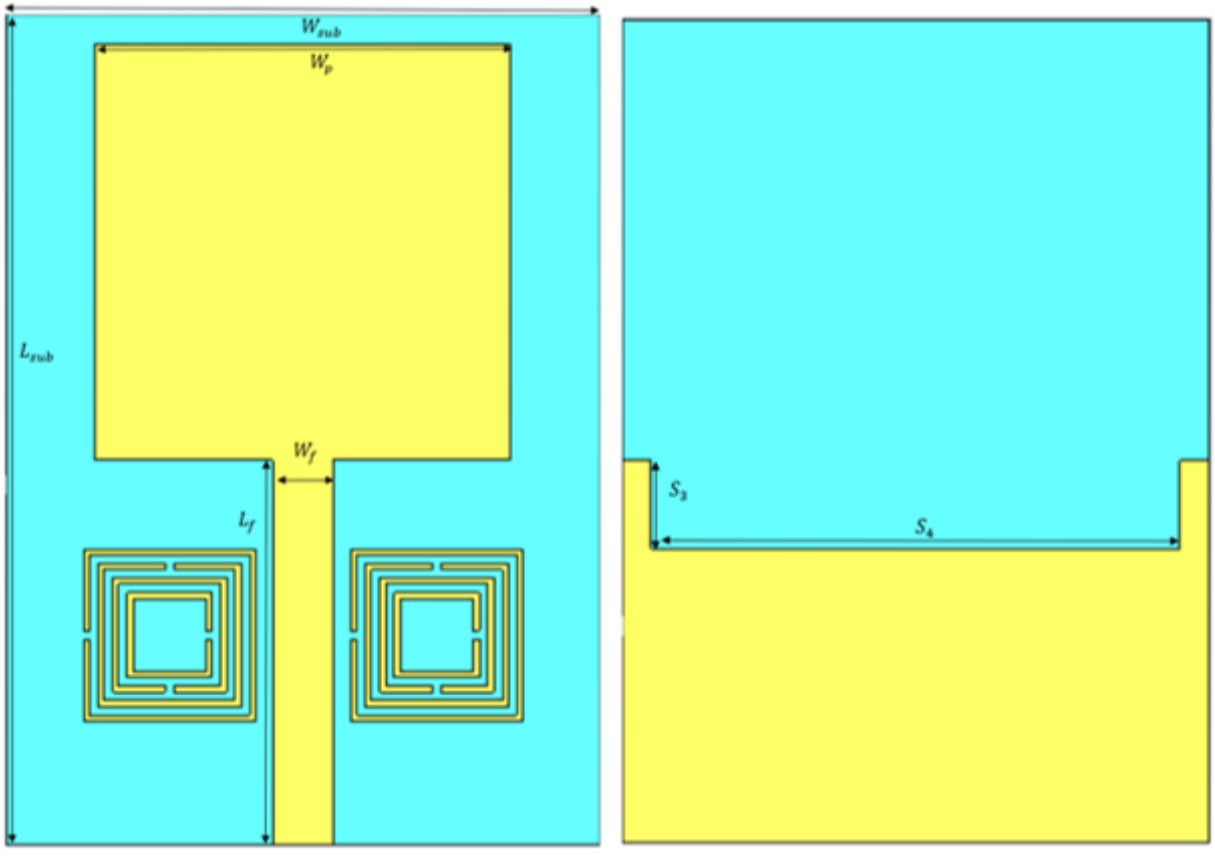

(a) (b)

Figure 4.3 Proposed design configuration. (a) Top view. (b) Back view.

4.3 Results and Discussion

The S-11 parameter of the basic rectangular patch antenna demonstrates a bandwidth extending from 3.42 GHz to 3.52 GHz, with a minimum value of -21 dB at 3.5 GHz. Additionally, a secondary bandwidth is observed between 5.43 GHz and 5.60 GHz, achieving a minimum value of -28 dB at 5.52 GHz, as depicted in Figure 4.4.

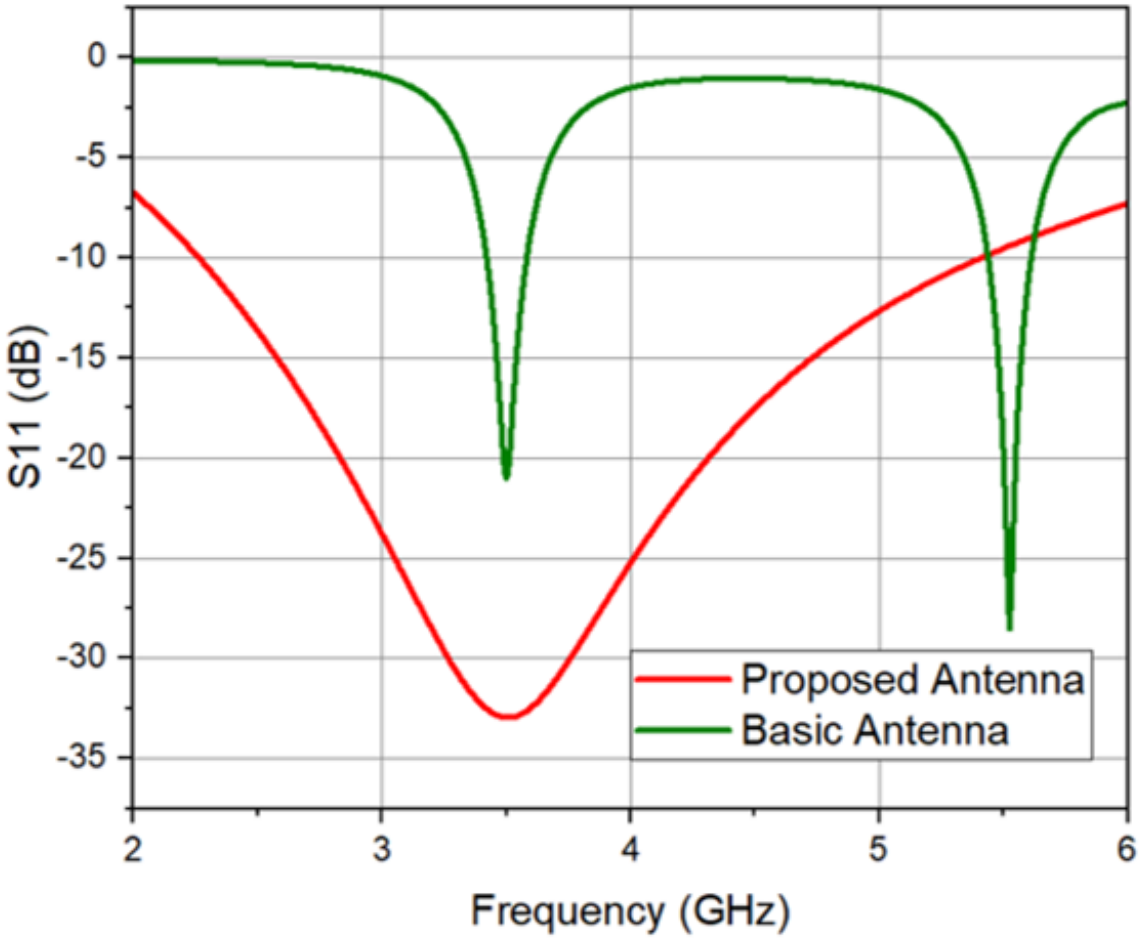

Figure 4.4 S-11 parameter of the basic and proposed design.

The S-parameters of the SRR unit cell, shown in Figure 4.5, reveal that the S-11 parameter attains values below -10 dB, indicating minimal reflection and maximal signal absorption at this frequency. This suggests that less than 1% of the incident power is reflected. The S-21 parameter displays values close to 0 dB, signifying maximal signal transmission through the system, with minimal loss, thereby indicating that nearly the entire signal is transmitted.

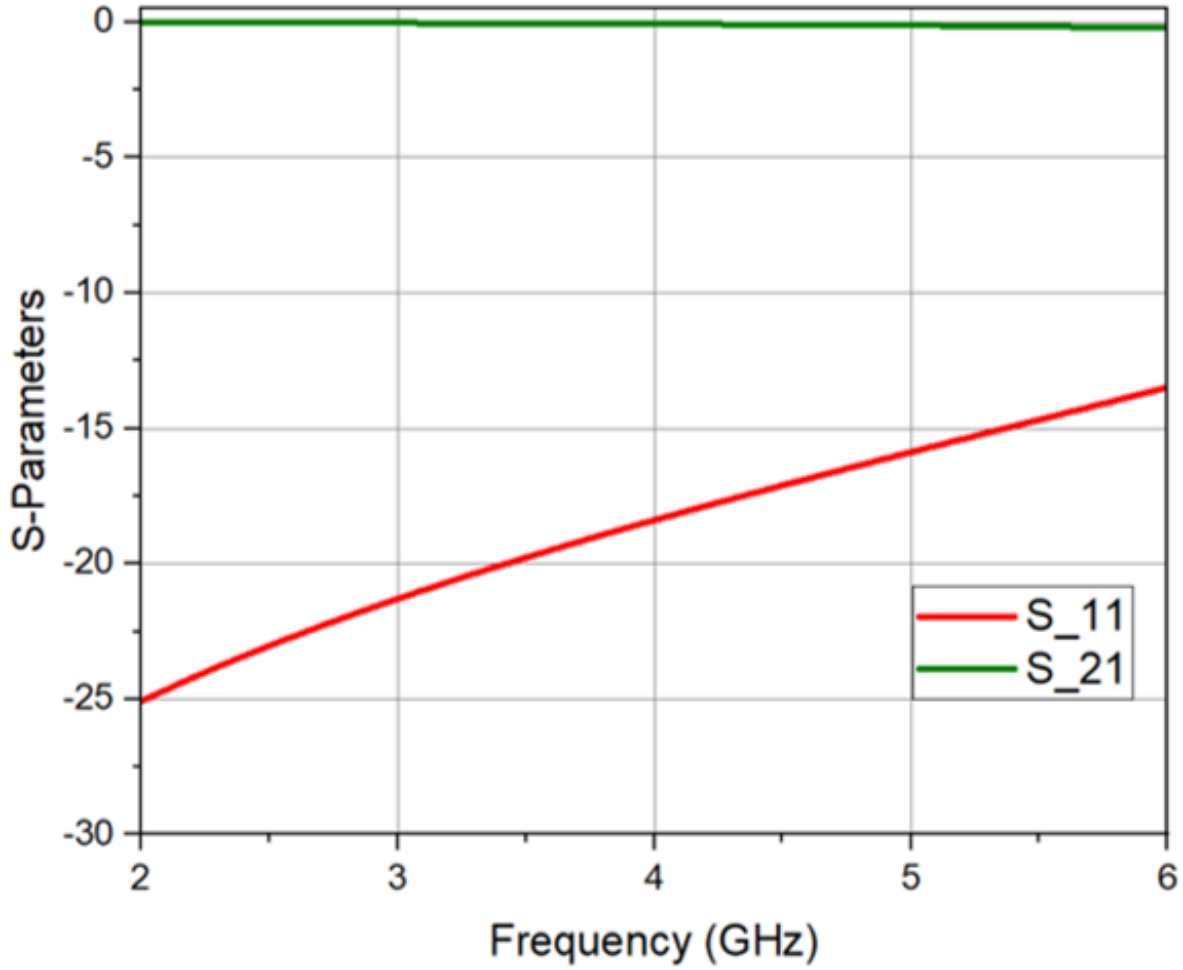

Figure 4.5 S-parameters of the SRR unit cell.

For the SRR unit cell to function effectively as a metamaterial, it should exhibit negative or near-zero values for the effective permittivity (ε), permeability (μ), and refractive index (n) at the target frequency. As illustrated in Figure 4.6, the real and imaginary components of permittivity (ε) demonstrate a transition from negative to positive values near the resonant frequency. This transition is attributed to the dispersive nature of the SRR, which behaves as a resonant material. Below 3.5 GHz, the real part of permittivity (Re(ε)) is negative, indicating the presence of a negative refractive index. The imaginary component (Im(ε)) is associated with material losses, and at the resonance frequency of 3.5 GHz, Im(ε) peaks, reflecting heightened absorption losses. As the frequency deviates from resonance, Im(ε) decreases, indicating reduced energy dissipation.

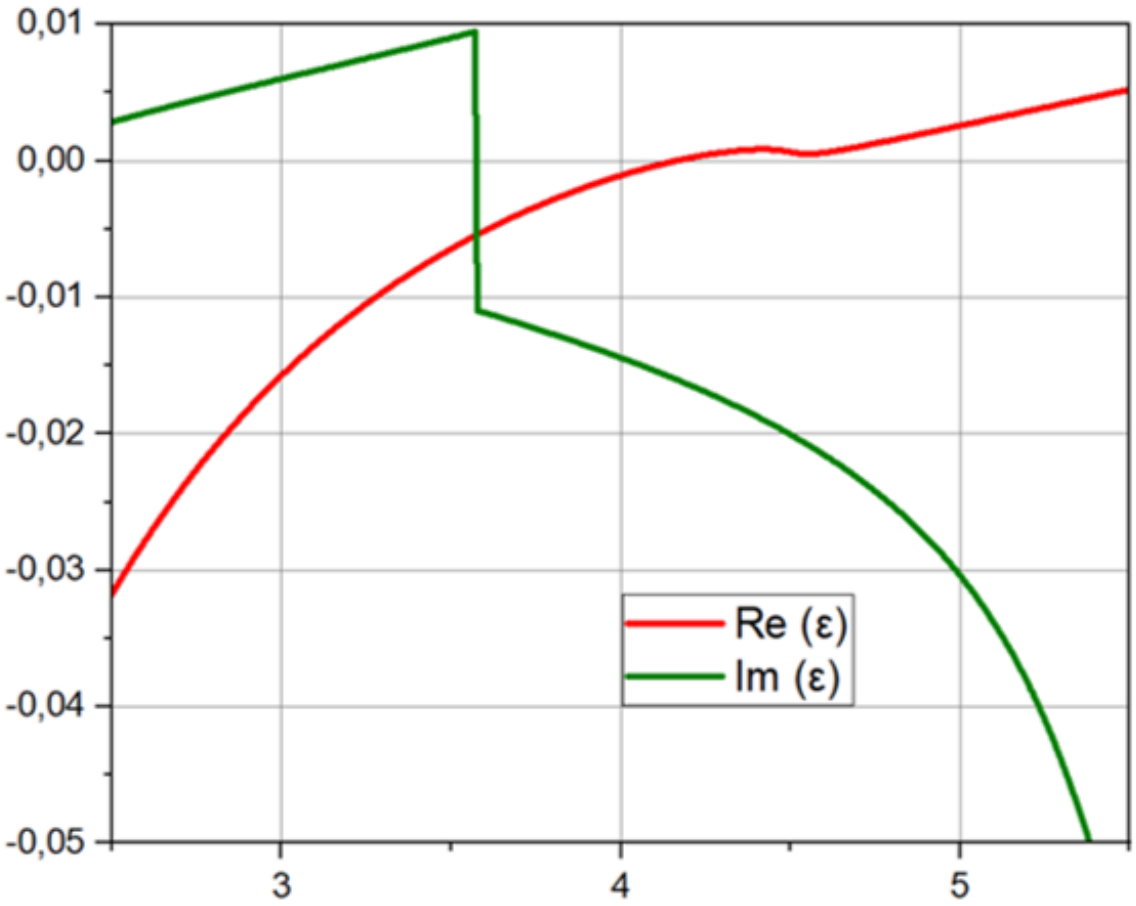

Figure 4.6 Real and imaginary parts of permittivity.

Figure 4.7 presents the real and imaginary components of permeability (μ). Similar to permittivity, the real part of permeability (Re(μ)) exhibits significant variation near the resonance frequency. Below 3.5 GHz, Re(μ) is negative, but as the frequency surpasses the resonance point, Re(μ) may become positive due to the inductive nature of the SRR. The imaginary component of permeability (Im(μ)) represents magnetic losses within the material, with a sharp decrease observed at 3.5 GHz, indicating heightened magnetic energy dissipation, which is characteristic of resonant structures such as SRRs.

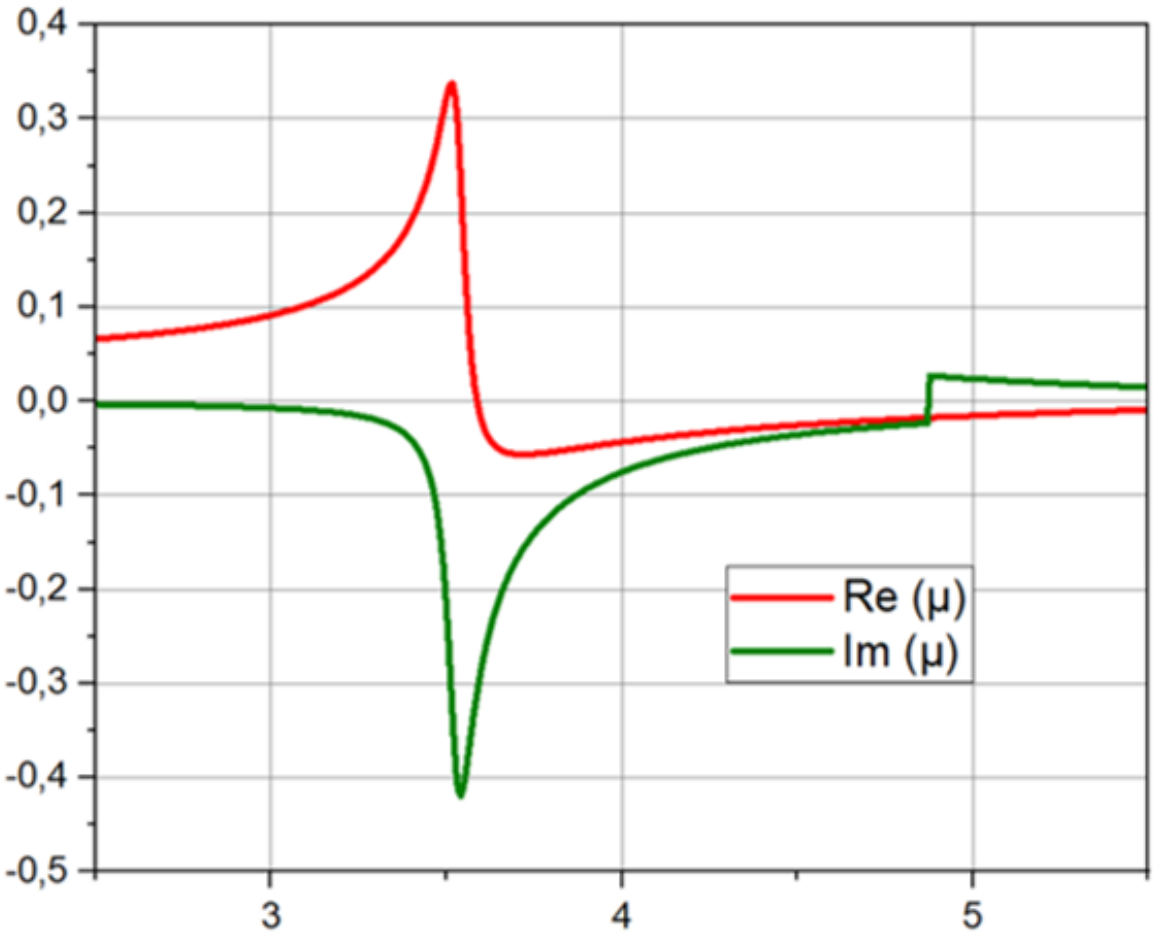

Figure 4.7 Real and imaginary parts of permeability.

The real and imaginary components of the refractive index (n) are depicted in Figure 4.8. Given that the SRR exhibits negative or near-zero permittivity and permeability around the resonance frequency, the real part of the refractive index (Re(n)) is also negative near 3.5 GHz. This negative refractive index is a distinctive feature of metamaterials, enabling unique electromagnetic behaviors. The imaginary component (Im(n)) is related to attenuation within the material. At resonance, Im(n) peaks, corresponding to maximum losses, and diminishes as the frequency moves away from 3.5 GHz. This behavior aligns with the loss characteristics observed in both permittivity and permeability.

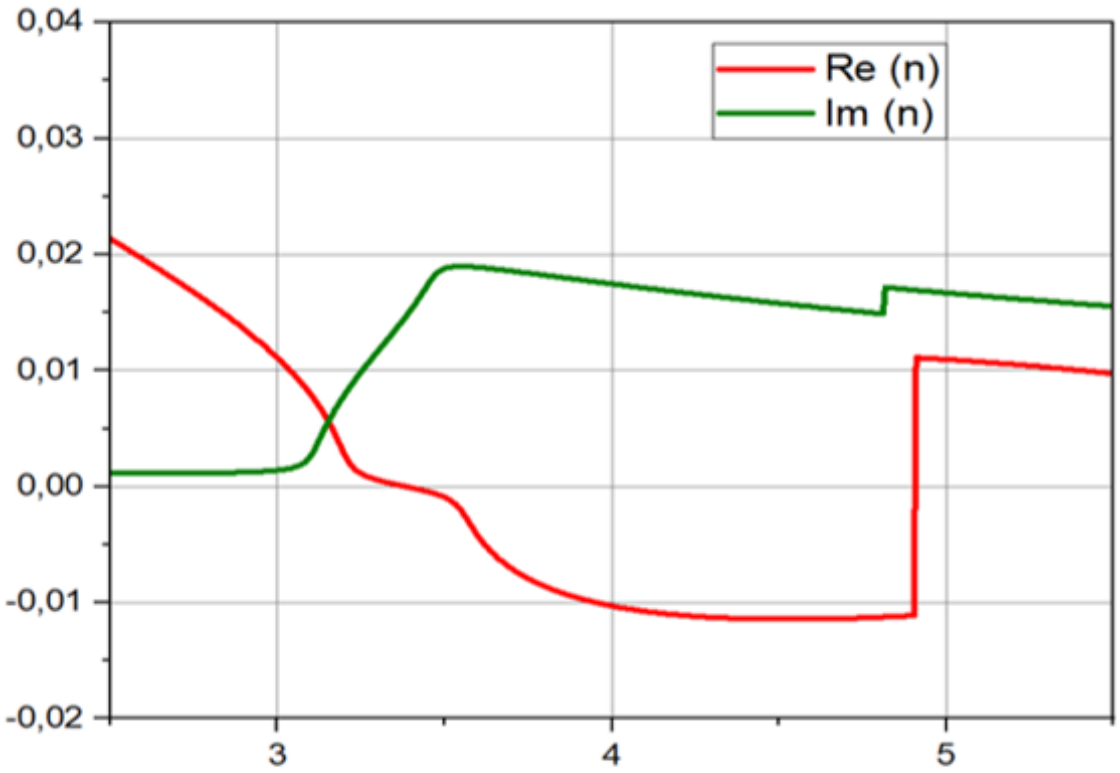

Figure 4.8 Real and imaginary parts of the refractive index.

The integration of two SRR unit cells near the feed line of the patch antenna, combined with the application of the DGS technique to the ground plane, is critical for optimizing antenna performance. The region near the feed line, where the electromagnetic field is strongest, benefits from the placement of SRRs and the introduction of a slot on the backside of this area. This configuration allows for effective coupling with the electric and magnetic fields, thereby amplifying the resonance effects and enhancing the overall electromagnetic interaction between the SRRs and the antenna. The inclusion of SRRs and DGS facilitates antenna miniaturization while preserving favorable operational characteristics, enhancing both the bandwidth and frequency response of the monopole, as illustrated in Figure 4.4. The S-11 parameter of the proposed antenna exhibits a bandwidth ranging from 2.26 GHz to 5.4 GHz, with a minimum value of -33 dB at 3.5 GHz. This modification also improves the monopole's gain, as evidenced in Figure 4.9, where the proposed design achieves a gain of 3.85 dB at 3.5 GHz and a peak gain of 4.15 dB at 5.2 GHz, compared to the basic design's peak gain of 2 dB at 3.5 GHz.

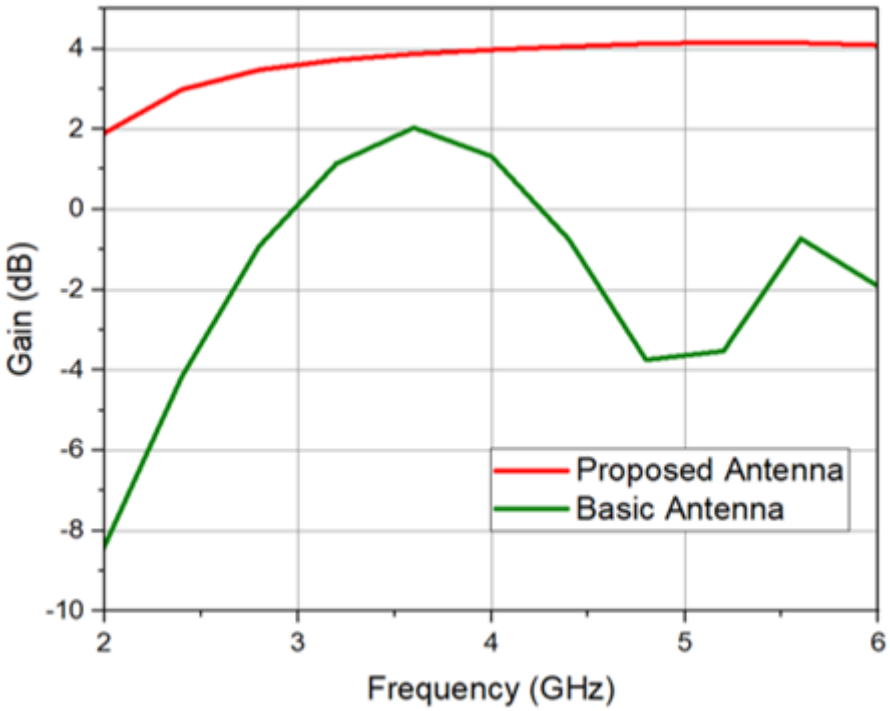

Figure 4.9 Realized gain of the basic and proposed antenna.

The simulated S-11 parameters, gain, and radiation pattern of both CST and HFSS software are presented in Figure 4.9, Figure 4.10, and Figure 4.11 respectively.

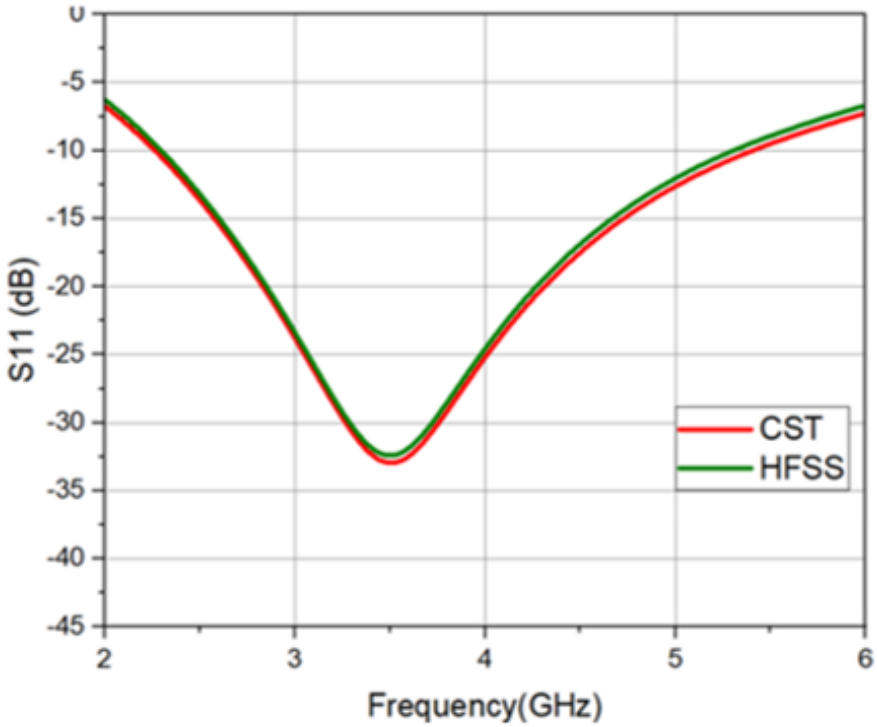

Figure 4.10 Simulated S-11 parameters CST versus HFSS.

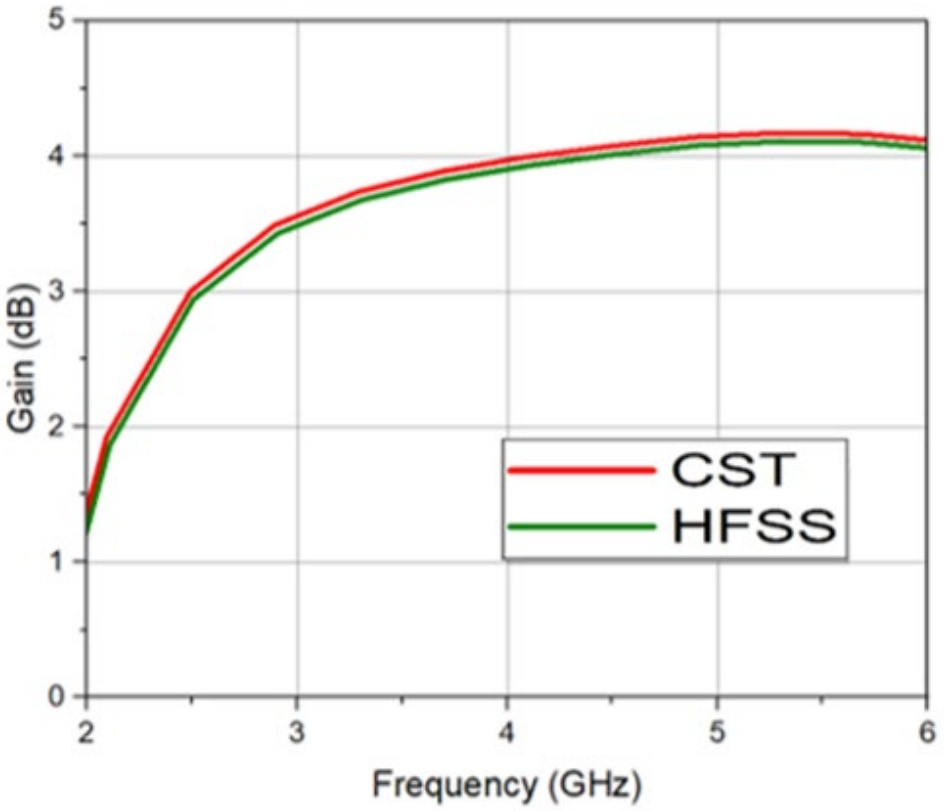

Figure 4.11 Simulated gain CST versus HFSS.

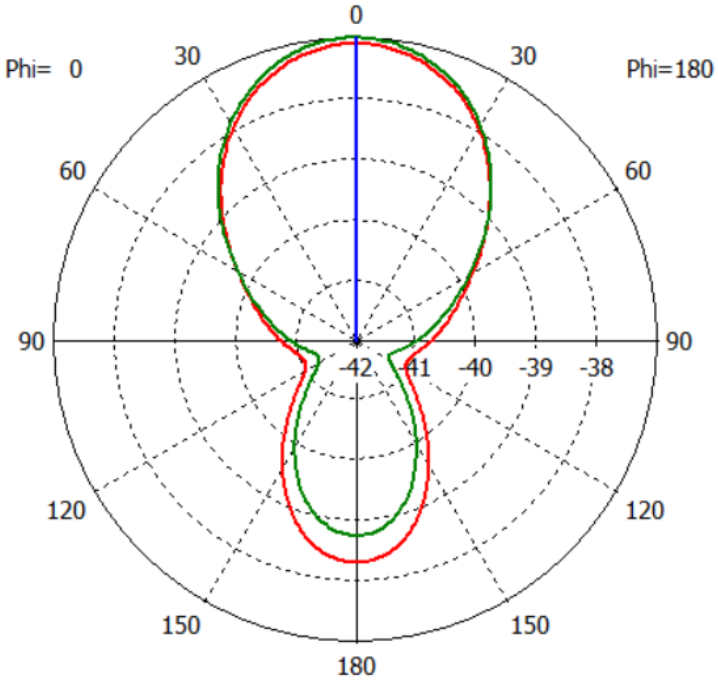

(a)

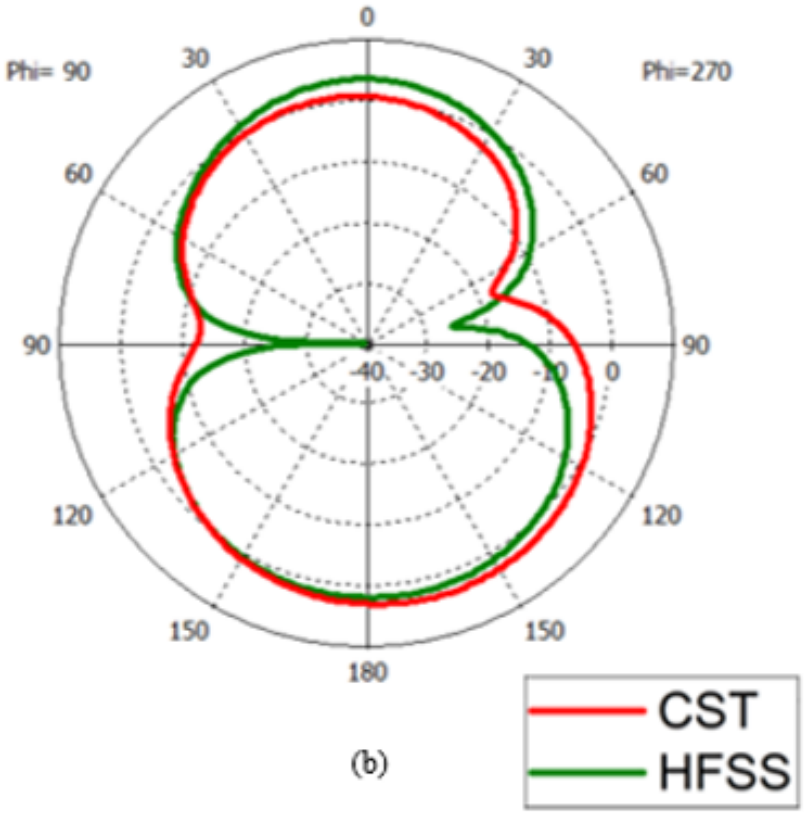

Figure 4.12 Simulated radiation pattern at 3.5 GHz CST versus HFSS. (a) E-plane. (b) H-plane.

4.4 Conclusion

This study demonstrates that integrating Split Ring Resonator (SRR) unit cells and a Defective Ground Structure (DGS) significantly enhances the performance of a rectangular patch antenna for 5G Sub-6 GHz applications. The modified design achieved substantial improvements in bandwidth, gain, and electromagnetic behavior. Specifically, the antenna's bandwidth expanded to 2.26 GHz–5.4 GHz, with a peak S-11 parameter of -33 dB at 3.5 GHz. The gain increased to 4.15 dB at 5.2 GHz, showcasing the effectiveness of SRRs and DGS in coupling electric and magnetic fields, thereby strengthening resonance effects. The SRR unit cells functioned as metamaterials, exhibiting negative or near-zero permittivity, permeability, and refractive index, contributing to the antenna's superior performance. This study highlights the potential of SRR and DGS techniques in advancing antenna design for modern communication systems, offering valuable insights for future research in the field. The proposed antenna is suitable for UWB applications, and 5G Sub-6 GHz Mid-band applications.

REFERENCES

[1] S. Chen, J. Zhao, IEEE Commun. Mag. 52(5), 36 (2014).
[2] M. Agiwal, A. Roy, N. Saxena, IEEE Commun. Surveys Tuts 18(3), 1617 (2016).
[3] Kumari R, Kumar M. Frequency reconfigurable multi-band inverted T-slot antenna for wireless application. In Proceedings of the 2014 International Conference on Advances in Computing, Communications and Informatics, ICACCI 2014. 2014:696–699.
[4] Balanis CA. Antenna Theory, Analysis and Design, 3rd ed. New Jersey: John Wiley & Sons; 2016.
[5] Al-Bawri SS, Islam MT, Islam MS, Singh MJ, Alsaif H. Massive metamaterial system-loaded MIMO antenna array for 5G base stations. Sci. Rep. 2022;12(1):1–16
[6] Rani SS, Naik KK. Design and analysis of complimentary split ring resonator with slot on rectangular patch antenna for wireless applications. Int. J. Recent Technol. Eng. 2019;7(6):50–53.
[7] Bose S, Ramaraj M, Raghavan S, Kumar S. Mathematical modeling, equivalent circuit analysis and genetic algorithm optimization of an n-sided regular polygon split ring resonator (NRPSRR). Procedia Technol. 2012; 6:763–770.
[8] Kumar G, Ray KP. Broadband microstrip antennas. MA, USA: Artech House; 2003.
[9] Huang Y, Boyle K. Antennas from Theory to Practice, 1st ed. West Sussex, United Kingdom: John Wiley & Sons; 2008.
[10] Balanis CA. Antenna Theory, Analysis and Design, 3rd ed. New Jersey: John Wiley & Sons; 2016.

CHAPTER V

a Compact Size Frequency Selective Surface Unit Cell Design for Ultra-Wideband Filtering and Shielding Applications

5.1 Introduction

The rapid advancement of mobile communications systems, particularly over the last two decades, has significantly heightened the interest in Frequency Selective Surface (FSS) applications. FSS structures have emerged as crucial components in various electromagnetic applications, including spatial filtering, electromagnetic shielding, and enhancing antenna performance by acting as reflectors to boost gain [1-3]. FSS technology is deeply rooted in electromagnetic theory, with its core functionality being derived from two-dimensional periodic arrays of metallic elements embedded in a dielectric substrate. These arrays demonstrate specific transmission and reflection characteristics at resonant frequencies, which are essential for their filtering capabilities [2].

However, conventional FSS designs have been limited by several challenges, particularly their insufficient spatial filtering performance and narrow bandwidth, which restrict their application in modern communication systems. Recent research efforts worldwide have concentrated on overcoming these limitations by miniaturizing FSS structures and enhancing their frequency bandwidth, especially under dual polarization and at higher incidence angles. These advancements aim to create more versatile and efficient FSS designs for broader electromagnetic applications [3-7].

In this chapter, we propose an FSS unit cell design intended to filter electromagnetic signals across the entire Ultra-Wideband (UWB) frequency range, spanning from 3.1 to 10.6 GHz [8]. The proposed FSS design achieves a wide stop-band response, characterized by a significant -10 dB attenuation, covering frequencies between 2 and 16 GHz, thus encompassing an impressive 14 GHz bandwidth. Furthermore, the design exhibits excellent shielding effectiveness, making it suitable for various high-performance applications. The simulation results, obtained through time-domain analysis using CST Microwave Studio software, demonstrate the potential of this FSS design in UWB filtering and shielding applications [9].

5.2 FSS Unit Cell Design

The geometry of the proposed single-layered Frequency Selective Surface unit cell is depicted in Figure 5.1(a). The design features a square patch with two reverse hexagonal slots embedded within it. This copper patch is deposited on the top surface of an FR4 substrate, which has a thickness of 1.6 mm. The overall dimensions of the unit cell are Wu × Lu = 6 × 6 mm. Detailed geometric parameters of the FSS unit cell can be found in Table 5.1.

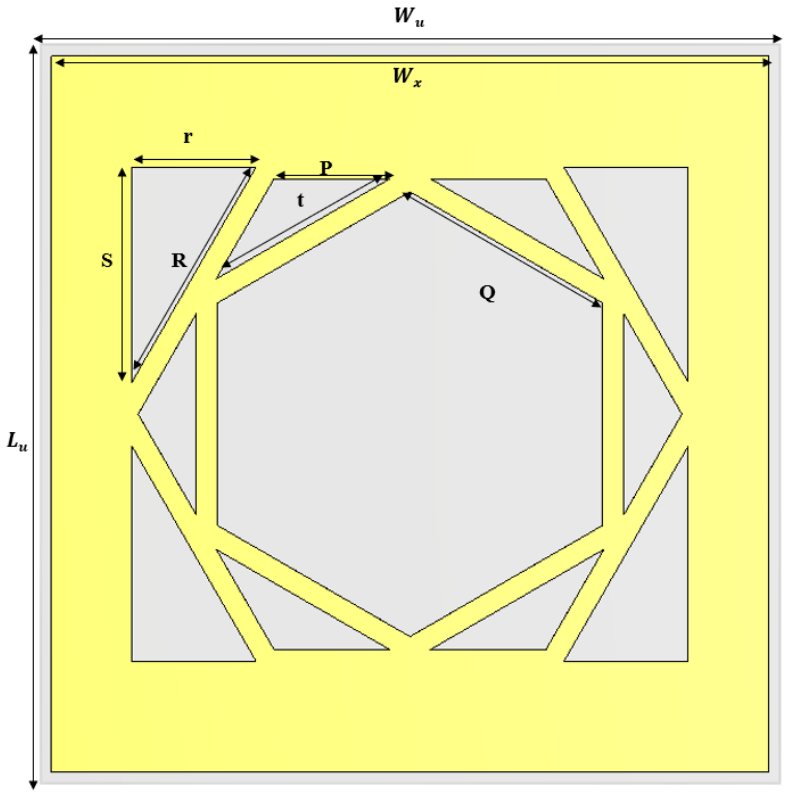

(a)

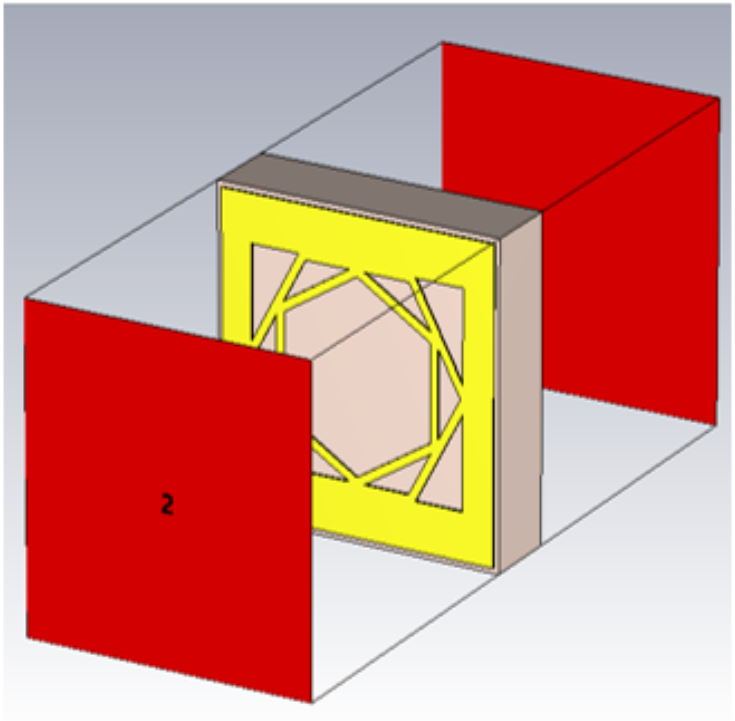

(b)

Figure 5.1. (a) Configuration of the unit cell. (b) Simulated model of the unit cell.

Table 5.1. Parameters' values of the unit cell.

Parameter	Value (mm)
Wu	6
Lu	6
Wx	5.8
R	2.01
r	1
s	1.74
p	0.94
t	1.62
Q	1.8

For the simulation of this FSS unit cell, CST Studio Suite, a comprehensive electromagnetic simulation software, was employed. This software utilizes the Finite Integration Technique (FIT) to accurately model and simulate electromagnetic behavior, making it well-suited for FSS structure analysis [10]. Figure 5.1(b) illustrates the simulation setup, where the FSS structure is aligned in the XY plane, positioned between two waveguide ports along the Z-axis, which represents the direction of wave propagation.

The boundary conditions applied to the simulation include a Perfect Electric Conductor (PEC) boundary along the X-axis and a Perfect Magnetic Conductor (PMC) boundary along the Y-axis. These boundary conditions are essential for ensuring accurate electromagnetic behavior representation, with the PEC serving as an idealized electric conductor and the PMC acting as its magnetic counterpart. This configuration enables precise analysis of the proposed FSS unit cell's performance under different electromagnetic conditions, allowing for optimization of the design for its intended filtering and shielding applications.

5.3 Results and discussion

5.3.1 Reflection/transmission coefficients

The reflection and transmission coefficients, denoted as S11 and S21 respectively, for the proposed unit cell (UC) are depicted in Figure 5.2. The performance analysis of these coefficients reveals that the designed UC effectively produces a broad stop-band response, which is essential for Ultra-Wideband (UWB) filtering applications. Specifically, the unit cell

achieves a significant stop-band characterized by a -10 dB reflection, covering a wide frequency range of 14 GHz, extending from 2 GHz to 16 GHz. This indicates that the UC is capable of attenuating signals across this broad spectrum, making it suitable for high-performance filtering and shielding in UWB applications.

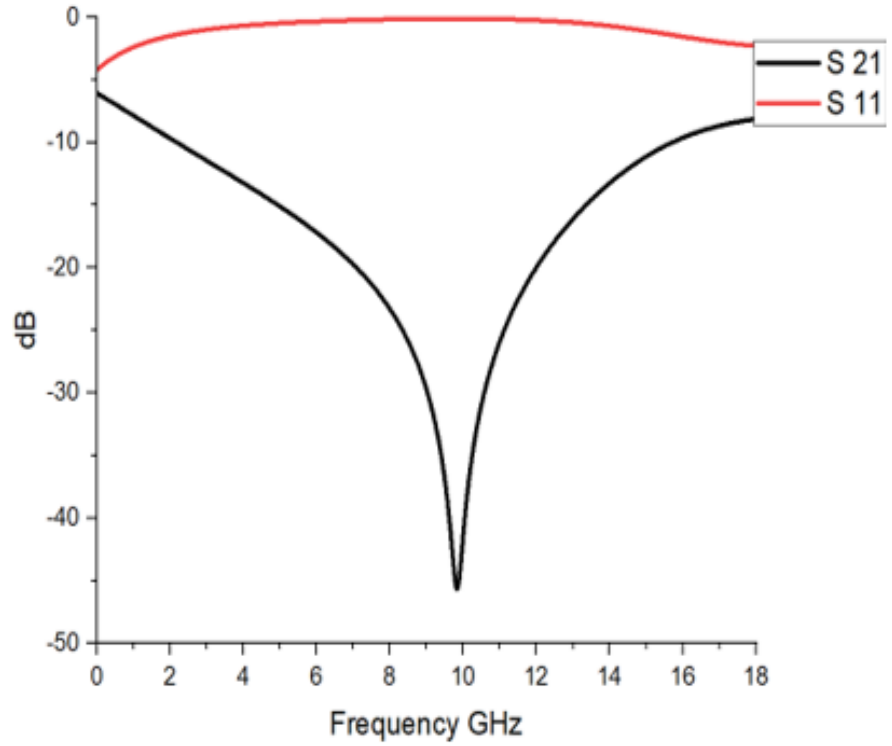

Figure 5.2. S-parameters of the unit cell.

Further analysis of the transmission coefficient (S21) is provided in Figure 5.3, where the effects of varying two key geometric parameters, Wx and Q, on the performance of the UC are examined. As shown in Figure 5.3(a), changes in the Wx parameter, which ranges from 5.6 mm to 5.9 mm, predominantly influence the upper frequency limit of the stop-band. This demonstrates that fine-tuning the Wx dimension can control the higher end of the frequency response.

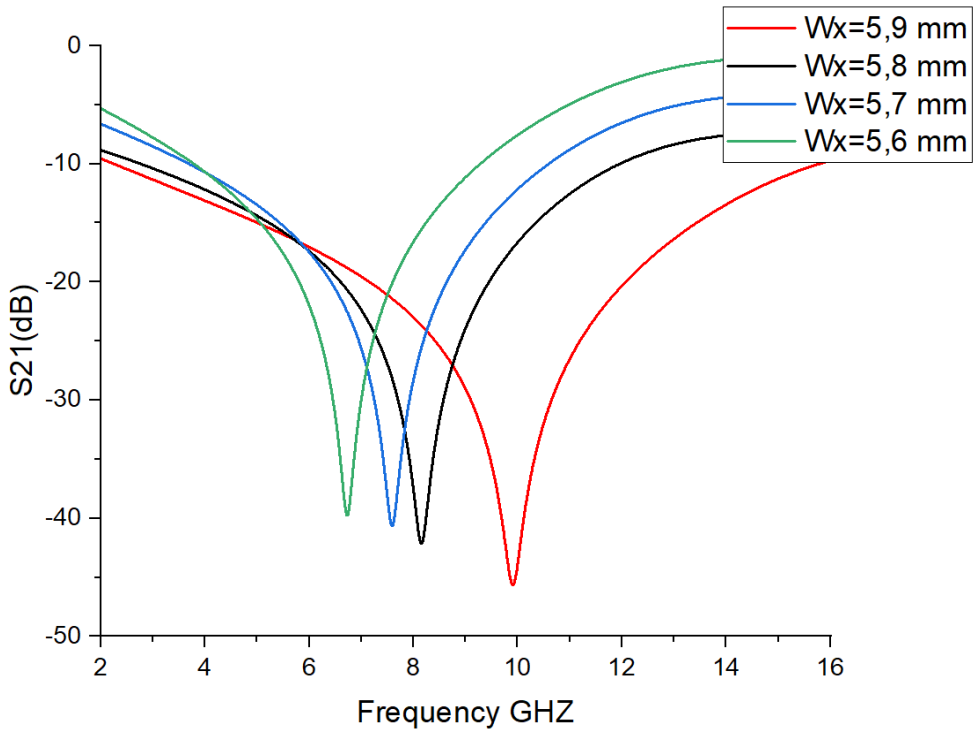

(a)

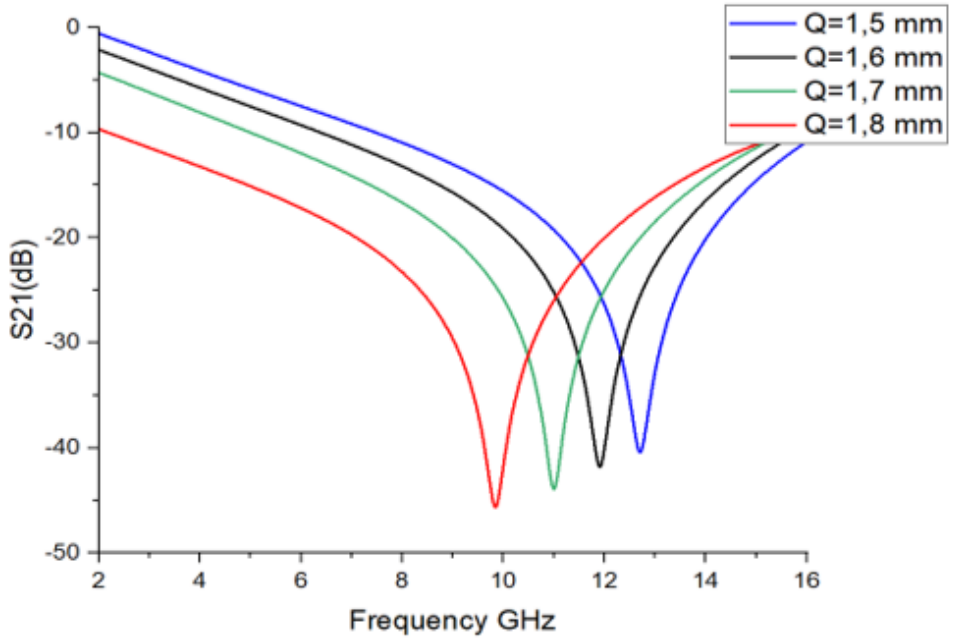

(b)

Figure 5.3. Simulated S-21 parameters of the unit cell for different values of (a) Wx and (b) Q.

Similarly, Figure 5.3(b) illustrates the impact of altering the Q parameter, which varies from 1.5 mm to 1.8 mm. In this case, modifying the Q dimension primarily affects the lower frequency limit of the stop-band. This sensitivity analysis highlights the importance of these parameters in shaping the overall frequency response of the UC, allowing for precise control over the filtering range to meet specific design requirements.

5.3.2 Shielding Effectiveness

Shielding effectiveness (SE) is a crucial metric in evaluating the performance of Frequency Selective Surfaces (FSS), particularly for electromagnetic shielding applications. SE is typically quantified by the ratio of the magnitudes of the incident electric field (E_i) to the transmitted electric field (E_t), and is often expressed in decibels (dB). The standard equation used to compute SE is as follows:

$$SE(dB) = 20 \cdot \log_{10}\left(\frac{E_i}{E_t}\right) \tag{22}$$

This equation allows for the evaluation of how effectively the FSS structure attenuates the electromagnetic waves passing through it.

As illustrated in Figure 5.4, the designed FSS structure demonstrates strong shielding effectiveness across a broad frequency band, from 2 GHz to 16 GHz. The SE remains consistently above 10 dB within this range, indicating effective attenuation of electromagnetic signals. Notably, the structure achieves a peak SE of 49.22 dB at 9.9 GHz, which highlights its capability to provide substantial shielding at that frequency. This performance underscores the suitability of the FSS design for applications requiring high levels of electromagnetic interference (EMI) suppression, making it an excellent candidate for UWB shielding applications.

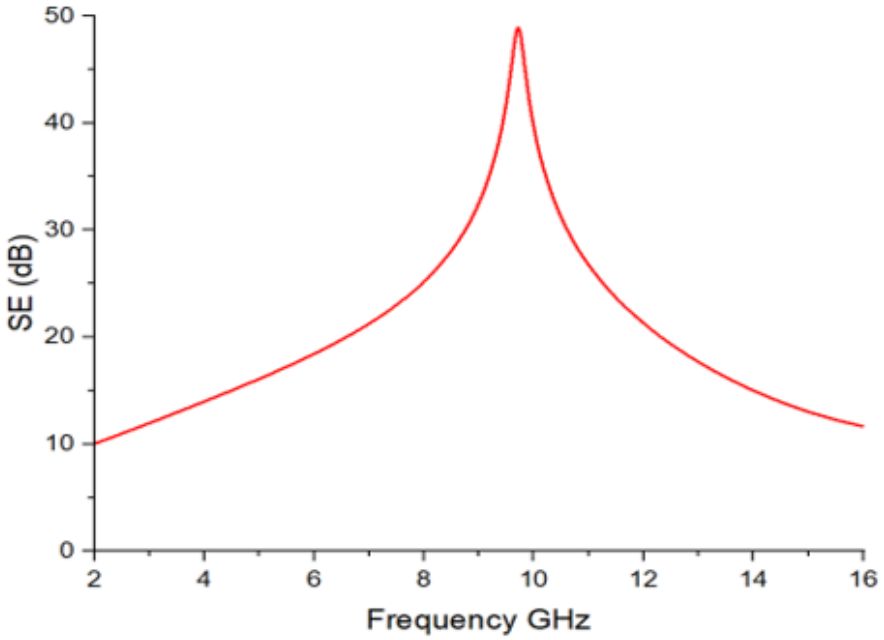

Figure 5.4. Shielding effectiveness of the designed FSS.

5.3.3 Array analysis

In many practical applications, a single unit cell (UC) is insufficient to provide adequate electromagnetic performance, particularly in terms of shielding and filtering effectiveness. Instead, an array of unit cells is typically required to achieve the desired electromagnetic characteristics. Figure 5.5 presents the simulated model setup for various array configurations, ranging from the previously discussed single UC (1x1 configuration) to larger arrays, including 2x2, 3x3, and 4x4 arrays. These configurations correspond to overall dimensions of 6x6 mm, 12x12 mm, 18x18 mm, and 24x24 mm, respectively.

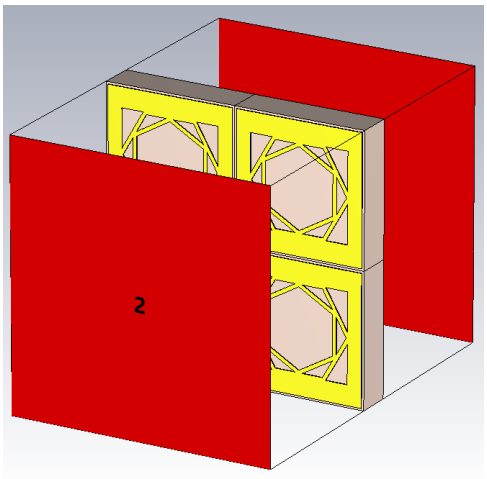

(a)

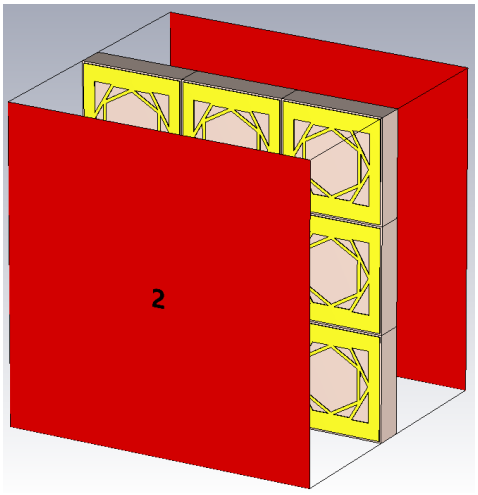

(b)

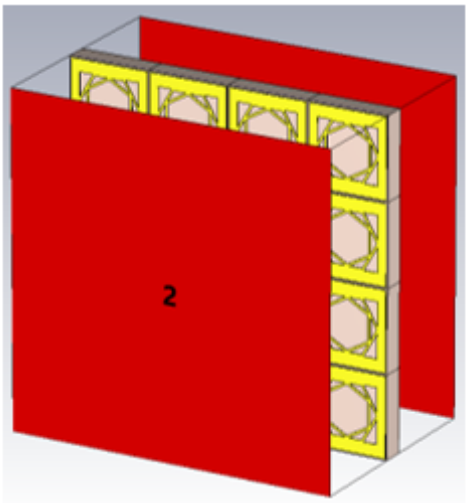

(c)

Figure 5.5. Simulated model setup of several array configurations: (a) 2x2, (b) 3x3, (c) 4x4.

The performance of these different array configurations is evaluated in terms of the transmission coefficient (S21) and shielding effectiveness (SE). The simulation results for the S21 parameter across the various array arrangements are displayed in Figure 5.6, while Figure 5.7 illustrates the corresponding SE values. The study reveals how increasing the array size improves the electromagnetic response, enhancing both the stop-band performance and the shielding effectiveness over a broader frequency range.

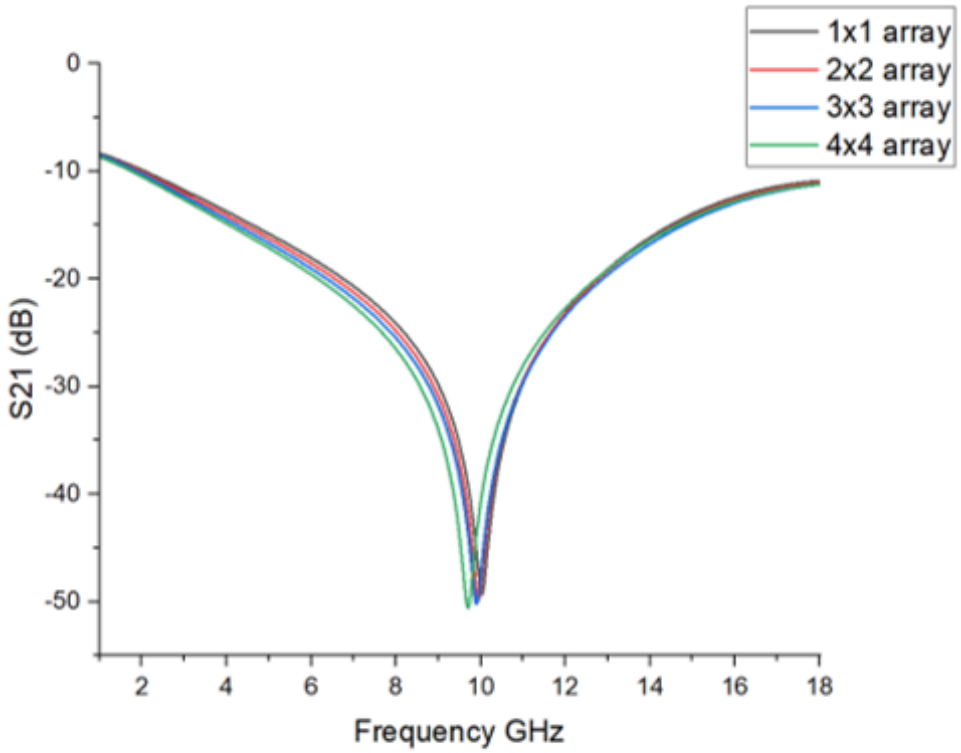

Figure 5.6. S21 of several array arrangements.

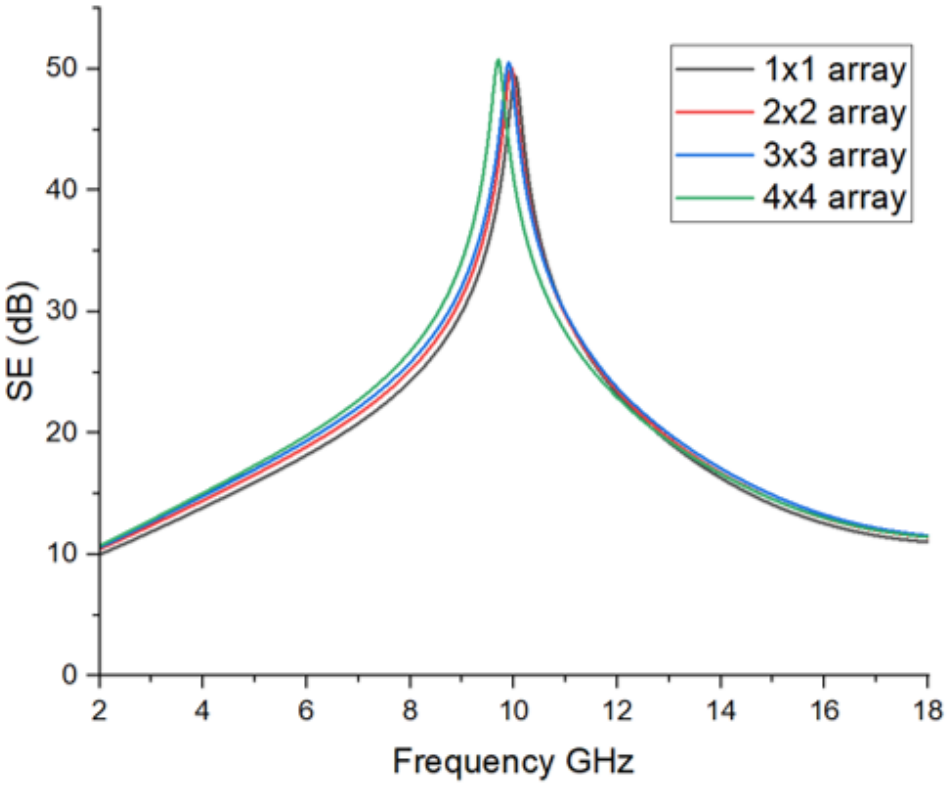

Figure 5.7. SE of several array arrangements.

The parameters derived from the analysis of these array configurations are summarized in Table 5.2. These findings demonstrate that larger arrays provide more effective electromagnetic shielding and filtering, making them more suitable for practical applications where enhanced performance is critical. This is particularly relevant for Ultra-Wideband (UWB) applications, where achieving broad stop-band coverage and high shielding effectiveness is essential. Table 5.3 contains a comparison of the proposed structure with similar works.

Table 5.2: Parameters of: 1x1, 2x2, 3x3, 4x4 arrays.

Configuration	Frequency Range (GHz)	S21 dips (dB)	Maximum SE (dB)
1x1	2-16	-49.22	49.22
2x2	1.94-17.84	-49.72	49.72
3x3	1.86-18.24	-50.22	50.22
4x4	1.75-18.67	-50.57	50.57

Table 5.3 a Comparison between the proposed FSS design and similar works.

Ref	UC Size (mm)	Substrate type	Substrate thickness	Stop-band (GHz)
11	10×10	FR-4	1.6	3.1-13.3
12	8×8	FR-4	1.6	2.7-13.23
This work	6×6	FR-4	1.6	2-16

5.4Conclusion

This section presents a design of a single-layered Ultra-Wideband Frequency Selective Surface (UWB-FSS) that functions as a band-stop spatial filter with ultra-wide stop-band characteristics. The structure has been implemented on a cost-effective FR4 substrate, making it a practical and affordable solution for various applications. The proposed FSS design

achieves an exceptionally wide stop-band, ranging from 2 GHz to 16 GHz, which is critical for effective signal filtering in the UWB frequency range.

In addition to its broad stop-band performance, the design also exhibits excellent shielding effectiveness, ensuring that electromagnetic interference (EMI) is effectively attenuated across the targeted frequency spectrum. The compact size of the FSS unit cell further enhances its suitability for integration into modern electronic systems where space is often a constraint. The simulation results confirm that the proposed structure meets the necessary performance criteria, making it an ideal candidate for UWB applications where both filtering and shielding are essential.

References

[1] De Sabata A, Matekovits L, Buta A, Dassano G, Silaghi A. Frequency Selective Surface for Ultra-Wide Band Filtering and Shielding. Sensors (Basel). 2022 Feb 28;22(5):1896. DOI: 10.3390/s22051896. PMID: 35271041; PMCID: PMC 8914931. J. Clerk Maxwell, A Treatise on Electricity and Magnetism, 3rd ed., vol. 2. Oxford: Clarendon, 1892, pp.68–73.
[2] Munk, B.A. Frequency Selective Surfaces: Theory and Design. In Frequency Selective Surfaces; John Wiley & Sons, Ltd.: Hoboken, NJ, USA, 2000.
[3] Anwar, R.S.; Mao, L.; Ning, H. Frequency Selective Surfaces: A Review. Appl. Sci. 2018, 8, 1689.
[4] Chiu, C.-N.; Chang, K.-P. A novel miniaturized-element frequency selective surface having a stable resonance. IEEE Antennas Wirel. Propag. Lett. 2009, 8, 1175–1177.
[5] Abdelrahman, A.H.; Elsherbeni, A.Z.; Yang, F. Transmission phase limit of multilayer frequency-selective surfaces for transmit array designs. IEEE Trans. Antennas Propag. 2014, 62, 690–697.
[6] Martinez-Lopez, L.; Rodriguez-Cuevas, J.; Martinez-Lopez, J.I.; Martynyuk, A.E. A multilayer circular polarizer based on bisected split-ring frequency selective surfaces. IEEE Antennas Wirel. Propag. Lett. 2014, 13, 153–156.
[7] Abadi, S.M.A.M.H.; Li, M.; Behdad, N. Harmonic-suppressed miniaturized-element frequency selective surfaces with higher order bandpass responses. IEEE Trans. Antennas Propag. 2014, 62, 2562–2571.
[8] S. E. I. Daira, M. Lashab and M. Belattar, "a Compact Size FSS Unit Cell Design for UWB Filtering and Shielding Applications," 2023 International Conference on Advances in Electronics, Control and Communication Systems (ICAECCS), BLIDA, Algeria, 2023, pp. 1-4.
[9] CST Microwave Studio, Computer Simulation Technology, commercial software version 2021.
[10] Gooch, J.W., Daher, J.K. (2007). Fundamentals of Electromagnetic Shielding. In: Electromagnetic Shielding and Corrosion Protection for Aerospace Vehicles. Springer, New York, NY. https://doi.org/10.1007/978-0-387-46096-3_3
[11] S. S. Sampath and R. Sivasamy, "A Single-Layer UWB Frequency-Selective Surface With Band-Stop Response," in IEEE Transactions on Electromagnetic Compatibility, vol. 62, no. 1, pp. 276-279, Feb. 2020,
[12] Paul, G.S., and Mandal, K., Polarization-Insensitive and Angularly Stable Compact Ultrawide Stop-Band Frequency Selective Surface; LAWP Sept. 2019 1917-1921.

CHAPTER VI

a Novel Curved Single-Layer Frequency Selective Surface for Gain Enhancement of a Compact Size Coplanar Waveguide UWB Antenna

6.1 Introduction

Ultrawideband communications networks have attracted significant interest from industry experts in recent years. Researchers assert that UWB technology may surpass other technologies in terms of efficiency and success [1]. UWB devices possess numerous notable features, including a slim profile, small dimensions, an ultra-wide impedance bandwidth, and affordable production expenses. Typically, these gadgets use planar antennas, mainly monopole and slot antennas, fed through a coplanar waveguide (CPW) [2–5]. Because printed antennas lose little radiation, CPW-feed lines work well with this kind of antenna because they are easy to connect to surface components and don't depend as much on the thickness of the substrate [6]. Unlike the traditional method in microstrip antennas, which separates the patch area from the ground plane using a dielectric substrate, in a CPW both the patch and ground are located on a single surface atop the substrate, as indicated by the acronym. Research efforts established various radiating part forms, such as hexagonal, triangular, circular, and rectangular, to offer a broad impedance bandwidth [7, 8]. Researchers are enhancing the antennas by using various slotted configurations in the feed line, ground plane, and patch, leading to a significant improvement in bandwidth [9]. For better accuracy and detection range in certain situations, like ground-penetrating radar (GPR) antenna radomes, radar cross section (RCS), and microwave imaging systems, it is important to use UWB devices with substantial gain and directivity [10, 11]. Different methods, such as AMCs [12], antenna arrays [13], RISs [14], and FSSs [15], can also enhance these attributes.

Frequency selective surface (FSS) effectively meets the increasing demand for wider bandwidth in mobile communications, as well as sophisticated applications that rely on a specified bandwidth for operation. Consequently, a global competition has emerged to develop advanced methods that effectively generate distinct signals over a broad spectrum of frequencies [16]. Frequency-selective surfaces exhibit a prompt reaction due to the duplication of a predetermined cell element. These materials consist of a printed arrangement of unit cell (UC) resonators over a substrate, serving as a spatial filter. This filter enables electromagnetic radiation to either reflect (stop-band filter) [17] or transmit (pass-band filter) [18] through the FSS system. Correctly conceived and constructed UWB FSS UC reflective elements have the potential to enhance the characteristics of a UWB antenna [19]. Furthermore, this design improves usability and protects UWB antennas from nearby metallic elements, thereby ensuring optimal performance. This feature also enables angular flexibility for UWB apps [20,

21]. Various methods involving multi- and single-layer configurations are employing FSS to enhance the gain of UWB transmitters [22, 23].

This chapter presents a new design that combines a curved single-layered frequency selective surface with a small coplanar waveguide ultra-wideband antenna to boost gain [1]. A CPW powers an UWB monopole and develops it on a FR-4 substrate. Subsequently, the monopole was positioned on top of the 11 × 11 curved frequency selective surface reflector, also made from FR-4 material, with each unit cell measuring 13 x 13 mm. The overall structure exhibits a very broad impedance bandwidth that spans 2.66 GHz to 17.98 GHz (148%), encompassing the entire ultra-wideband frequency spectrum. The integration of the monopole and curved reflector results in a substantial increase in gain, which fluctuates between 0.2 ~ 5.4 dB and 8.8 ~ 14.9 dB across the working range. The design directs the radiation patterns, achieving a peak gain boost of 10 dB at 10.6 GHz. We conducted an analysis to evaluate the essential design features, comparing the conventional FSS approach with the suggested alternative through simulations and tests. The outcomes were highly satisfactory. We subjected the paired antenna-curved FSS reflective elements to a comparative analysis with previously published studies of a similar nature. The proposed framework is suitable for ultra-wideband and ground-penetrating radar systems.

6.2 Antenna Design

The proposed antenna is constructed on a 1.6-mm-thin FR-4 substrate. It has extremely small dimensions of 20 × 25 mm^2, a relative permittivity of ε_r= 4.4, and a loss tangent of tan δ = 0.025. The structure comprises of a square-shaped patch that emits radiation and a metallic ground plane, both manufactured from annealing copper. We position these components over the substrate. The setup consists of a 50 Ω microstrip line with a feed line length of 6 mm and a width of 2 mm. To evaluate the design process, we can use formulas (23) through (28) to determine the physical dimensions of the monopole:

$$\frac{\lambda_L}{4} < L_{sub} < \frac{\lambda_L}{3} \quad (23)$$

$$W_{sub} \approx \frac{\lambda_L}{5} \quad (24)$$

$$\frac{\lambda_L}{6} < W_p < \frac{\lambda_L}{5} \quad (25)$$

$$W_g \approx \frac{\lambda_L}{11} \quad (26)$$

$$L_g = 3 \times h \quad (27)$$

$$L_f \approx L_g + h \quad (28)$$

λ_L represents the wavelength at the lowest boundary of the ultra-wideband frequency spectrum, measuring 3.1 GHz. 'h' denotes the depth of the substrate.

Computing simulation software is utilized to optimize parameters. Figure 6.1 provides the configuration of the monopole, and Table 6.1 contains the parameter values for the prescribed design.

Table 6.1 Values of the design parameters.

Parameter	Value (mm)	Parameter	Value (mm)
W_{sub}	20	a	3.75
L_{sub}	20	b	4.02
W_p	18	c	2.75
W_g	8.7	d	12.75
L_g	4.8	i_1	0.5
W_f	2	i_2	0.25
L_f	6	j	2

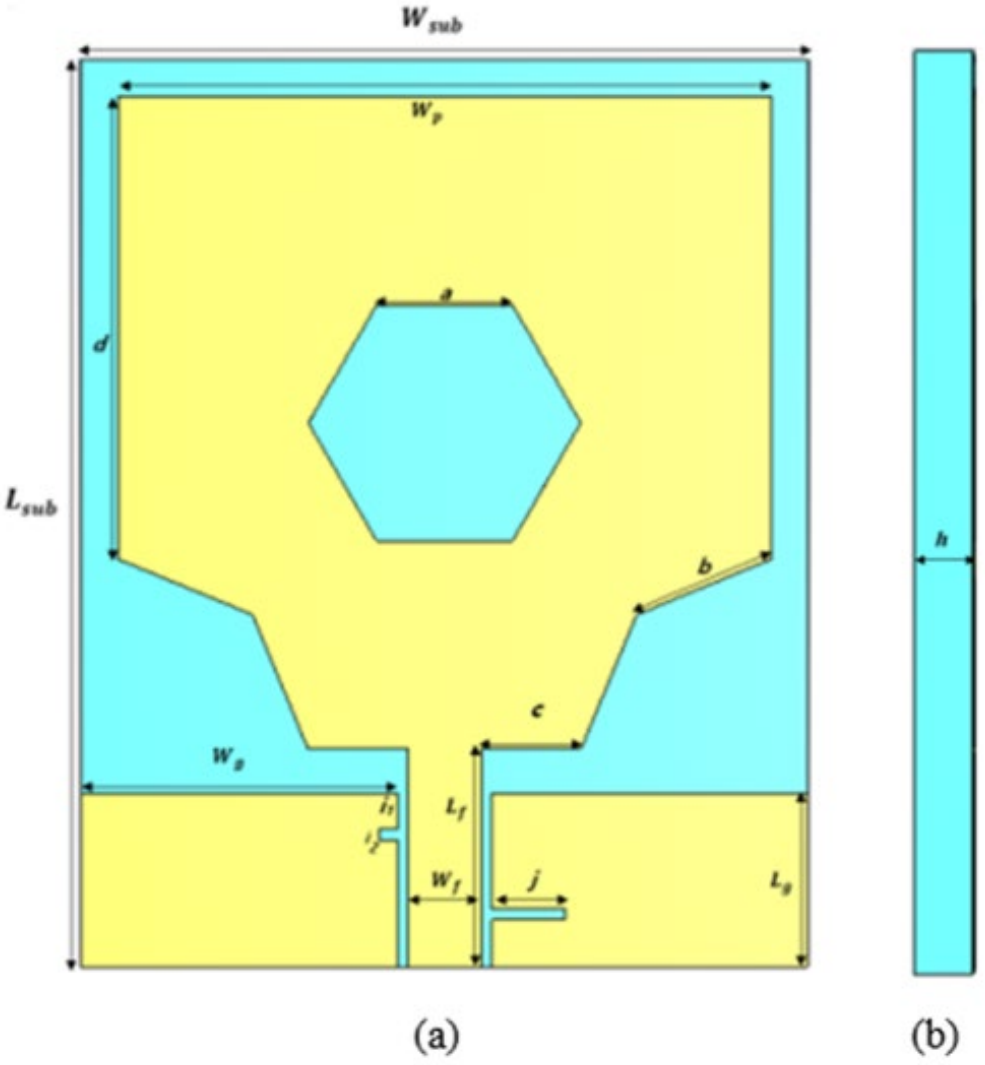

Figure 6.1 Proposed design configuration. (a) Top view. (b) Side view.

To expand the bandwidth across the entire UWB frequency range (3.10~10.60 GHz), different slots have been added to the monopole, as shown in Figure 6.2. Removing twin tiny sections from the ground plane, creating a hexagonal opening in the patch's center, and then making two similar cuts at the patch's lower ends. These alterations have the potential to alter the existing arrangement and impact the capacitance and inductance, leading to an expanded range of frequencies for the antenna.

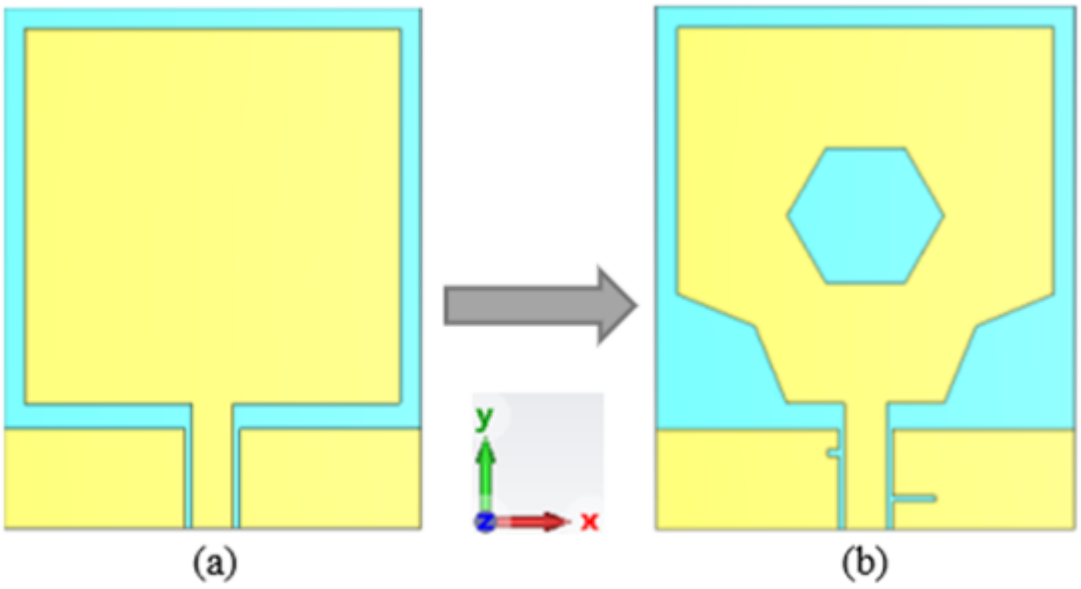

Figure 6.2 (a) Basic antenna. (b) Proposed antenna.

Figure 6.3 depicts the return loss properties of each of the conventional and suggested antennas. The fundamental layout exhibits a limited impedance bandwidth (−10 dB) spanning 3.35 to 4.94 GHz (24%), indicating a significant impedance mismatch. Conversely, the proposed monopole demonstrates a significantly broad impedance bandwidth spanning 2.8 to 17.91 GHz (146%), including the entire UWB spectrum. It also displays favorable impedance matching and resonates at 3.7 GHz and 13.58 GHz.

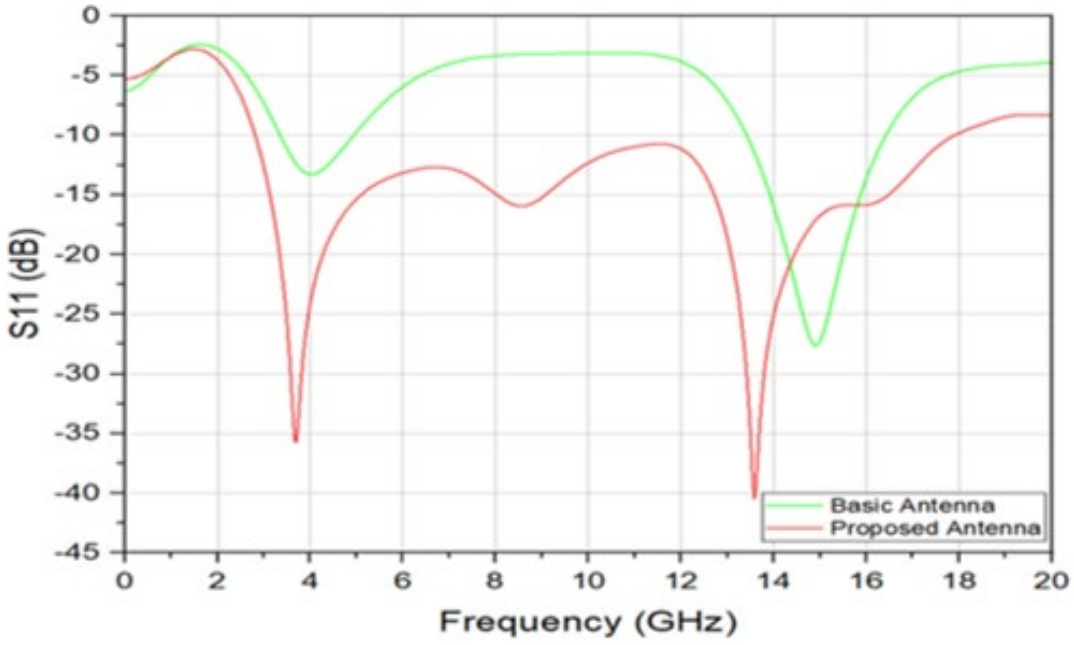

Figure 6.3 Simulated S-11 Vs frequency.

6.3 Unit Cell Design

Signal processing systems operating in the microwave and optic frequency ranges widely recognize spatial filtering as a highly effective procedure [24]. We employ FSS, also known as spatial filters, to modify incident electromagnetic waves and produce dispersive reflecting and/or transmitting characteristics [25]. Based on their operation, we can categorize FSSs into high-pass, low-pass, bandpass, and band-stop filters. Normally, periodic arrays of metal components (patches and slots) etched on a dielectric material have been utilized to construct FSSs [26, 27]. One of the increasingly important steps in the design phase is selecting the appropriate parts, parameters, forms, and substrate materials for the FSS array [28, 29].

Figure 6.4 depicts the configuration of the single-layer FSS UC. Table 6.2 provides the physical parameters for this layout. The setup consists of a square patch featuring a 3 × 3 grid of hexagon-shaped holes that hold miniature hexagonal shapes. Mounted on a FR4 substrate, the copper radiating square boasts a total dimension of 13 x 13. The FSS UC arrangement employs hexagonal slots due to their advantageous characteristics. These include significant symmetry, promoting a uniform spread of energy, and minimizing unneeded resonances. Additionally, the hexagonal holes enable the effective utilization of space, resulting in enhanced frequency selectivity along with an extra small yet effective means of reaching the targeted frequency response. Furthermore, the relative simplicity of creating hexagonal holes simplifies the manufacturing process. A 3×3 FSS UC configuration may be selected for various reasons, such as enhanced performance, expanded bandwidth, and greater design adaptability. As the number of subcells increases, both the complexity and size of the frequency-selective surface increase. This is precisely why the recommended cell consists of a 3×3 subcell array. This configuration provides symmetry, allowing it to minimize unwanted resonances while maintaining an acceptable equilibrium regarding the number of subcells and the dimension of the FSS. As a result, the FSS delivers an acceptable harmony in efficiency, complexity, and size.

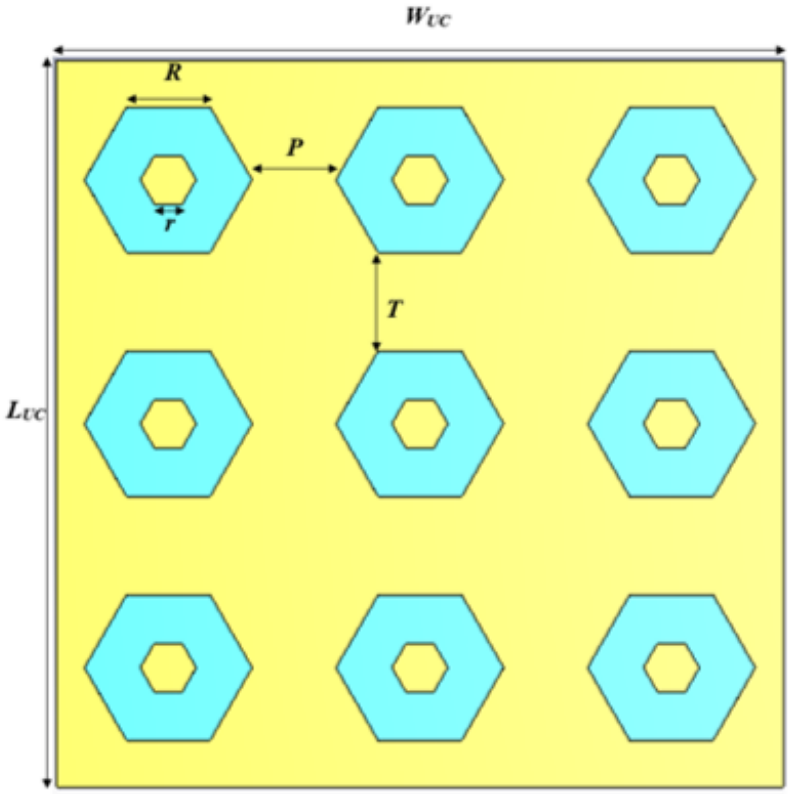

Figure 6.4 FSS unit cell geometry.

Table 6.2 Values of the FSS unit cell design parameters.

Parameter	Value (mm)	Parameter	Value (mm)
W_{uc}	13	R	0.5
L_{uc}	13	P	1.5
R	1.5	T	1.77

Figure 6.5 (a) and (b) depict the S_11 and S_21 coefficients for the constructed unit cell. It is evident that the reflection value is approximately 0 dB, while the transmission value is below -10 dB. These measurements are taken in a frequency spectrum spanning from 0 up to 18 GHz. To achieve reflection on the frequency-selective surface, one must have a phase response that decreases linearly throughout the baseline. This ensures the correct propagation path of the transmitted and reflected waves.

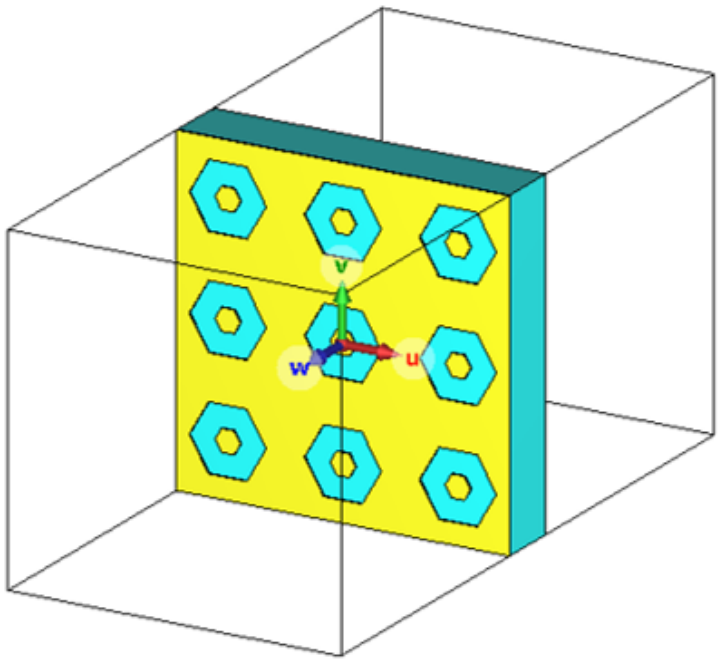
v
w
u

(a)

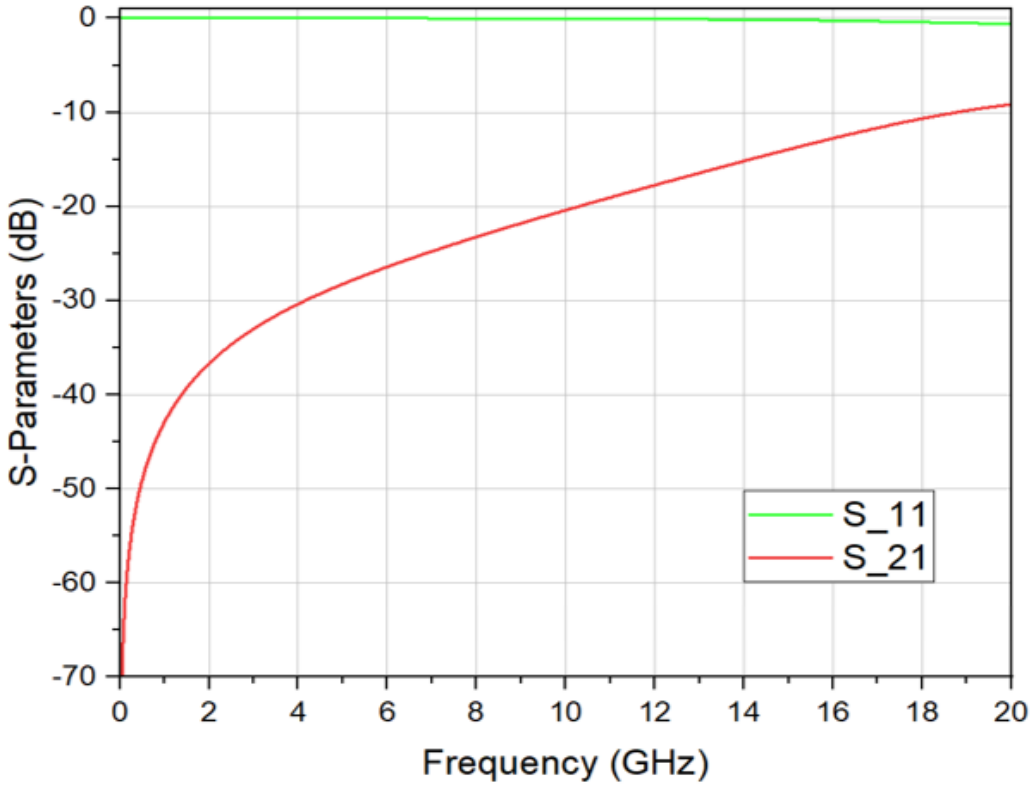
S-Parameters (dB)
0
-10
-20
-30
-40
-50
-60
-70
0
2
4
6
8
10
12
14
16
18
20
Frequency (GHz)
S_11
S_21

(b)

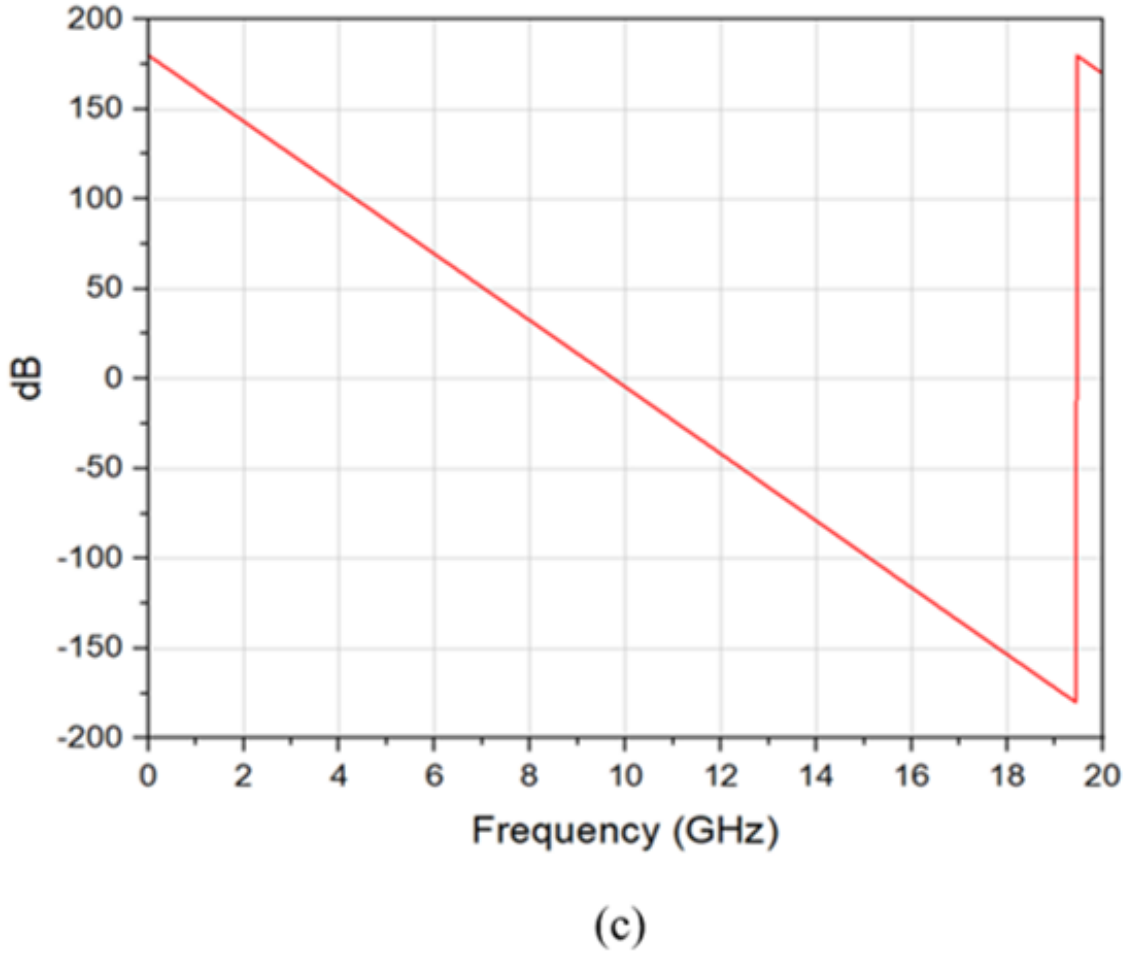

Figure 6.5 (a) UC simulation. (b) Transmission and reflection coefficients. (c) Reflection phase of the UC.

6.4Merged Antenna-FSS Design

The primary distinction between a metallic ground and a unit cell resides in the corresponding design and functionality. An FSS's UC is a structured arrangement that discriminates microwaves based on their frequency range. The main function of this arrangement is to selectively manipulate the reflection, absorption, or transmission of radio waves at specified frequencies. The dimensions, arrangement, and form of the unit cell, along with the dielectric characteristics of the substrate, influence the system's performance. A metallic ground is a solid piece of metal that serves as an anchor plane for electrical systems and offers a conducting channel for electromagnetic waves, acting as a barrier preventing interference. This clarifies the utilization of the FSS reflector to augment the gain of the monopole being suggested.

6.4.1 Flat Design

To achieve a significant increase in gain while receiving directed radiation across the ultra-wideband frequency range, the monopole antenna was positioned above the reflector array of the frequency-selective surface FSS. An extensive parametric analysis was carried out to ascertain the optimal quantity of UCs and the precise distance between the monopole and the structure.

We first examined the antenna's reflection coefficient for various amounts of 'd' (5, 10, 15, 20, and 25 mm) to analyze the impact of the spacing separating the monopole from the structure, as shown in Figure 6.6(a). When anticipated, the frequency-selective surface unit cells have an influence on the antenna's bandwidth, demonstrating that as the parameter "d" grows, the antenna's bandwidth also grows.

In addition, the impact of "d" on the monopole's gain performance is illustrated in Figure 6.6(b), where the gain is computed across the UWB spectrum for numerous amounts of “d”.

Ultimately, the separation space between the antenna and the reflector significantly influences the operating frequency range and the highest gain of the antenna. Based on this study, it is evident that the optimal “d” number is 25 mm, where “d” is approximately equal to $\lambda_L/4$. This particular value provides satisfactory performance throughout an entire range of frequencies.

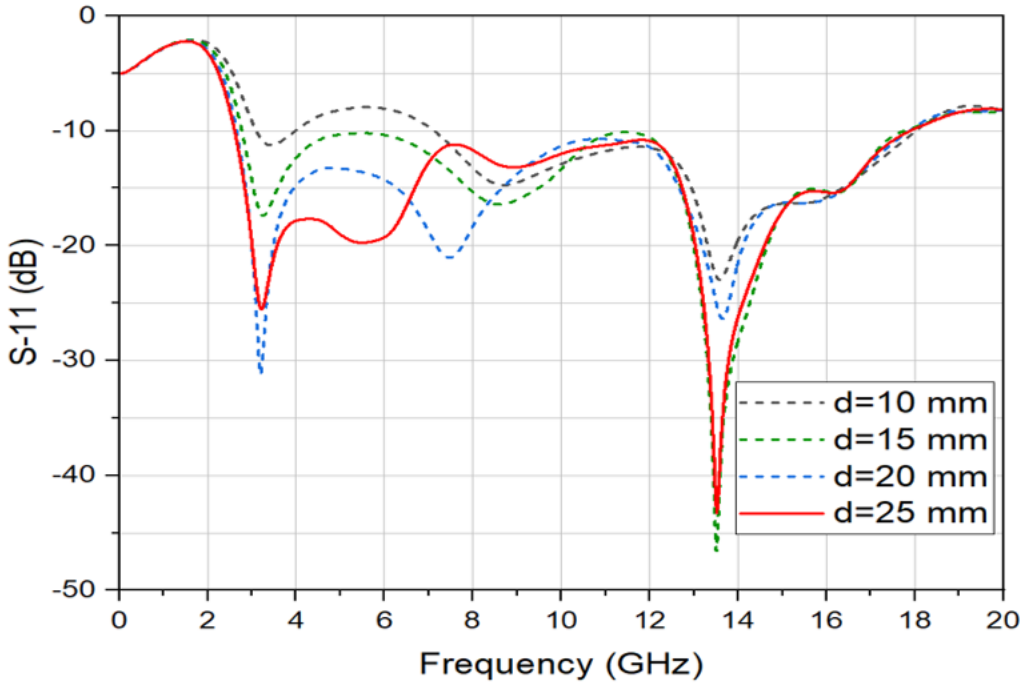

(a)

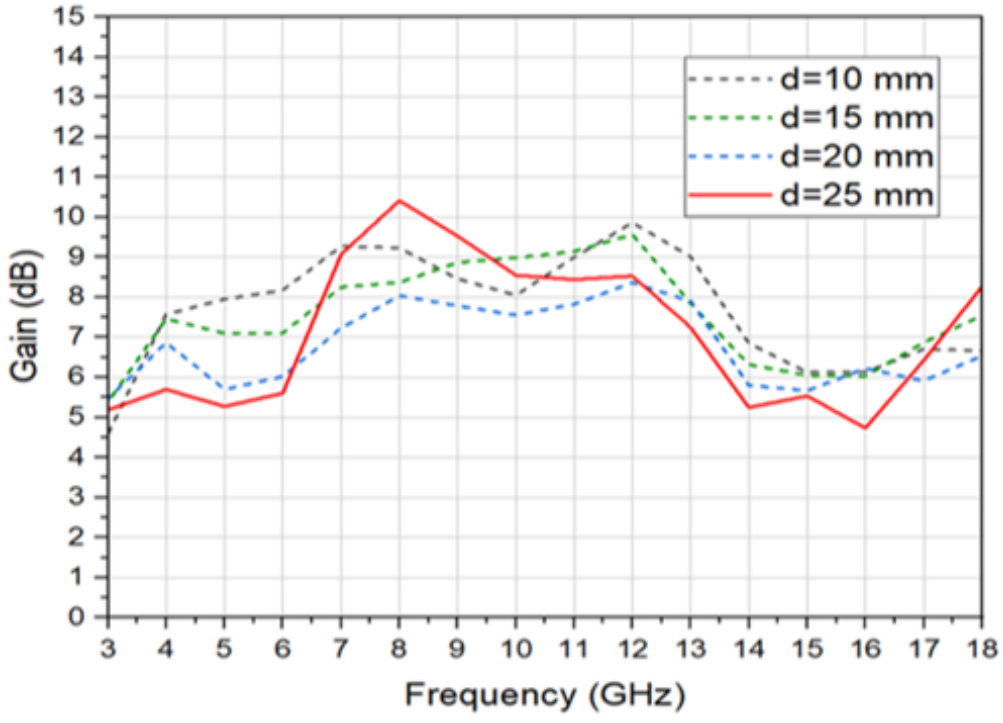

(b)

Figure 6.6 Parametric study of the distance "d" between the antenna and the FSS reflector. (a) Reflection coefficient for different values of "d". (b) Realized gain for different values of "d".

Figure 6.7 displays the findings of the study, which investigated the influence of the quantity of UCs on performance. We determine the reflective outcomes of the UC by calculating its size in relation to the antenna. In this case, the bandwidth is the only aspect of the FSS that matters. Figure 6.7(a) shows the S-11 of the unified structure, which has different numbers of UCs. Figure 6.7(b) illustrates a parametric evaluation of the antenna's realized gain, demonstrating that an FSS reflective material with 121 components (11 × 11) exhibits superior gain compared to reflectors with 81 components (9 × 9) and 49 components (7 × 7). This indicates that the gain is directly related to the number of unit cells (UCs), as raising the total number of UCs results in a boost in gain throughout the ultra-wideband spectrum.

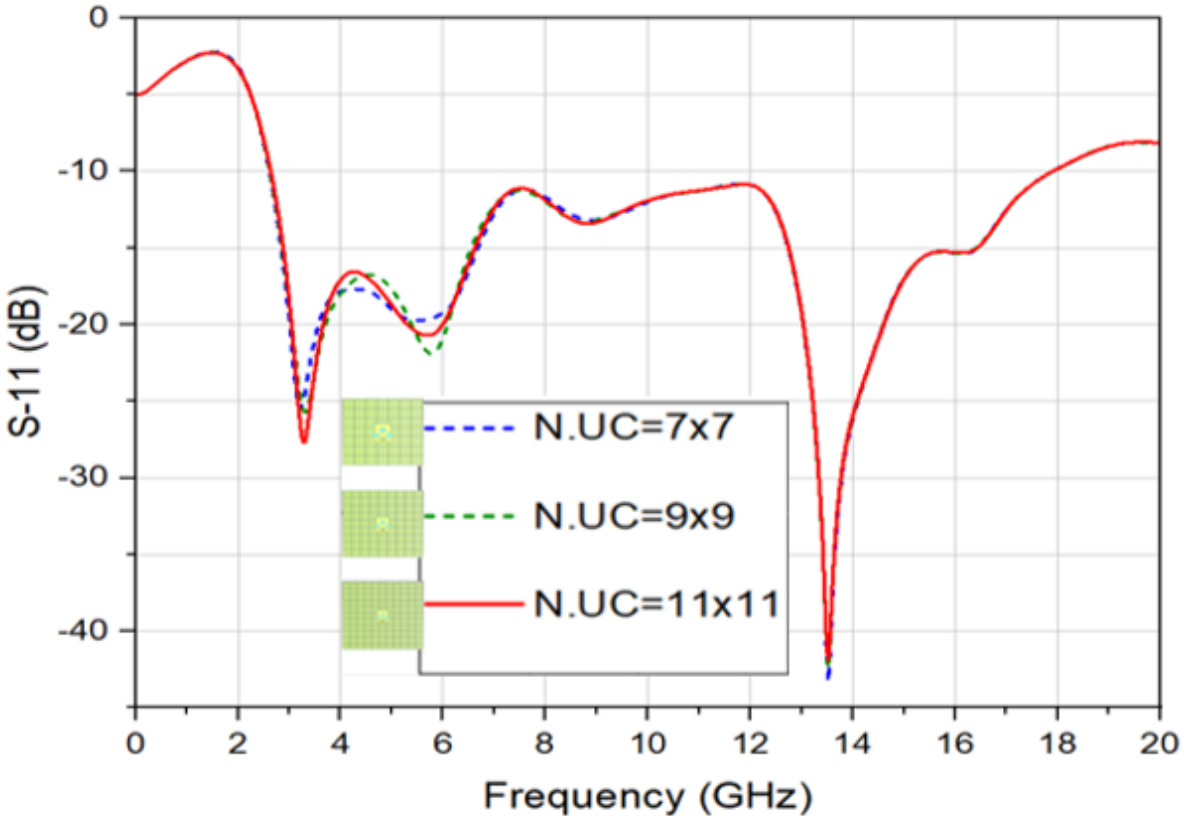

(a)

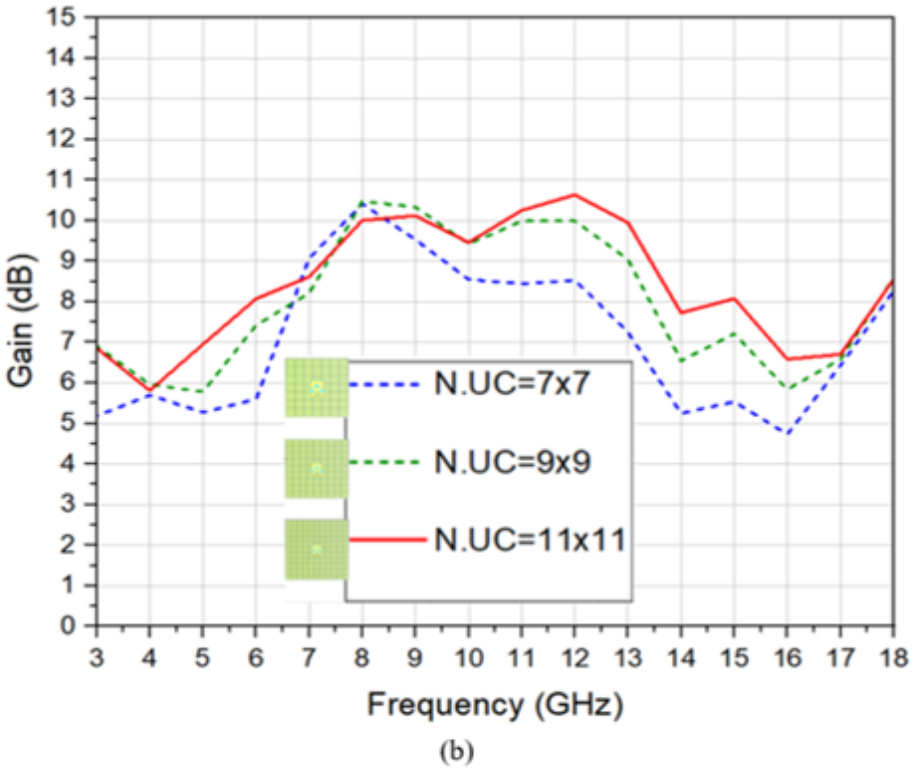

Figure 6.7 Parametric study about the effect of number of UCs on the antenna. (a) Reflection coefficient for different Number of UCs. (b) Realized gain for different Number of UCs.

6.4.2 Curved Design

The following subsection proposes a novel FSS configuration. We provide an example to elucidate the operating concept: we can describe a basic lamp that emits light uniformly in every direction as having an isotropic radiation pattern. We'll say that the beam of light emitted by the lamp is not bright enough for anyone to see; therefore, we are unable to increase its intensity. However, we do notice that a significant amount of light generated by the lamp is being emitted in unwanted directions. Placing a mirror above the lamp effectively doubles the brightness beneath it, reflecting all the dispersed illumination in that direction. To increase the number of beams, one can extend the setup by adding a second mirror at an angle. Additionally, we could potentially use a concave mirror to produce a highly luminous yet focused light beam. In our scenario, the term "lamp" denotes the antenna, whereas the term "mirror" signifies the FSS reflector. The antenna converts electrical power into electromagnetic radiation, which can travel throughout space. Typically, we position a flat frequency-selective surface configuration at a distance "d" beneath the radiating antenna to increase the gain by two times, as shown in Figure 6.8. In order to increase the amount of gain, it is feasible to flex the flat FSS at a specific

angle to form a curved configuration, as illustrated in Figure 6.9. The value of β, which is equal to 10°, denotes the angle among one UC and another in the curving orientation. We acquired this value through a series of experiments using an optimization tool.

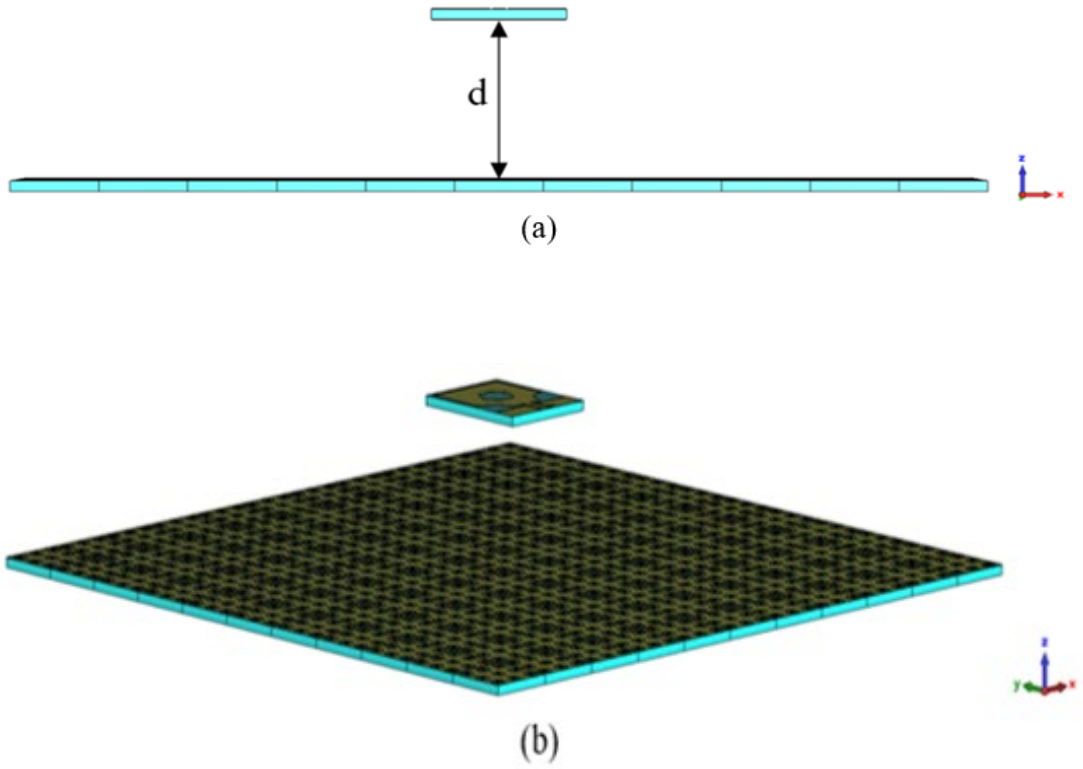

Figure 6.8 Combined antenna + flat FSS structure configuration. (a) Side view. (b) Angular view.

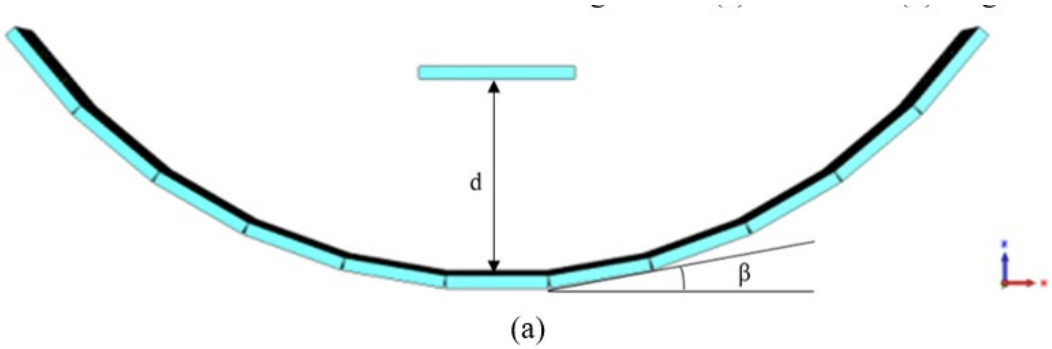

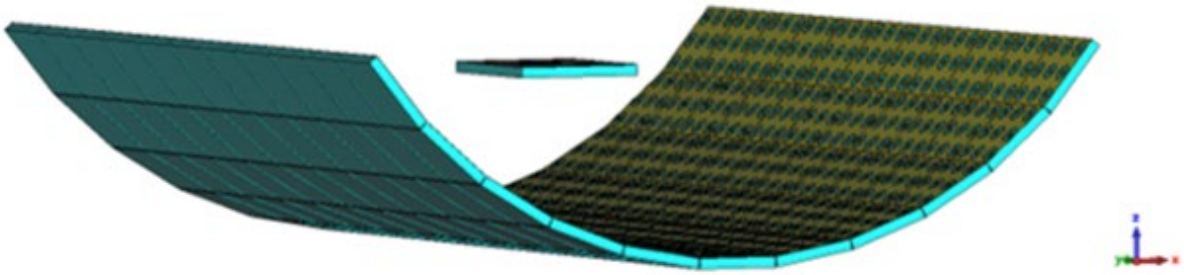

(b)

Figure 6.9 Combined antenna + curved FSS structure configuration. (a) Side view. (b) Angular view.

6.4.3 Flat Vs Curved FSS Design

Figure 6.10(a) displays S11 for both curved and flat constructions. It is evident that the reflection coefficient values for each of the merged curved and flat frameworks are nearly equal, indicating that curving the FSS has no impact on the antenna's bandwidth. By bending the frequency-selective surface, the gain improved significantly from 5.9 ~ 10.6 dBi to 8.8 ~ 14.9 dBi, as depicted in Figure 6.10(b). We observed this gain improvement in contrast to the configuration's S11 features. The electromagnetic characteristics of an FSS setup can impact the antenna's effectiveness by modifying its bending angle. Although the connection between the monopole gain and the curving degree of an FSS is not straightforward, they are connected in such a manner that a well-constructed FSS using an appropriate bending degree may enhance the monopole's performance. Reducing interference, improving the radiation pattern, or enhancing the directivity can all lead to increased antenna gain, as mentioned above.

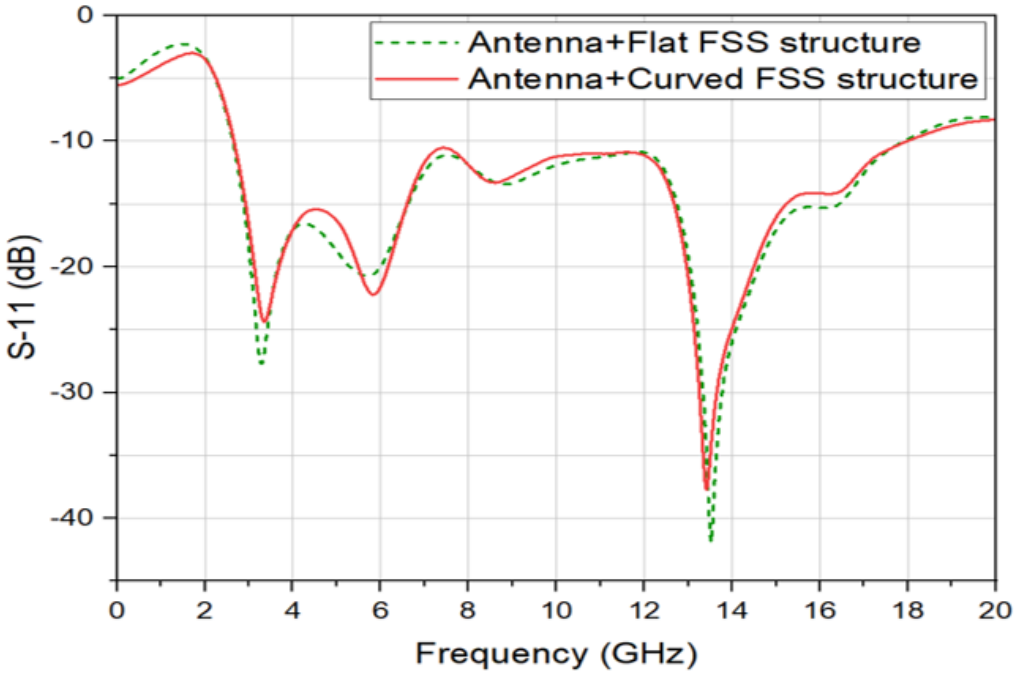

(a)

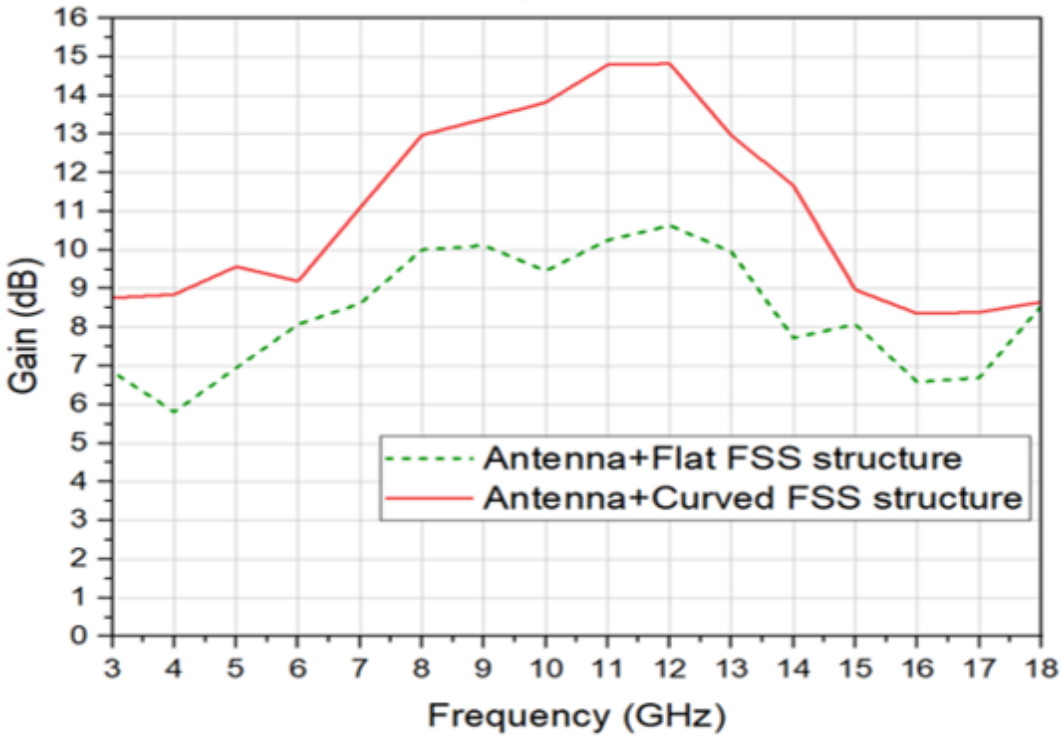

(b)

Figure 6.10 (a) Reflection coefficient and (b) Realized gain of the curved and flat FSS.

6.4.4 Simulation and measurements

This research has assessed the outcomes of simulations of the coplanar waveguide antenna using and without the curved structure to ascertain the characteristics of the constructed prototype. Figure 6.11 depicts the manufacturing of the layout on a FR-4 substrate.

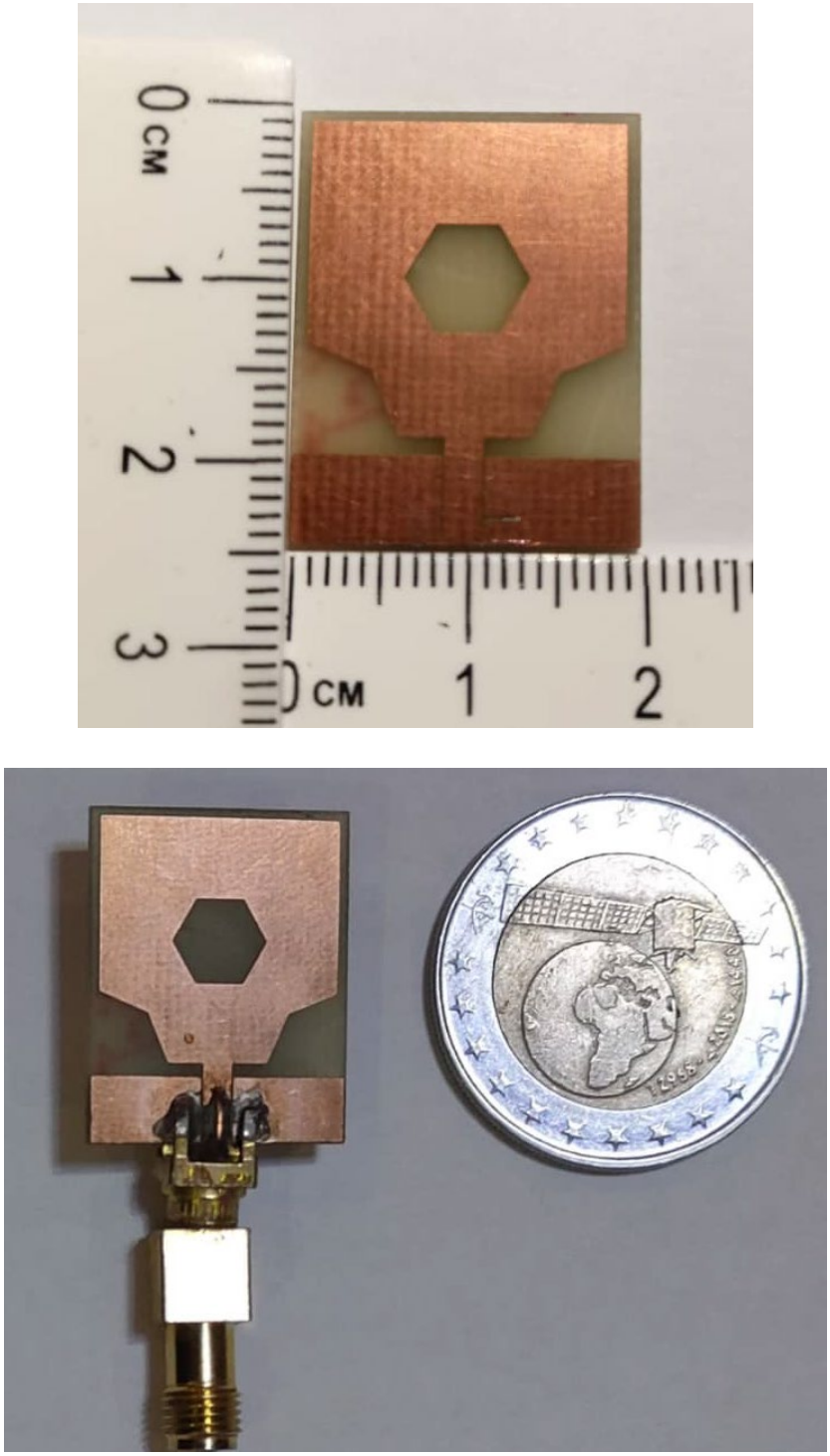

(a)

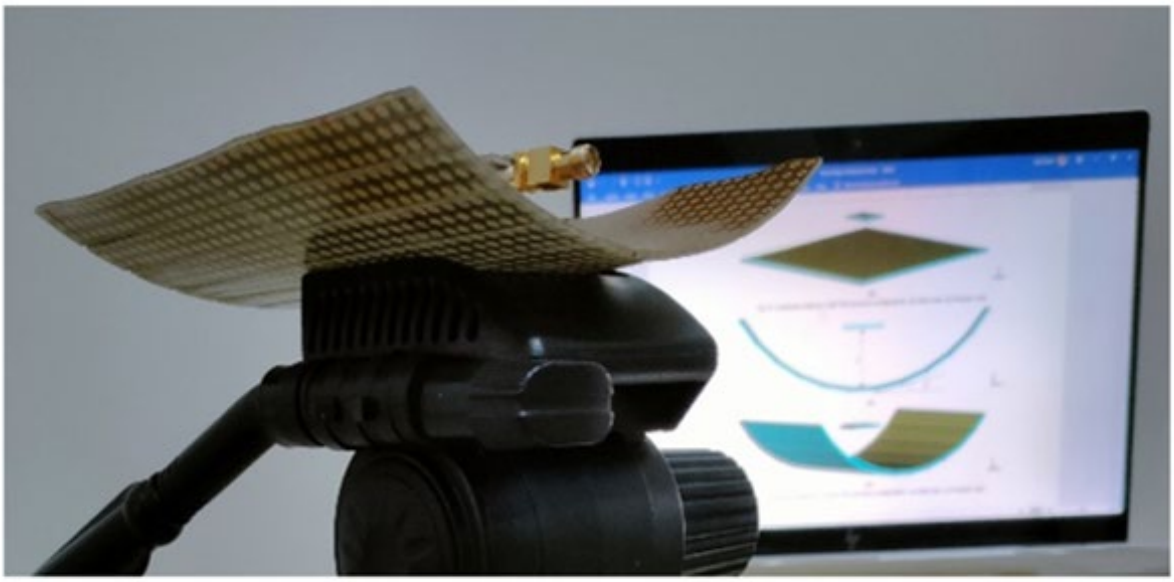

(b)

Figure 6.11 Fabricated designs. (a) UWB CPW-fed antenna. (b) Combined antenna-curved FSS reflector.

Figure 6.12 shows the simulated and measured reflection coefficients of the indicated UWB antenna, both alongside and without the curved structure. The independent monopole has a simulated bandwidth of 2.80 GHz to 17.8 GHz as well as a measured bandwidth of2.79 GHz to17.6 GHz. On the other hand, the merged structure has a simulated bandwidth of2.66 GHz to17.98 GHz as well as a measured bandwidth of2.39 GHz to 17 GHz. This indicates that the reflective elements do not significantly affect the monopole's bandwidth.

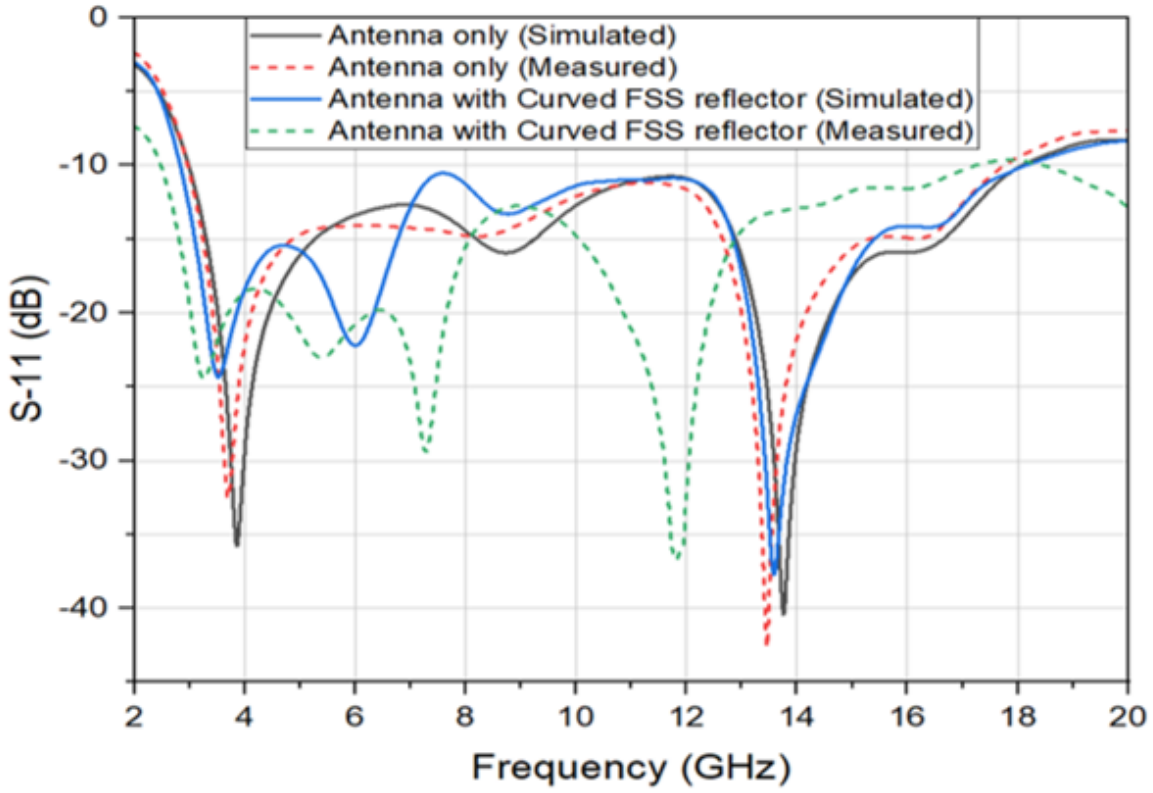

Figure 6.12 Simulated and measured S-11 of the suggested UWB monopole with and without the curved FSS reflector.

However, the peak gain rose significantly, as illustrated in Figure 6.13. The results show that the merged design has a simulated gain range of 8.8~14.9 dB as well as a measured gain of 8.9~14.8 dB. This indicates a substantial rise in the highest achievable gain compared to the lone antenna, which possesses a simulated gain variance of 0.2~5.4 dB and a measured one of 0.15~5.3 dB. The merged configuration exhibits a maximum top gain of 14.9 dBi across the working frequency spectrum around 10.6 GHz; the maximal gain spanning the ultra-wideband spectrum is 14.5 dB, which represents a significant improvement of 10 dB vs. the standalone antenna.

The disparities that exist between measurements and the simulation results of the S-11 and the gain are predominantly attributed to manufacturing imperfections.

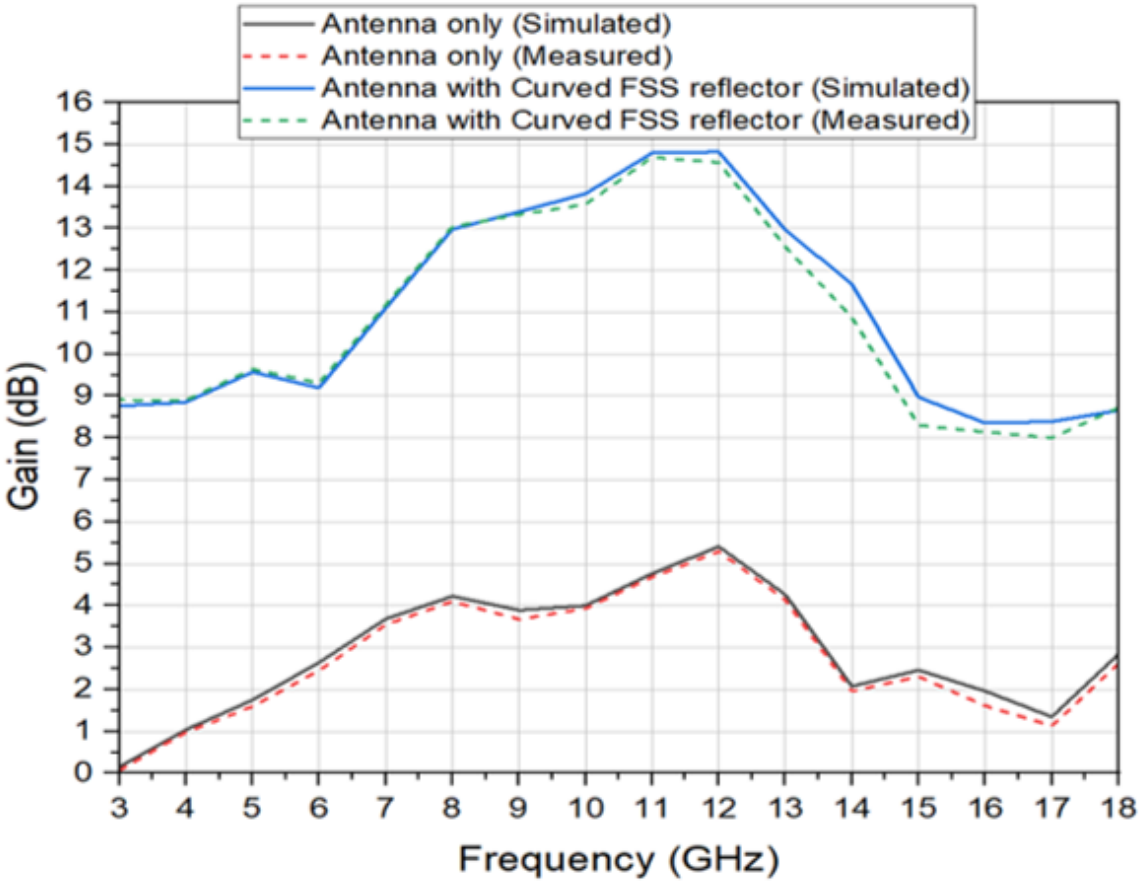

Figure 6.13 Simulated and measured gain of the suggested UWB monopole with and without the curved FSS reflector.

Figure 6.14 displays the measured and simulated E-field and H-field of the proposed ultra-wideband antenna alongside and without the bent-frequency selective surface reflector at frequencies of 3.6 GHz, 5.8 GHz, and 8.6 GHz. The CPW-fed monopole, with no curved structure, exhibits a figure-8 pattern across the H-plane and a virtually omni-directional pattern across the E-plane. Nevertheless, the radiation pattern acquired a specific directionality following the implementation of the bent design, hence augmenting the directivity of the layout under consideration.

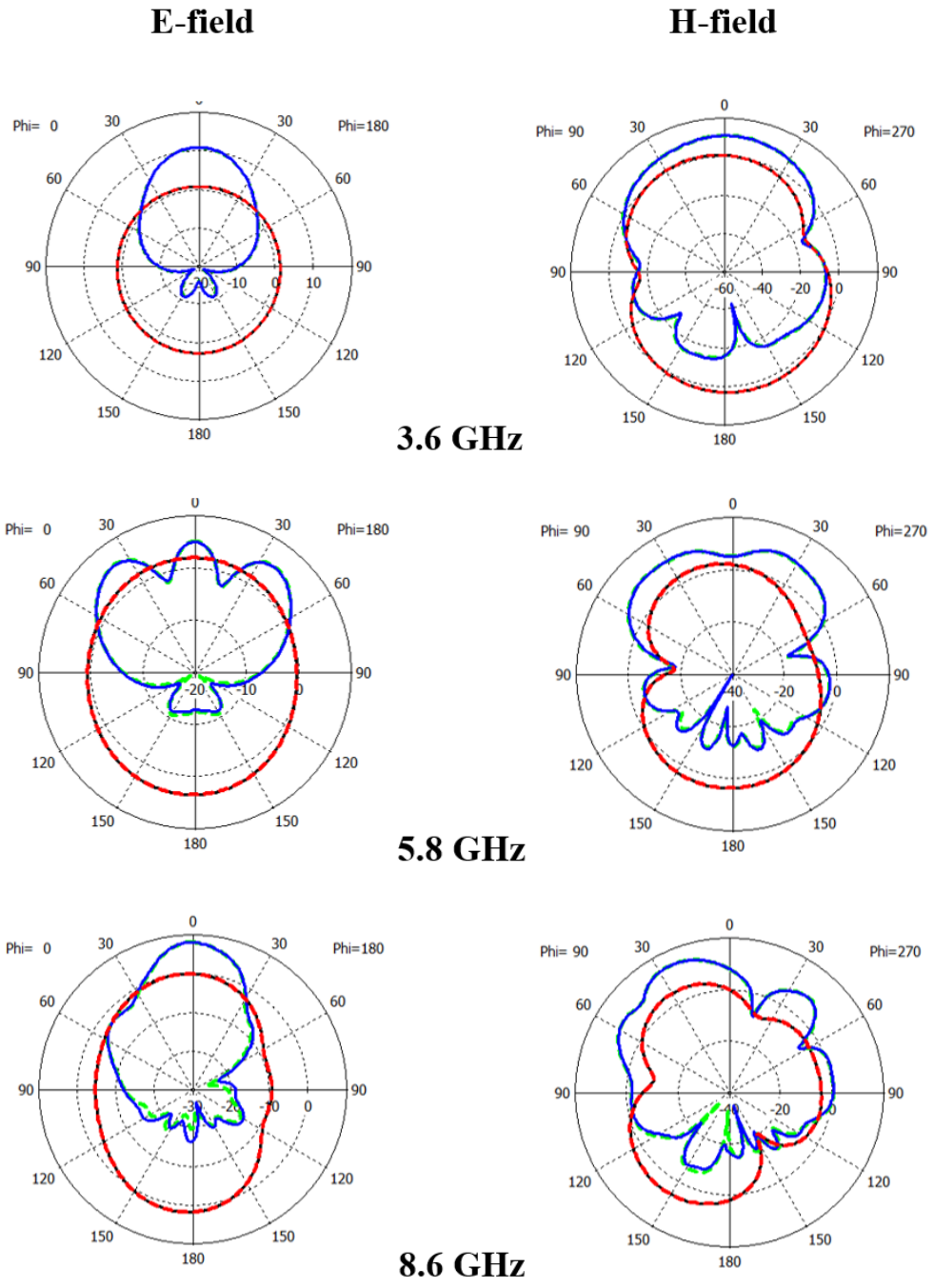

Figure 6.14 Simulated and measured E-field and H-field of the suggested UWB monopole with and without the curved FSS reflector at 3.6 GHz, 5.8 GHz, and 8.6 GHz.

Table 6.3 displays a comparison with contemporary works of a similar nature.

Table 6.3 Comparison between the suggested design and similar works.

REF	Antenna size (mm)	Number of FSS	Bandwidth (GHz)	Gain (dB)
30	31.9×30×1.6	Single	3.8-10.6	3.5-8
31	27×20×1.6	Single	4.7-14.9	5-8.7
32	36×24×0.8	Single	2.94-15.26	5.5-8.5
33	26×26×1.6	Single	3.05-11.9	7.87-9.68
This work	20×25×1.6	Single	2.66-17.98	8.8-14.9

6.5Conclusions

This work aims to optimize the greatest gain of a UWB antenna. This study introduces a new design for a bent UWB-stop-band single-layered FSS. The CPW-Fed monopole, spanning 20 × 25 mm^2, is positioned atop the curve-shaped Structure. The reflector consists of an 11x11 array of UCs, each measuring 13 × 13 mm. The combined configuration, when coupled, reaches a bandwidth of 15.32 GHz, ranging from 2.66 to 17.98 GHz, which encompasses the whole UWB spectrum. It also exhibits a considerable gain of 8.8 to 14.9 dB, including a top gain improvement of 10 dB at 10.6 GHz. Additionally, it displays directed radiation patterns. We conducted an analysis on fundamental design aspects and compared the newly developed FSS design process to the commonly employed method, yielding favorable outcomes. The proposed configuration exhibits a diminutive and condensed form, showcases exceptional attributes, and can be utilized in ultra-wideband and ground-penetrating radar apps.

REFERENCES

[1] Daira SEI, Lashab M, Berkani HA, Belattar M, Gharbia I, Abd-Alhameed RA. A curved single-layer FSS design for gain improvement of a compact size CPW-fed UWB monopole antenna. Microw Opt Technol Lett. 2023;1-12.

[2] E. S. Angelopoulos, A. Z. Anastopoulos, D. I. Kaklamani, A. A. Alexandridis, F. Lazarakis, and K. Dangakis, ‘‘Circular and elliptical CPW-fed slot and microstrip-fed antennas for ultrawideband applications,’’ IEEE Antennas Wireless Propag. Lett., vol. 5, pp. 294–297, 2006.

[3] S. Chaimool and K. L. Chung, ‘‘CPW-fed mirrored-L monopole antenna with distinct triple bands for WiFi and WiMAX applications,’’ Electron. Lett., vol. 45, no. 18, p. 928, 2009.

[4] Mohamed Lashab, Chemss Eddine, Naeem Ahmed Jan, F Benabdelaziz, RA Abd-Alhameed, Marl Child, “CPW-Fed antenna based on Metamaterial for Broadband application,” Loughborough Antennas and Propagation Conference (LAPC) 2014, pp. 144-147, Loughborough, UK.

[5] Naeem Ahmed Jan, Mohamed Lashab, Chemss-Eddine Zebiri, Djouablia Linda, RA Abd-Alhameed, Fatiha Benabdelaziz Compact, “CPW antenna loaded with CRLH-TL and EBG for multi-band and gain Enhancement,” Loughborough Antennas & Propagation Conference (LAPC) 2016, Loughborough, UK.

[6] T. C. Edward and M. B. Steer, Foundations for microstrip circuit design, 4 st ed., John Wiley & Sons, Chichester (United Kingdom), p. 659, 2016.

[7] R. Cicchetti, E. Miozzi, and or. Testa, “Wideband and UWB antennas for wireless applications: A comprehensive review,” International Journal of Antennas and Propagation, Article ID 2390808, 45 pages, 2017.

[8] A. Esmaeilkhah, Ch. Ghobadi, J. Nourinia, and M. Majidzadeh, “On effect of planar scaling on microstrip patch antenna performance,” Advanced Electromagnetics, vol. 8, no. 1, pp. 1-7, March 2019.

[9] I. Amdaouch, O. Aghzout, A. Naghar, and A. V. Alejos, F. Falcone, “Design of UWB compact slotted monopole antenna for breast cancer detection,” Advanced Electromagnetics, vol. 8, no. 5, pp. 1-6, December 2019.

[10] Jamlos, M. A., M. F. Jamlos, S. Khatun, and A. H. Ismail, “A compact super wide band antenna with high gain for medical applications,” IEEE Symposium on Wireless Technology and Applications (ISWTA), Kota Kinabalu, Malaysia, 2014.

[11] Ali, J., “Ultra-wideband antenna design for GPR applications: A review,” International Journal of Advanced Computer Science and Applications, Vol. 8, 392–400, 2017.

[12] F. Mouhouche, A. Azrar, M. Dehmas, and K. Djafer, “Gain Enhancement of Monopole Antenna using AMC Surface,” Advanced Electromagnetics, 7, 3, 2018, pp. 69-74.

[13] K. P. Rao, R. M. Vani, and P. V. Hunagund, “Planar Microstrip Patch Antenna Array with Gain Enhancement,” Procedia computer science, 143, 2018, pp. 48-57.

[14] J. Chatterjee, A. Mohan and V. Dixit, «Broadband Circularly Polarized H-Shaped Patch Antenna Using Reactive Impedance Surface, » IEEE Antennas Wireless Propag. Lett., 17, 4, 2018, pp. 625-628.

[15] R. Yahya, A. Nakamura, M. Itami and T. A. Denidni, "A Novel UWB FSS-Based Polarization Diversity Antenna, » in IEEE Antennas and Wireless Propagation Letters, 16, 2017, pp. 2525-2528.

[16] Al-Gburi, A.J.A.; Ibrahim, I.M.; Zakaria, Z.; Abdulhameed, M.K.; Saeidi, T. Enhancing Gain for UWB Antennas Using FSS: A Systematic Review. Mathematics 2021, 9, 3301.

[17] S. E. I. Daira, M. Lashab and M. Belattar, "a Compact Size FSS Unit Cell Design for UWB Filtering and Shielding Applications," 2023 International Conference on Advances in Electronics, Control and Communication Systems (ICAECCS), BLIDA, Algeria, 2023, pp. 1-4.

[18] J. D. Ortiz, J. D. Baena, V. Losada, F. Medina, R. Marques, and J. L. A. Quijano, ‘‘Self-complementary metasurface for designing narrow band pass/stop filters,’’ IEEE Microw. Wireless Compon. Lett., vol. 23, no. 6, pp. 291–293, Jun. 2013.

[19] Ranga, Y., L. Matekovits, and K. P. Esselle, “Multioctave frequency selective surface reflector for ultrawideband antennas,” IEEE Antennas and Wireless Prop. Letters, Vol. 2011, 10, 219–222.

[20] Jan, N.A.; Kiani, S.H.; Muhammad, F.; Sehrai, D.A.; Iqbal, A.; Tufail, M.; Kim, S. V-Shaped Monopole Antenna with Chichena Itzia Inspired Defected Ground Structure for UWB Applications. Comput. Mater. Contin. 2020, 65, 19–32.

[21] Narayan, S.; Jha, R.M. A novel metamaterial FSS-based structure for wideband radome applications. Comput. Mater.Contin. 2013, 37, 97–108.

[22] Askari, H.; Hussain, N.; Choi, D.; Abu Sufian, M.; Abbas, A.; Kim, N. An AMC-Based Circularly Polarised Antenna for 5G sub-6 GHz Communications. Comput. Mater.Contin. 2021, 69, 2997 3013.

[23] Liu, C.; Bai, Y.; Jing, L.; Yang, Y.; Chen, H.; Zhou, J.; Zhao, Q.; Qiao, L. Equivalent energy level hybridisation approach for high-performance metamaterials design. Acta Mater. 2017, 135, 144–149.

[24] A. Kapoor, R. Mishra, P. Kumar, Frequency selective surfaces as spatial filters: fundamentals, analysis and applications. Alexandria Eng. J. 61(6), 4263–4293 (2022).

[25] Anwar, R.S.; Mao, L.; Ning, H. Frequency Selective Surfaces: A Review. Appl. Sci. 2018, 8, 1689.

[26] R. A. Abdulhasan, R. Alias, K. N. Ramli, F. C. Seman, and R. A. Abd-Alhameed, ‘‘High gain CPW-fed UWB planar monopole antenna-based compact uniplanar frequency selective surface for microwave imaging,’’ Int. J. RF Microw. Comput.-Aided Eng., vol. 29, no. 8, 2019, Art. no. e21757.

[27] P. Das and K. Mandal, "Modelling of ultra-wide stop-band frequency-selective surface to enhance the gain of a UWB antenna," IET Microwaves, Antennas & Propagation, 13, no. 3, 2019, pp. 269-277.

[28] S. Kundu, "Gain Improvement of Ultra-Wideband antenna using compact Frequency Selective Surface," 2020 URSI Regional Conference on Radio Science (URSI-RCRS), Varanasi, India, 2020, pp. 1-4.

[29] A. J. A. Al-Gburi, I. B. M. Ibrahim, M. Y. Zeain and Z. Zakaria, "Compact Size and High Gain of CPW-Fed UWB Strawberry Artistic Shaped Printed Monopole Antennas Using FSS Single Layer Reflector," in IEEE Access, vol. 8, pp. 92697-92707, 2020.

CHAPTER VII

Conclusions and Future Work

7.1 Conclusions

The present research has undertaken a comprehensive exploration of ultra-wideband (UWB) antenna design tailored for fifth-generation (5G) mobile communication systems. With the advent of 5G technology, the demand for antennas that offer ultra-wideband performance, miniaturized dimensions, multi-band capabilities, and high gain has become increasingly critical. The research aimed to address these complex challenges by investigating and developing innovative antenna designs that integrate fractal techniques, metamaterials, and advanced methods.

Throughout the course of this study, several key objectives were identified and pursued. The initial goal was to design a UWB antenna using fractal techniques. We then developed an antenna using metamaterials, specifically Split Ring Resonators (SRRs) and Defective Ground Structures (DGS), to promote miniaturization and enhance performance. Additionally, the research explored the design of a multi-band antenna suitable for 5G applications, considering the integration of different polarization schemes necessary for 5G communication. We extensively employed commercial simulation software, CST Studio Suite, to model, simulate, and optimize the antenna designs, which we subsequently fabricated and tested to validate the theoretical findings.

The research has made significant contributions to the field of UWB and 5G antenna design, particularly in the following areas:

A novel UWB antenna design was created through the study. It used fractal geometry to create a UWB antenna with a wide impedance bandwidth and high gain across the UWB spectrum. The fractal technique, along with the designed Frequency Selective Surface (FSS) structure, proved to be effective in miniaturizing the antenna while preserving its operational characteristics, thereby addressing one of the key challenges in UWB antenna design.

An innovative single-layered UWB Frequency Selective Surface Unit Cell designed for effective band-stop spatial filtering and electromagnetic shielding across a broad frequency range. Implemented on a cost-efficient FR4 substrate, the proposed layout demonstrates superior performance, achieving a wide stop-band with excellent shielding effectiveness. Overall, the compact and efficient design of the proposed FSS makes it a strong candidate for UWB applications where wideband filtering and robust EMI protection are critical.

Metamaterial-Based Antenna for 5G: Putting SRR unit cells and DGS techniques together in a UWB patch antenna for 5G applications below 6 GHz showed big gains in bandwidth, gain, and overall electromagnetic performance. The SRR and DGS structures

enabled a strong resonance effect, which was crucial for miniaturization and enhancing the antenna's performance within the specified frequency range.

Simulation and Fabrication: Through extensive use of simulation tools, we gained a detailed understanding of the electromagnetic behavior of the proposed designs, further reinforced by experimental validation. The fabricated prototypes exhibited performance metrics that were in close agreement with the simulated results, thereby validating the design methodologies and the effectiveness of the proposed solutions.

Gain Enhancement Techniques: We introduced a novel approach that involves a curved single-layer frequency selective surface (FSS) to enhance the gain of a compact coplanar waveguide (CPW) UWB antenna. This design achieved a substantial gain improvement across the UWB spectrum, making it suitable for applications in UWB and ground-penetrating radar systems.

The findings of this research have significant implications for the development of advanced antenna systems, which are essential for the realization of 5G communication networks. This study has given us useful information and useful solutions that help antenna technology keep getting better by looking at the important problems that come up with UWB antenna design and combining new methods and techniques like fractals, metamaterials, and advanced methods.

7.2 Future Work

While this research has made significant progress in the field of UWB and 5G antenna design, there are still several avenues for future investigation. These potential research areas offer opportunities to further improve the performance and applicability of the indicated antenna designs, as well as to explore new frontiers in antenna technology.

Exploration of Additional Metamaterial Structures: To further enhance antenna performance, future research could focus on the exploration and integration of other metamaterial structures, such as electromagnetic bandgap (EBG) materials and artificial magnetic conductors (AMCs). These materials have the potential to offer additional advantages in terms of bandwidth enhancement, gain improvement, and miniaturization.

Extension to Millimeter-Wave Frequencies: The current study primarily focused on UWB and sub-6 GHz frequency bands. However, the extension of the proposed designs to millimeter-wave (mmWave) frequencies, which are a critical component of 5G networks, presents a promising area for future research. Looking into how fractal and metamaterial

techniques can be used at mmWave frequencies could lead to useful discoveries and help the creation of very effective mmWave antennas.

Integration with Reconfigurable Antenna Technologies: Reconfigurable antennas, which can dynamically adjust their operating frequency, polarization, or radiation pattern, are increasingly relevant in modern communication systems. In the future, researchers might look into how to add reconfigurable parts to the proposed UWB and 5G antennas so that they can adapt to changing network conditions and needs.

Environmental and Wearable Applications Investigation: The miniaturized and high-performance nature of the proposed antennas makes them suitable for environmental and wearable applications, such as IoT devices and body-worn sensors. Future studies could explore the deployment of these antennas in such applications, addressing challenges related to environmental conditions, human body effects, and power efficiency.

Development of antenna arrays for MIMO systems: Multiple-input multiple-output (MIMO) technology is a key enabler of high data rates and reliability in 5G networks. Future research could focus on developing antenna arrays based on the proposed designs, optimized for MIMO systems. This includes exploring array configurations, mutual coupling reduction techniques, and beamforming capabilities.

Further Optimization of Polarization Techniques: This would involve studying the impact of polarization on antenna performance in different environments and developing strategies to mitigate polarization mismatches and enhance signal quality.

Simulations and controlled experiments have validated the proposed designs, but future work could involve extensive experimental testing in real-world scenarios like urban environments, indoor settings, and mobile platforms. This would provide valuable insights into the practical performance and reliability of the antennas in diverse and dynamic conditions.

Collaboration with Industry for Commercialization: Finally, collaboration with industry partners to transition the proposed antenna designs from research prototypes to commercially viable products represent a crucial step towards real-world impact. Future research could focus on optimizing the designs for mass production, cost-effectiveness, and integration into commercial 5G communication devices and systems.

In conclusion, this research has laid a solid foundation for the development of advanced UWB and 5G antennas, offering innovative solutions to the challenges posed by modern communication networks. The proposed designs have demonstrated significant improvements in performance, paving the way for future advancements in antenna technology. The outlined

future work serves as a roadmap for continued exploration and innovation, ensuring that the findings of this research contribute to the ongoing evolution of 5G and beyond.